Titre: Title:	Développement d'un procédé sans collision pour la fabrication de tresses 3D avec géométries variables
Auteur: Author:	Pascal Assi
Date:	2023
Type:	Mémoire ou thèse / Dissertation or Thesis
Référence: Citation:	Assi, P. (2023). Développement d'un procédé sans collision pour la fabrication de tresses 3D avec géométries variables [Thèse de doctorat, Polytechnique Montréal]. PolyPublie. https://publications.polymtl.ca/53425/

URL de PolyPublie: PolyPublie URL:	https://publications.polymtl.ca/53425/
Directeurs de recherche: Advisors:	Louis Laberge Lebel, & Sofiane Achiche
Programme: Program:	Génie mécanique

POLYTECHNIQUE MONTRÉAL

affiliée à l'Université de Montréal

Développement d'un procédé sans collision pour la fabrication de tresses 3D avec géométries variables

PASCAL ASSI

Département de génie mécanique

Thèse présentée en vue de l'obtention du diplôme de *Philosophiæ Doctor*

Génie mécanique

Avril 2023

POLYTECHNIQUE MONTRÉAL

affiliée à l'Université de Montréal

Cette thèse intitulée :

Développement d'un procédé sans collision pour la fabrication de tresses 3D avec géométries variables

présentée par **Pascal ASSI**

en vue de l'obtention du diplôme de *Philosophiæ Doctor*

a été dûment acceptée par le jury d'examen constitué de :

Aurelian VADEAN, président

Louis LABERGE LEBEL, membre et directeur de recherche

Sofiane ACHICHE, membre et codirecteur de recherche

Maxime RAISON, membre

Simon JONCAS, membre externe

DÉDICACE

To my beloved mom

REMERCIEMENTS

Je tiens tout d’abord à remercier mes directeurs de recherche, Louis Laberge Lebel et Sofiane Achiche, pour m’avoir guidé et formé tout au long de mon parcours doctoral. Je vous remercie pour votre aide et support constant ainsi que le temps que vous avez investi pour que j’acquière et développe mes compétences.

Je remercie également Aurelian Vadean, Maxime Raison et Simon Joncas pour avoir accepté de siéger sur le comité de cette thèse.

J’aimerais remercier les membres du personnel technique de Polytechnique Montréal, particulièrement Guy Gironne, Bénédict Besner et Fabrice Danet. Je vous remercie de m’avoir aidé à réaliser les montages expérimentaux tout au long de mes études universitaires. Sans vous, mes idées n’auraient jamais vu le jour.

Je remercie également FilSpec Inc, Pultrusion Techniques et Bauer Hockey ltd, pour leur soutien financier tout au long de mon doctorat.

Je tiens à remercier Rita pour les sacrifices qu’elle a faits pour me supporter tout au long de ma formation académique. Merci pour l’encouragement, le support et d'avoir constamment veillé à ma réussite.

Finalement, un grand merci à Clarice d’avoir été à mes côtés toutes ces années. Merci de me supporter dans les projets que j’entreprends, de m’écouter et de m’avoir relu à maintes reprises!

RÉSUMÉ

Les matériaux composites offrent de fortes propriétés mécaniques, et ce, pour une fraction de la masse habituelle. Ils contribuent donc à réduire le poids des véhicules terrestres, marins et aériens, ce qui permet d'augmenter l'efficacité énergétique de ces derniers. Les matériaux composites se retrouvent souvent sous la forme de fibres noyées dans une résine de polymère. Les fibres peuvent être sous la forme d'un tissu, d'une tresse, ou de fibres unidirectionnelles. Comparativement aux tissus et aux fibres unidirectionnelles, les tresses ont l'avantage d'être fabriquées aux dimensions finales de la pièce, ce qui permet de réduire considérablement la quantité de rebuts non recyclable produit. Cependant, les métiers à tresser possèdent des lacunes limitant l'utilisation des tresses pour les matériaux composites.

Les tresses sont produites par l'entrelacement de fils. Pour ce faire, les bobines de fil sont fixées sur des chariots qui se déplacent sur un plan de travail suivant une trajectoire qui s'entrelace. Néanmoins, la trajectoire de ces derniers est fixe, ce qui limite la fabrication de nouvelles géométries de tresses. De plus, les chariots doivent se déplacer sans rentrer en collisions. Pour ce faire, la position initiale des chariots, aussi appelée l'arrangement des chariots, dois être sélectionné correctement, sans quoi, une collision se produira. Or, à ce jour, il n'existe aucune méthode permettant de valider ou d'invalider l'arrangement des chariots, et ce, peu importe le métier à tresser.

Le premier objectif de cette thèse est de développer un algorithme permettant de détecter des collisions entre les chariots basés sur l'arrangement des chariots, permettant ainsi de valider ou d'invalider ce dernier. L'algorithme se base sur la théorie des graphes. Pour ce faire, le plan de travail est représenté par un graphe constitué de faces, de nœuds et d'arêtes. La trajectoire de chaque chariot est définie par une série de nœuds, représentant chacun une position sur le plan de travail. Une collision se produit lorsque deux chariots se trouvent au même endroit simultanément. Sur le graphe, cela implique que deux chariots se trouvent simultanément sur le même nœud. L'algorithme vérifie donc que chaque nœud est uniquement occupé par un chariot en tout temps. L'algorithme a été validé par deux études de cas. La première étude a été effectuée sur un métier à tresser traditionnel, tandis que la deuxième étude a été effectuée sur un métier à tresser pour des tresses en forme de « T ».

Le second objectif de cette thèse est de développer un procédé de fabrication pour les tresses permettant de positionner en tout temps et de façon indépendante les chariots supportant les bobines de fil. Pour ce faire, un nouveau chariot a été conçu. Ce dernier est composé d'une chaîne de trois maillons. Il se déplace sur un plan de travail composé de roues à encoches. Ces dernières sont positionnées selon un arrangement hexagonal compact. Le déplacement du chariot s'effectue par l'entremise des roues à encoches. Le système est similaire à celui d'un système chaîne-pignon. Un prototype a été fabriqué pour valider le concept. À partir de ce prototype, deux tresses ont été fabriquées. La première est une tresse standard à trois fils. La deuxième est une tresse comprenant deux changements de section transversale. Cette dernière débute par une tresse standard à trois fils. Elle se transforme par la suite en un enroulement filamentaire de 3 fils, où deux fils s'enroulent ensemble et le troisième enroule les deux premiers à un pas différent. Finalement, l'enroulement filamentaire se transforme en tresse standard à 3 fils. Ces changements de section ont été effectués de façon automatique, sans arrêter le procédé de fabrication. Il est donc possible de contrôler la position de chaque chariot.

Le troisième objectif de cette thèse est de développer un algorithme permettant d'éviter les collisions dans les métiers à tresser à trajectoires non fixes en exploitant la flexibilité du déplacement des chariots. Cet algorithme se base également sur la théorie des graphes. Similaire au premier objectif, le plan de travail est représenté par un graphe constitué de faces, de nœuds et d'arêtes. La trajectoire de chaque chariot est définie par une série de nœuds, représentant chacun une position sur le plan de travail. Les collisions sont évitées en prescrivant un délai à un ou plusieurs chariots. Les délais retardent le déplacement des chariots, évitant ainsi les collisions. Une étude de cas a été effectuée sur un prototype d'un métier à tresser à trajectoires variables pour valider l'algorithme. Lors du déplacement simultané de trois chariots, une collision a été évitée en retardant le déplacement d'un chariot par un délai prescrit par l'algorithme.

Les trois objectifs ont été atteints. En premier lieu, une solution simple et automatique est proposée pour valider ou infirmer l'arrangement des chariots. Cette dernière peut être utilisée sur n'importe quel métier à tresser. De plus, une méthode automatique réduit le risque d'erreur qui peut être coûteux en termes de matériels endommagés ou rendre la machine inopérable. En second lieu, un procédé de fabrication est présenté. Ce dernier permet de contrôler la position et l'orientation de chaque fils, ce qui permet la fabrication de pièces en composites tressés mieux adaptée aux requis de forme et offre une plus grande liberté de conception aux ingénieurs. Les pièces à géométrie complexe, telles que les cadres et les fourches de vélos, peuvent désormais être fabriquées en une seule étape de fabrication, et ce, de façon automatique. Finalement, l'algorithme permettant d'éviter les collisions dans les métiers à tresser à trajectoires variables servira de jalon pour la programmation automatique des métiers à tresser, favorisant ainsi l'exploitation des fortes propriétés mécaniques des composites tressés 3D. À ce jour, il n'existe aucune méthode reliant la géométrie du textile aux trajectoires des chariots (cinématique inverse). La capacité à déduire l'entrelacement des fils, or la trajectoire des chariots, à partir d'une tresse ou d'un modèle de tresse donné est réservée aux experts. Il serait intéressant d'élaborer une méthode pour résoudre la cinématique inverse.

ABSTRACT

Composite materials offer strong mechanical properties at a fraction of the usual weight. Therefore, they contribute to reducing the weight of land, sea and air vehicles, which increases the energy efficiency of these vehicles. Composite materials are often found in the form of fibers embedded in a polymer resin. The fibers can be in the form of a fabric, a braid, or unidirectional fibers. Compared to woven fabrics and unidirectional fibers, braids have the advantage of being manufactured to the final dimensions of the part, which greatly reduces the amount of non-recyclable waste produced. However, braiding machines have shortcomings that limit the use of braids for composite materials.

Braids are produced by intertwining yarns. To do this, the spools of yarn are attached to carriers that move along an intertwining path on a bedplate. The path of the carriers is fixed, which limits the manufacture of new braid geometries. In addition, the carriers must move without colliding. To do this, the initial position of the carriers, also called the carrier arrangement, must be selected correctly, otherwise, a collision will occur. However, there is no method to validate or invalidate the carriage arrangement, regardless of the braiding machine.

The first objective of this thesis is to develop an algorithm to detect collisions between carriers based on the carrier arrangement, thus allowing to validate or invalidate the latter. The algorithm is based on graph theory. To do this, the bedplate is represented by a graph made of faces, vertices and edges. The trajectory of each carrier is defined by a series of vertices, each representing a position on the bedplate. A collision occurs when two carriers are in the same location simultaneously. On the graph, this implies that two carriers are simultaneously on the same vertex. Therefore, the algorithm checks that each vertex is only occupied by one carrier at all times. The algorithm was validated by two case studies. The first study was performed on a traditional braiding machine, while the second study was performed on a braiding machine, which produces "T" shaped braids.

The second objective of this thesis is to develop a manufacturing process for braids that allows the positioning of the carrier at all times and in an independent manner. For this purpose, a new carrier is designed. It is composed of a three-link chain. It moves on a bedplate composed of horngears. The horngears are positioned in a compact hexagonal arrangement. The carrier is moved by the horngears. The system is similar to a chain-sprocket system. A prototype was built to validate the

concept. From this prototype, two braids were manufactured. The first is a standard three yarns braid. The second is a braid with two cross-section changes. The latter starts with a standard three yarns braid. It then changes to a filament winding, where two yarns are winded together and the third yarn winds the first two at a different pitch. Afterward, the filament winding changes to a standard three yarns braid. These section changes were performed automatically, without stopping the manufacturing process. It is therefore possible to control the position of each carrier.

The third objective of this thesis is to develop an algorithm to avoid collisions in braiding machines with non-fixed paths by exploiting the flexibility of the carrier's movement. This algorithm is also based on graph theory. Similar to the first objective, the bedplate is represented by a graph consisting of faces, vertices and edges. The path of each carrier is defined by a series of vertices, each representing a position on the bedplate. Collisions are avoided by prescribing a delay to one or more carriers. Delays postpone the movement of the carriers, thus avoiding collisions. To validate the algorithm, a case study was performed on a prototype of a braiding machine with variable carrier's paths. Three carriers were moved simultaneously. A collision was avoided by delaying the movement of one carrier, as prescribed by the algorithm.

All three objectives have been achieved. First, a simple and automatic solution is proposed to validate or invalidate the arrangement of the carriers. This solution can be used on any braiding machine. Moreover, an automatic method reduces the risk of error, which can be costly in terms of damaged materials or can render the machine inoperable. Secondly, a manufacturing process is presented. This process allows to control the position and the orientation of each carrier, which allows for the fabrication of braided composite parts that are better suited to shape requirements and provides greater design freedom to engineers. Parts with complex geometries, such as bicycle frames and forks, can now be manufactured in a single automatic step. Finally, the algorithm for preventing collisions in variable path braiding machines will serve as a milestone for programming variable paths braiding machines, thus promoting the exploitation of the strong mechanical properties of 3D braided composites. To date, there is no method linking the textile geometry to the carriers' trajectories (inverse kinematics). The ability to deduce the yarn crossovers, therefore the carrier's trajectory, from a given braid or braided geometry is reserved to experts. It would be interesting to develop a method to solve the inverse kinematics.

TABLE DES MATIÈRES

LISTE DES TABLEAUX

LISTE DES FIGURES

LISTE DES SIGLES ET ABRÉVIATIONS

CCW	Counterclockwise
CW	Clockwise
DS	Displacement step
HG	Horngear
IC	Interconnection
MMP	Multi-criteria mechatronic profile
PAN	Polyacrylonitrile
UAV	Autonomous unmanned aerial vehicles

LISTE DES ANNEXES

CHAPITRE 1 INTRODUCTION

Réduire les émissions de gaz à effet de serre est l'un des principaux défis auquel notre société ainsi que l'industrie du transport sont confrontées. L'utilisation des matériaux composites semble être une partie intégrante de la solution, car ils possèdent de bonnes propriétés mécaniques pour une fraction de la masse habituelle. Cela permet donc de réduire le poids de véhicules et augmenter leur efficacité énergétique. L'utilisation des matériaux composites ne cesse d'augmenter dans divers secteurs tels que l'aéronautique, l'automobile et les sports de performance. Au cours des 20 dernières années, le pourcentage massique des aéronefs attribué aux matériaux composites est passé de 15 à 53% [1], tandis que le pourcentage volumique atteint désormais 80% [2].

Par définition, un matériau composite est un assemblage d'au moins deux composants différents créant un matériau non homogène [3]. On retrouve souvent un renfort fibreux noyé dans une résine polymérique. Le renfort peut être un tissé, une tresse, des fils placés selon une direction bien définie ou des fils placés de façon aléatoire. Traditionnellement, les techniques de fabrication superposent, couche par couche, des renforts tissés plans (2D). La superposition des tissés 2D est longue et coûteuse. Suite à l'imprégnation des renforts par la résine, les fils sont généralement coupés aux dimensions finales de la pièce, créant ainsi énormément de rebuts. Pour pallier ces limitations, les procédés textiles tridimensionnels (3D), tels que le tressage, permettent la fabrication de tissus multicouches reliés par des fils du renfort. Pouvant être fabriquées aux dimensions finales de la pièce, les tresses 3D contribuent à la diminution des rebuts et éliminent des étapes d'usinage. Cependant, la fabrication de tresses 3D reste contrainte par les métiers à tresser qui imposent l'orientation des fils et par le fait même, la géométrie du textile.

L'objectif général de cette thèse est de développer un procédé de fabrication pour les tresses 3D permettant de positionner et de contrôler l'orientation des fils en tout temps. Tout d'abord, une revue de la littérature est présentée, faisant état des procédés de fabrication textiles tressés ainsi que de leurs lacunes. Par la suite, la méthodologie permettant d'atteindre l'objectif de recherche est présentée, suivie d'une discussion des résultats de trois articles scientifiques publiés dans le cadre des travaux de recherche, d'une conclusion et de recommandations futures.

CHAPITRE 2 REVUE CRITIQUE DE LA LITTÉRATURE

2.1 Les tresses

Le tressage est un procédé textile qui s'inspire fortement des tresses à cheveux. Le principe consiste à entrelacer au minimum trois fils parallèles pour former une structure continue [4]. Le tressage est traditionnellement utilisé pour la fabrication de cordes d'escalade, de lacets et de filets de pêche [4]. Les tresses ont également fait leur apparition dans les structures composites, telles que les cadres de fuselages d'avions, les tuyères de moteurs et les hélices marines [4-7].

Il existe 2 grandes familles de textiles tressés : les tresses planes (2D) et les tresses tridimensionnelles (3D). Parmi les tresses 2D, on retrouve les tresses plates et les tresses tubulaires [7]. Les tresses tubulaires, fréquemment utilisées, se divisent en trois principales catégories selon leurs architectures d'entrelacement : diamants, régulières et hercules. La Figure 2.1a), b) et c) présentent schématiquement les trois types de tresses tubulaires. Les tresses Diamants se caractérisent par une architecture 1x1 : altération d'un fil passant au-dessus et en dessous d'un autre fil. Les tresses régulières se caractérisent par une architecture 2x2 : altération d'un fil passant au-dessus et en dessous de deux autres fils. Les tresses Hercules se caractérisent par une architecture 3x3. Il existe aussi différentes autres architectures d'entrelacement comme 1x2, 2x3 ou 1x3. Parmi les tresses 2D, on retrouve aussi les tresses triaxiales. Ces dernières se caractérisent par la présence de fils de renforcement axial. Ces fils ont une orientation de 0 degré par rapport à l'axe longitudinal de la tresse. La Figure 2.1d) présente une section d'une tresse tubulaire triaxiale ayant une architecture 2x3. Les tresses 2D qui ne comportent aucun fil axial sont appelées tresses biaxiales.

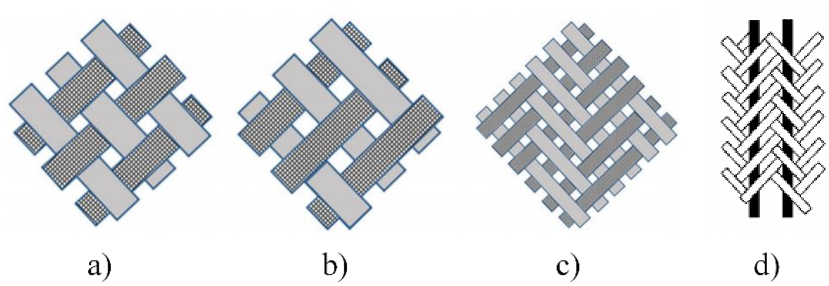

Figure 2.1 : Représentation schématique des tresses tubulaires et triaxiales a) Diamant b) régulière c) Hercule d) Tresse triaxiale [7, 8].

La différence entre les tresses 3D et les tresses 2D se trouve au niveau du croisement des fils [4, 7]. Par exemple, pour renforcer ou épaissir une tresse tubulaire, il faut tresser, de nouveau, par-dessus. Le résultat est donc deux tresses tubulaires concentriques ayant des diamètres différents. Cet assemblage est une tresse 2D. Une tresse 3D est similaire, car elle est aussi constituée de plusieurs couches. Par contre, chacune des couches est interreliée par des fils de la tresse. Autrement dit, des fils de la tresse doivent être orientés dans la direction de l'épaisseur pour relier chacune des couches entre elles afin d'être considérée comme une tresse 3D.

2.2 Les caractéristiques et les avantages des composites tressés

L'architecture de la tresse influence grandement ses propriétés mécaniques [9]. Elle est définie par la position et l'angle de chaque entrelacement de fils. L'angle d'une tresse est mesuré entre les fils et l'axe central de cette dernière. La Figure 2.2 présente une tresse tubulaire sur un mandrin cylindrique. L'angle (α) et l'axe central y sont illustrés. Par des essais de traction, il a été démontré que le module de traction et la charge maximale que peut supporter une tresse diminuent avec l'augmentation de l'angle [10]. Ce phénomène peut être expliqué par l'orientation des fils. En effet, lorsque l'angle augmente, les fils sont de moins en moins parallèles avec l'axe de la tresse. Dans un même ordre d'idées, il a été démontré, par des essais de flexion 3 points, que le module en flexion d'une tresse diminue avec l'augmentation de son angle [11]. D'un autre côté, des essais en torsion sur différentes tresses ont démontré que les propriétés en cisaillement augmentent avec l'augmentation de l'angle [12]. Par ailleurs, l'ajout de fils axiaux renforce les propriétés mécaniques en traction ainsi qu'en flexion [10]. Toutefois, leur impact est minime sur la rigidité en torsion.

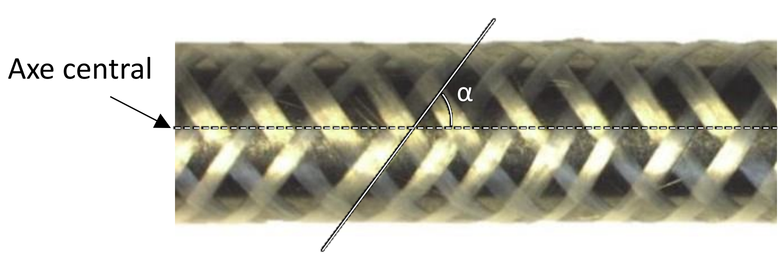

Figure 2.2 : Représentation de l'angle et de l'axe central de la tresse.

Les composites tressés offrent un meilleur comportement en fatigue et une meilleure ténacité par rapport aux composites laminés. L'entrelacement des fils permet de freiner la propagation des fissures [7, 13]. De plus, l'ajout de fils axial offre un comportement plus stable et confère aux matériaux des propriétés quasi isotropes [13]. En outre, les trous formés par le retrait de goupilles positionnées dans une tresse lors de sa fabrication démontrent une robustesse 1.8 fois plus grande que les trous percés en raison de la continuité des fils [13]. Les tresses confèrent aussi aux renforts fibreux une forme presque identique au produit final [6]. Ceci permet d'éliminer toute forme de rebut engendré par les étapes d'usinage subséquentes du renfort permettant d'atteindre les dimensions de la pièce finale.

Comparativement aux tresses 3D, les tresses 2D possèdent de meilleures propriétés selon l'axe de la tresse. En effet, les fils d'une tresse 2D sont moins ondulés que celles d'une tresse 3D, car les fils d'une tresse 2D ne relient pas plusieurs couches adjacentes. Or, plus l'ondulation des fils est élevée, plus les propriétés selon l'axe sont réduites [14]. Toutefois, ce manque de fils selon l'épaisseur entraîne certains désavantages. Les tresses 2D sont plus propices à la délamination lors d'un impact et elles possèdent de faibles propriétés mécaniques selon la direction de l'épaisseur [5, 15]. D'un autre côté, les tresses 3D possèdent une résistance à la délamination et à l'impact nettement supérieur [5, 15-17] en raison des fils orientés selon l'épaisseur du renfort. Elles possèdent aussi de plus grandes propriétés en cisaillement que les tresses 2D [7].

2.3 Procédé de fabrication

La Figure 2.3a) illustre un métier à tresser traditionnel. Les tresses sont fabriquées par le déplacement de chariots sur un plan de travail. Sur chacun des chariots se trouve une bobine de fil. Les chariots se déplacent sur le plan de travail suivant des trajectoires qui s'entrecroisent permettant ainsi d'entrelacer les fils et de créer une tresse. Un mécanisme de traction est aussi positionné au-dessus du plan de travail dans le but de tirer la tresse et les fils à l'écart de ce dernier. Chacune des bobines est positionnée sur un mécanisme d'ajustement de tension nommé tendeur. Le tendeur permet de maintenir une tension constante dans les fils au cours du procédé de fabrication.

Les premiers brevets concernant les métiers à tresser remontent au 18^{e} siècle [18]. Le système le plus utilisé pour déplacer les chariots sur le plan de travail est celui des roues à encoches [19]. Les chariots se logent dans les encoches de ces roues. Par la rotation de ces dernières, les chariots peuvent se déplacer selon une trajectoire prédéfinie. La trajectoire des chariots est rainurée sur le plan de travail. Les roues à encoches doivent donc être positionnées en fonction de la trajectoire. La Figure 2.3b) présente une vue de haut du plan de travail. La moitié des roues ne sont pas présentées à la Figure 2.3b) afin de visualiser la trajectoire qui se trouve en dessous de ces dernières.

Chaque roue à encoches tourne dans le sens contraire à sa voisine. Lorsque deux encoches de roues adjacentes sont face à face, le chariot peut être transféré d'une roue à l'autre et ainsi se déplacer sur le plan de travail. La Figure 2.3c) illustre le transfert d'un chariot entre deux roues. Chaque chariot est muni d'un pied de direction. Le pied de direction est une section extrudée positionnée en dessous du chariot qui glisse dans la rainure de la trajectoire. La Figure 2.3c) i) présente la position initiale des roues et du pied de direction. La Figure 2.3c) ii) présente la position intermédiaire. À ce stade, la trajectoire contraint le transfert du chariot à la roue suivante. À la Figure 2.3c) iii), le transfert est terminé et le chariot se déplace par l'entremise d'une nouvelle roue à encoches. Une roue à encoches peut accueillir plusieurs chariots. Toutefois, un seul chariot à la fois peut être transféré entre deux roues adjacentes.

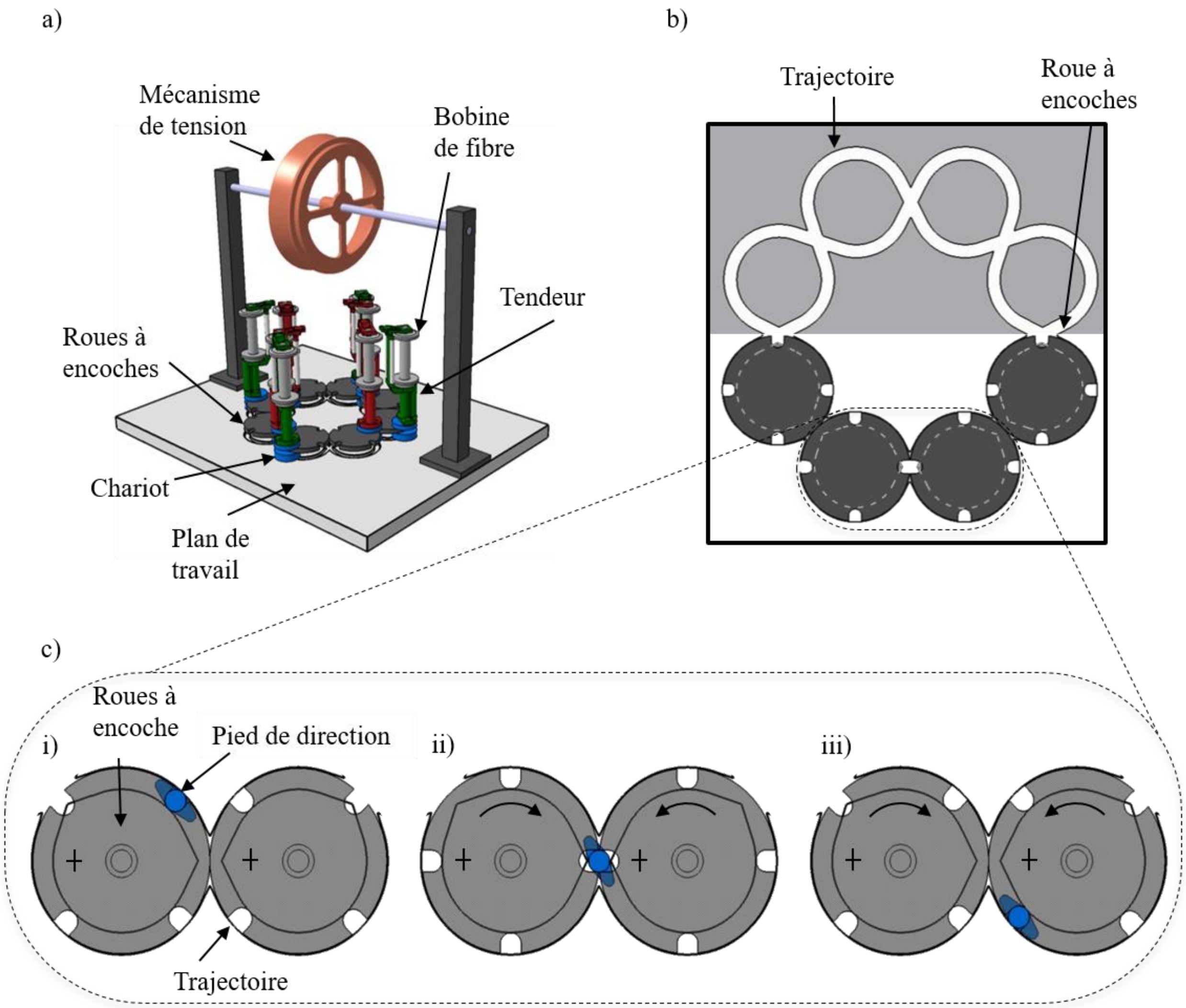

Figure 2.3 : Fonctionnement d’un métier à tresser a) vue isométrique d'un métier à tresser avec les composants importants. b) vue de haut du plan de travail. La moitié des roues à encoches sont présentées pour visualiser la trajectoire située en dessous des roues. c) transfert de chariot entre deux-roues i) position initiale ii) position intermédiaire iii) position finale.

La Figure 2.4 présente les principales caractéristiques d’une tresse : le diamètre, l’angle et le pas. Le pas P [mm] est défini comme étant la distance de la section répétable de la tresse. Cette distance est mesurée selon l’axe de la tresse. Elle peut être calculée à partir de la vitesse d’avance du mécanisme de tension V [mm/s] et du nombre de révolutions par seconde des chariots ω [sec $^{-1}$] autour de plan de travail [20] comme indiqué par l’Équation (2.1).

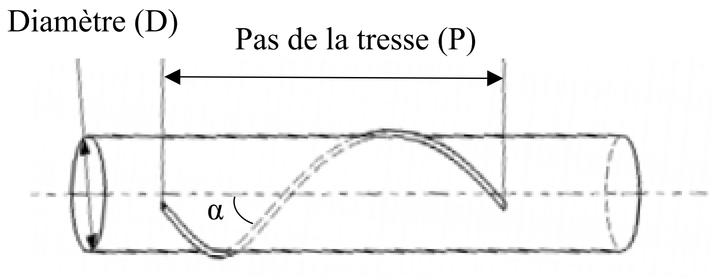

Figure 2.4 : Paramètres de la tresse : diamètre, pas de la tresse et l'angle [20].

$$P = \frac{V}{\omega} \tag{2.1}$$

À partir de l'Équation (2.1), l'angle α d'une tresse tubulaire peut être calculé par

$$\tan\alpha = \frac{\pi D}{P} \tag{2.2}$$

Où D [mm] représente le diamètre interne de la tresse.

À partir de l'Équation (2.1), l'angle α d'une tresse plate peut être calculé par

$$\tan\alpha = \frac{2W}{P} \tag{2.3}$$

Où W [mm] représente la largeur de la tresse.

2.3.1 Configuration du plan de travail et arrangement des chariots

La configuration du plan de travail réfère à l'arrangement des roues à encoches par rapport aux trajectoires rainurées. L'arrangement des chariots réfère à la position initiale des chariots par rapport à la configuration du plan de travail. L'arrangement des chariots ainsi que la configuration du plan de travail ont un impact direct sur l'architecture de la tresse et la topologie des croisements de fils. Cependant, il existe très peu de directives de conception concernant la configuration du plan de travail ainsi que l'arrangement des chariots pour la création de tresses complexes [6, 21].

En réorganisant la configuration du plan de travail des métiers à tresser traditionnels, Tada [21] a démontré qu'il était possible de fabriquer des tresses à section transversale carrée, rectangulaire et en forme de « L ». Chacune des sections transversales énumérées requiert un arrangement de chariots et une configuration du plan de travail différent.

L'arrangement des chariots joue un rôle important lors de la conception d'une tresse. Les chariots doivent être placés d'une certaine façon afin d'éviter une collision durant le procédé de fabrication. Une collision se produit lorsque deux chariots se retrouvent au même endroit simultanément. Cela se produit généralement à l'intersection de deux trajectoires lors du transfert d'un chariot d'une roue à l'autre.

Les notions théoriques concernant l'arrangement des chariots sont sous-développées. Les ingénieurs dépendent grandement de leur expérience ainsi que d'essais-erreur pour trouver un arrangement de chariot ne causant aucune collision [22, 23], ce qui peut être très inefficace en termes de temps et de ressources.

2.3.2 Développements technologiques

Les métiers à tresser traditionnels comportent une lacune majeure : la trajectoire des chariots est fixe et elle ne peut être modifiée au cours du procédé. Ceci limite la fabrication de tresses à une seule structure. Pour modifier la géométrie du produit final, il faut reconfigurer l'arrangement des roues à encoches ainsi que la trajectoire des chariots [22]. Toutefois, en modifiant la vitesse de déplacement des chariots ou la vitesse du mécanisme de traction placé au-dessus du plan de travail, l'angle de la tresse peut être modifié entre 10° à 85° [7]. Pour créer des renforts fibreux à forme complexe, tels que les pales d'une turbine à gaz, des fourches de vélo et les collecteurs d'entrée d'air des moteurs à combustion, la trajectoire des chariots doit pouvoir être modifiable.

Durant les années 1970, plusieurs mécanismes de transfert de chariots ont été inventés afin de modifier la trajectoire de ces derniers [4]. Reichel (1975) [24] et Berger (1975) [25] ont développé des commutateurs rectilignes similaires permettant de transférer un chariot d'un groupe de roues à encoches à un autre. Ce mécanisme a permis la fabrication de filets sans nœuds. Bock [26] a proposé un mécanisme de transfert, similaire à celui d'un aiguillage ferroviaire, placé entre chaque roue à encoches, permettant de transférer ou non le chariot d'une roue à une autre libérant ainsi partiellement la trajectoire des chariots. Cette idée a par la suite été reprise par Laourine [27] et Schneider [28, 29]. Les sections suivantes présentent plus en détail l'invention semblable à l'aiguillage ferroviaire ainsi que les métiers à tresser permettant la fabrication de tresses à forme variables et tridimensionnelles.

2.3.2.1 Aiguillage ferroviaire

À partir de l'invention de Bock [26], Laourine (2000) [27] et Schneider (2000) [28, 29] ont développé un métier à tresser à trajectoire variable en introduisant un module similaire à un aiguillage ferroviaire placé entre chaque roue à encoches. Ce dernier possède un ensemble de deux trajectoires. La Figure 2.5 illustre schématiquement les deux trajectoires possibles. La Figure 2.5a) présente une trajectoire en forme de X qui permet le transfert d'un chariot entre deux roues adjacentes. La Figure 2.5b) présente une trajectoire constituée de deux arcs de cercle qui introduisent une discontinuité de la trajectoire entre les roues adjacentes. Cette discontinuité empêche le transfert du chariot. Dans les deux cas, le trait noir opaque illustre le trajet du chariot. Lorsque la seconde trajectoire est sélectionnée, comme à la Figure 2.5b), le chariot tourne autour de la même roue.

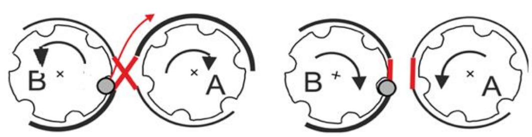

a) b)

Figure 2.5 : Illustration des deux positions possibles du module a) transfert b) aucun transfert [30]

De plus, chaque roue à encoches est équipée d'un système de frein et d'embrayage pour être en mesure de s'arrêter et de tourner de façon indépendante. Chaque module est aussi contrôlé de façon indépendante. En modifiant la position de chaque module, la trajectoire des chariots peut ainsi être modifiée. Toutefois, lorsqu'un chariot se retrouve par-dessus un module, ce dernier ne peut pas changer de position [31]. De plus, deux chariots ne peuvent être transférés simultanément d'une roue à une autre par l'entremise du même module. Il faut donc prévoir des encoches libres afin d'assurer le transfert de chariots entre deux roues. Par ailleurs, la machine doit s'arrêter complètement avant d'effectuer un changement de position du module. En effet, les roues à encoches ne peuvent tourner durant l'activation du module. Le procédé est donc séquentiel.

Puisque le procédé de fabrication utilise des roues à encoches pouvant accueillir plusieurs chariots, ces derniers ne peuvent se déplacer de façon complètement indépendante. Lorsqu’une roue tourne, la position de tous les chariots sur cette dernière est affectée. En outre, la programmation et le contrôle d’une telle machine sont très complexes [31].

Dans le but de rendre le procédé plus fluide, une étude sur la grosseur des roues a été effectuée [32]. En agrandissant le diamètre des roues, le chariot parcourt une plus grande distance. Le module possède ainsi suffisamment de temps pour changer de position avant qu’un chariot se retrouve par-dessus. Ceci permet d’éliminer les arrêts occasionnés par l’activation des modules. Néanmoins, cette approche possède une limite. Pour déplacer les chariots à une plus grande vitesse, le diamètre des roues à encoches doit augmenter en conséquence.

2.3.2.2 La fourche rotative

Mungalov et Bogdanovich (2002-2004) [33-37] ont développé un mécanisme permettant le transfert simultané de deux chariots entre deux roues à encoches adjacentes. Ce mécanisme est présenté à la Figure 2.6. La Figure 2.6a) présente la roue à encoches. La Figure 2.6b) présente le chariot. La Figure 2.6c) présente la fourche rotative, tandis que la Figure 2.6d) présente l’assemblage des trois composants. Une fourche rotative est positionnée entre chaque roue. Elle est actionnée de façon indépendante. Elle peut accommoder deux chariots à la fois. Une fois actionnée, elle effectue une rotation de 180°. En pivotant, la fourche entraîne les deux chariots placés de chaque côté de cette dernière. Après la rotation, les chariots ont échangé de position et ils se retrouvent sur une nouvelle roue à encoches. Lorsque la fourche reste immobile, les chariots ne peuvent être transférés. Ils tournent donc autour de la même roue à encoches. Cette innovation permet d’occuper toutes les encoches d’une roue créant ainsi des tresses avec beaucoup plus de fil. Par ailleurs, en actionnant la rotation des fourches, la trajectoire des chariots peut être modifiée.

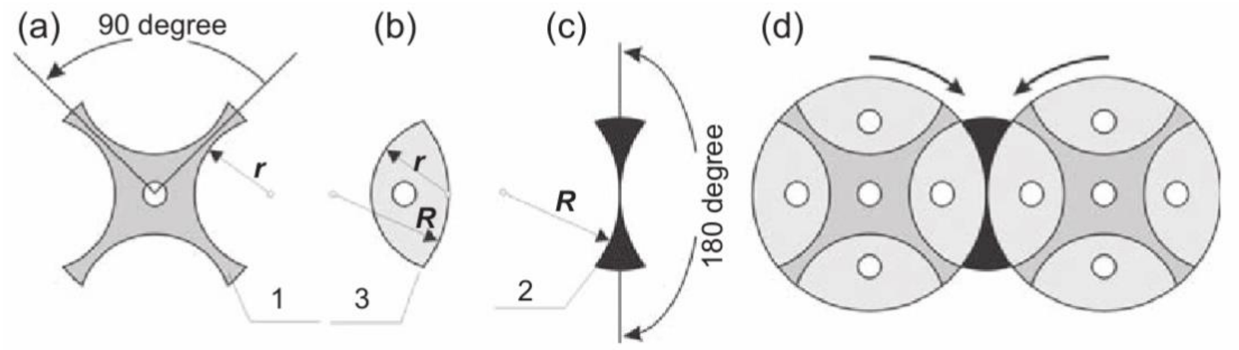

Figure 2.6 : Les différentes parties du système à fourche rotative a) roue à encoches b) chariot c) fourche rotative d) assemblage du système [4].

Toutefois, le procédé reste un procédé pas à pas. Les roues doivent être immobiles pour effectuer une rotation de la fourche. De plus, un arrêt de la machine ainsi qu'une intervention manuelle de l'opérateur sont requis pour ajouter ou retirer des bobines de fil contribuant à la formation de la tresse [37]. Par ailleurs, puisque ce type de métier à tresse utilise des roues à encoches sur lesquelles reposent plusieurs chariots, les déplacements de ces derniers ne sont pas indépendants. En outre, l'addition d'un mécanisme de transfert indépendant ajoute un niveau de complexité dans la programmation et le contrôle d'une telle machine et rend difficiles la conception et la fabrication de nouveau produit tressé [38].

Cette technologie a été reprise par Schreiber [39]. Il a agencé les roues à encoches sur le plan de travail selon un arrangement hexagonal compact. Il a également augmenté le nombre d'encoches par roue. Ceci lui a permis de minimiser l'empreinte du plan de travail tout en augmentant le nombre de chariots.

2.3.2.3 Métiers à tresser 3D divers

Il existe également différents types de métiers à tresser permettant la fabrication de tresse 3D tout en ayant une trajectoire de chariots fixe. Parmi ceux-ci, on retrouve les machines circulaires 3D et les machines cartésiennes.

La Figure 2.7 présente le plan de travail d'une machine circulaire 3D. La Figure 2.7a) illustre le plan de travail complet, tandis que la Figure 2.7b) présente un agrandissement d'une section du plan de travail. Chaque trajectoire est également illustrée et numérotée par la lettre P. Les machines circulaires 3D fonctionnent de façon semblable aux machines traditionnelles. Elles sont équipées de roues à encoches et la trajectoire des chariots est rainurée sur le plan de travail. Cependant, les roues à encoches forment plusieurs cercles concentriques de différents diamètres. La trajectoire relie chacun de ces cercles. Chaque cercle permet la fabrication d'une tresse tubulaire. Puisque les chariots sont en mesure de traverser les couches adjacentes, le résultat final est une tresse tubulaire 3D [40].

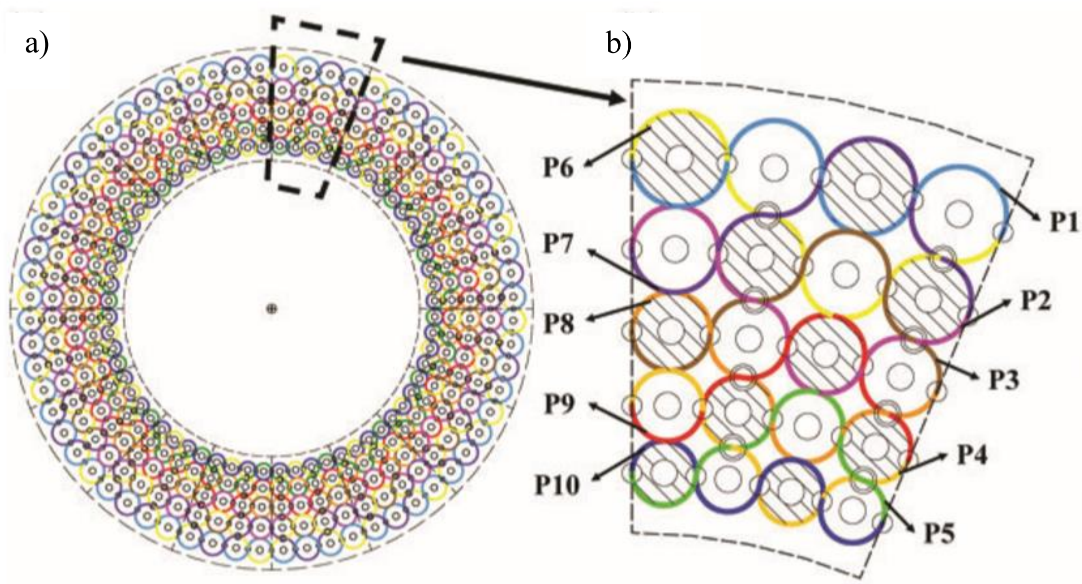

Figure 2.7 : Machine circulaire 3D a) plan de travail complet b) agrandissement d'une section du plan de travail. Les trajectoires des chariots sont énumérées et dénotées par la lettre P [5].

La Figure 2.8 présente schématiquement le plan de travail d'une machine cartésienne. Chaque cercle représente un chariot sur le plan de travail. Ces derniers sont placés selon un arrangement de lignes et de colonnes. La Figure 2.8a) illustre la position initiale des chariots. Les lettres b) – e) de la Figure 2.8 présentent les séquences de déplacement des chariots. Les machines cartésiennes confèrent aux chariots des trajectoires rectilignes uniquement. Tous les chariots sur une même ligne ou sur une même colonne se déplacent simultanément et dans la même direction. Les lignes choisies sont déplacées d'un incrément prédéfini. Les colonnes sont par la suite déplacées à leur tour [41]. Le cycle recommence en croisant ainsi les fils.

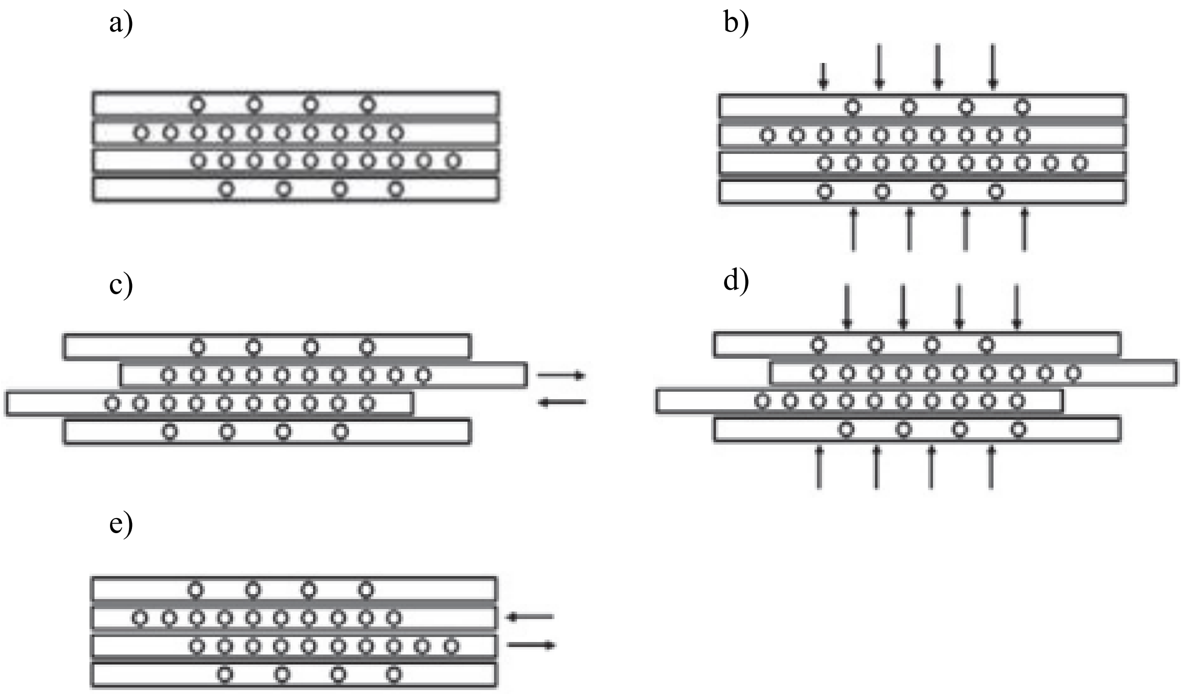

Figure 2.8 : Représentation du plan de travail d'une machine cartésienne. Chaque cercle représente un chariot a) position initiale des chariots b)-e) séquences de déplacement des chariots b) mouvement rectiligne des colonnes c) mouvement rectiligne des lignes d) mouvement rectiligne des colonnes e) mouvement rectiligne des lignes [42].

Le Tableau 2.1 résume les différents types de métiers à tresser. Les avantages et désavantages de chacun sont présentés. On y retrouve également une figure rappelant le principe de fonctionnement de chaque métier à tresser.

Tableau 2.1 : Résumé des métiers à tresser ainsi que leurs avantages et désavantages.

Types de métiers à tresser	Avantages	Lacunes
Traditionnel 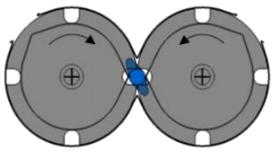	Simple à utiliser	- Trajectoire fixe rainurée dans le plan de travail - Réorganisation du plan de travail pour changer la forme de la tresse - Trajectoire des chariots non modifiable
Aiguillage ferroviaire  a) b)	Trajectoire de chariots modifiable	- Un chariot à la fois peut se faire transférer entre deux roues - Complexité du contrôle par l'ajout d'un mécanisme de transfert indépendant - Contrôle partiel sur la position des chariots
Fourche rotative 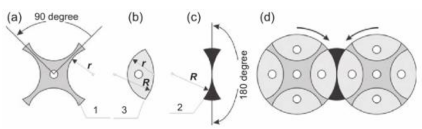	- Trajectoire des chariots modifiable - Transfert de deux chariots simultanément entre deux roues : fabrication de tresse avec un plus grand nombre de fils	- Complexité du contrôle par l'ajout d'un mécanisme de transfert indépendant - Contrôle partiel sur la position des chariots - Arrêt et intervention humaine pour rajouter ou enlever des chariots lors du procédé
Traditionnel 3D 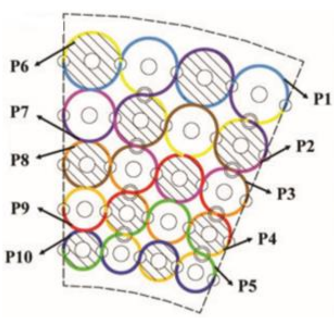	- Simple à utiliser - Fabrication de tresses 3D	- Trajectoire fixe rainurée dans le plan de travail - Trajectoire des chariots non modifiable
Cartésien 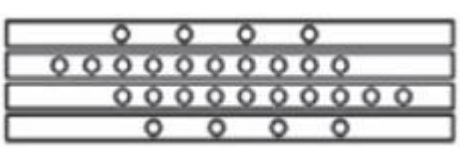	- Simple à utiliser - Fabrication de tresses 3D	Trajectoire des chariots non modifiable

2.4 Détection des collisions

Comme mentionné à la section 2.3.1, peu d'études se sont penchées sur la détection des collisions entre chariots dans les machines à trajectoires fixes. Yu *et al.* [6] ont proposé une méthode permettant de vérifier si les chariots allaient rentrer en collision afin de valider l'arrangement des chariots. La méthode a été développée pour des tresses complexes obtenues en épissant des trajectoires de métiers à tresser traditionnels. Cela signifie que la configuration du plan de travail est composée de différentes trajectoires de tresses plates reliées entre elles pour former une tresse complexe. Chengjie *et al.* [23] ont développé un modèle mathématique permettant de valider l'arrangement des chariots en se concentrant sur les machines traditionnelles 3D permettant la fabrication de tresses à section transversale symétrique. Kyosev [22] a pour sa part modélisé les pièces critiques d'un métier à tresser. Ces dernières sont les roues à encoches, les chariots ainsi que les trajectoires rainurées dans le plan de travail. En modélisant chacune des pièces, le procédé de tressage peut désormais être modélisé. Par conséquent, les collisions des chariots peuvent être détectées par simulation. Toutefois, le temps de calcul devient un facteur limitant de cette méthode pour des machines à plus grandes échelles. Kyosev a par ailleurs appliqué sa méthode sur les métiers à tresser à trajectoires variables [22, 30]. Ceci lui a permis de détecter des collisions entre les chariots par simulation. Toutefois, aucune méthode n'est proposée pour éviter les collisions lorsqu'elles sont détectées.

CHAPITRE 3 OBJECTIFS DE RECHERCHE ET COHÉRENCE DES ARTICLES

3.1 Synthèse de la problématique

En résumé, les métiers à tresser traditionnels comportent une lacune majeure : la trajectoire des chariots est fixe et elle ne peut pas être modifiée au cours du procédé, ce qui limite la fabrication à des tresses à une seule structure uniforme. Les avancements technologiques permettent une modification de la trajectoire des chariots permettant ainsi la création de tresses complexes à géométries variables. Toutefois, ces avancements comportent encore des lacunes. En effet, le déplacement des chariots n'est pas complètement indépendant les uns des autres. À haute densité de chariot, plusieurs chariots se retrouvent sur la même roue à encoches. Lorsque cette dernière pivote, la position de chaque chariot se trouvant sur la roue est altérée. Le déplacement d'un chariot implique donc nécessairement le déplacement d'un autre. À ce jour, la modification de la trajectoire nécessite un mécanisme de transfert indépendant placé entre chaque roue à encoches rajoutant ainsi un niveau de complexité au contrôle et à la programmation des métiers à tresser. Il est aussi impossible de retirer ou d'insérer des bobines de fil dans le procédé de tressage sans intervention humaine et sans arrêter le procédé de fabrication.

De plus, déterminer l'arrangement des chariots d'un métier à tresser traditionnel demeure une tâche compliquée à réaliser. Bien que différentes méthodes aient été développées pour valider l'arrangement des chariots avant le procédé de fabrication, elles restent compliquées, coûteuses en temps de calcul ou sont spécifiques à un seul type de métier à tresser ou à une seule configuration du plan de travail. Aucune méthode permettant de valider l'arrangement des chariots n'est assez polyvalente et facilement mise en œuvre pour être utilisée sur n'importe quel métier à tresser.

Finalement, concernant les métiers à tresser à trajectoires variables, il n'existe aucune méthode permettant de prévenir les collisions lorsqu'elles sont détectées. Présentement, pour éviter une collision, l'arrangement des chariots doit être modifié manuellement avant le procédé de tressage. Donc, la flexibilité dans la trajectoire des chariots n'est pas exploitée à sa pleine capacité pour prévenir des collisions durant le procédé. Par conséquent, pour obtenir un processus sans collision, plusieurs essais-erreur sont encore nécessaires pour trouver un bon arrangement de chariots.

3.2 Objectifs de recherche

À la lumière de la revue de littérature et de la problématique soulevée à la section précédente, l'objectif principal de recherche est de :

Développer un procédé de fabrication pour les tresses 3D permettant de positionner en tout temps et de façon indépendante les chariots supportant les bobines de fil.

Trois sous objectifs découlent de l'objectif général.

1. Développer un algorithme pour la détection de collisions entre les chariots pouvant être facilement mis en œuvre peu importe le métier à tresser.
2. Concevoir et fabriquer un métier à tresser permettant un déplacement indépendant des chariots.
3. Développer un algorithme permettant d'éviter les collisions dans les métiers à tresser à trajectoires variables.

3.3 Cohérence des articles

Les sous-objectifs de recherche ont été atteints. Ils sont présentés sous la forme d'articles scientifiques au chapitre 4, 5 et 6.

Le chapitre 4 présente le premier sous objectif. Les résultats sont présentés sous la forme d'un article scientifique publié dans *The International Journal of Advanced Manufacturing Technology* en mars 2023. L'article est intitulé « Application of graph theory for detecting carriers' collisions in braiding machines ». Il présente une nouvelle méthode, basée sur la théorie des graphes, permettant de détecter les collisions entre les chariots. La méthode proposée offre une solution simple et unique pour la détection des collisions entre les chariots, et ce, peu importe la configuration du plan de travail. Deux études de cas, une simple et une complexe, sont présentées pour démontrer le fonctionnement ainsi que la polyvalence de la méthode.

Le chapitre 5 présente le deuxième sous objectif sous la forme d'un article scientifique publié dans *CIRP Journal of Manufacturing Science and Technology* en février 2021. L'article est intitulé « 3D printing process for textile composites ». Il présente un nouveau concept de métier à tresser 3D. Les lignes directrices de conception ainsi que le principe de fonctionnement du concept y sont détaillés. Une validation expérimentale est également présentée. De plus, une comparaison quantitative est effectuée avec les différents métiers à tresser existants, ce qui permet de conclure sur les avantages du nouveau concept.

Le chapitre 6 présente le troisième sous objectif. Les résultats sont présentés sous la forme d'un article scientifique, intitulé « Application of graph theory for preventing carriers' collisions in variable path braiding machines », publié dans *The International Journal of Advanced Manufacturing Technology* en avril 2023. Il présente une nouvelle méthode, basée sur la théorie des graphes, permettant de prévenir les collisions entre les chariots dans les métiers à tresser à trajectoires variables. Pour ce faire, des délais sont introduits dans le déplacement des chariots, ce qui permet d'exploiter la flexibilité du déplacement des chariots pour éviter une collision.

CHAPITRE 4 ARTICLE 1 : APPLICATION OF GRAPH THEORY FOR DETECTING CARRIERS' COLLISIONS IN BRAIDING MACHINES

P.Assi[1,2], S. Achiche[2], L. Laberge Lebel[1]

[1]Advanced Composites and Fibers Structures Laboratory (ACFSlab), High Performance Polymer and Composite Systems (CREPEC), Polytechnique Montreal, 2500 ch. Polytechnique, Montreal, Qc, Canada, H3T 1J4

[2]Laboratoire de Conception de Systèmes Intelligents et Mécatroniques(CoSIM), Polytechnique Montreal, 2500 ch. Polytechnique, Montreal, Qc, Canada, H3T 1J4

Publié dans *The International Journal of Advanced Manufacturing Technology* – 8 mars 2023

Abstract

Traditionally manufactured for ropes and fishing lines, braids are now found in structural composite parts used in the transportation industries and the medical sector. Braiding machines are increasing in size and complexity. However, engineers mostly rely on expertise and on trials and errors to select a collision-free carrier arrangement, which is inefficient in terms of both time and resources. In this paper, we propose a method, based on graph theory, to detect collisions between carriers for any braiding machine configuration and for any number of carriers. To do so, the braiding machine is modeled as a graph. Each horngear is represented by a face and each horngear slot is represented by a vertex. A collision detection algorithm is developed, which validates or invalidates the proposed carrier arrangement. Two case studies are carried out to demonstrate the algorithm. The first one is carried out on a traditional maypole braiding machine, while the second one is done on a T-shape braider. The T-shape braider has a more complex configuration with horngears having different number of slots and diameters. The developed solution is an efficient method to detect collisions based on any carrier arrangement.

4.1 Introduction

Reducing greenhouse gases is a crucial challenge in the context of global warming. Using lightweight composite materials to improve weight efficiency of transport vehicles, such as airplanes, cars, and drones, is an integral part of the solution. Composite materials offer excellent strength and stiffness to weight ratio, which explains its climbing use over the past two decades in the aviation industry. The volume percentage of aircraft attributed to composite materials has reached 80% [2], while the mass percentage has jumped from 15% to 53% [1].

Composites are a combination of at least two components forming a heterogeneous material [3]. Textile fabrics, such as braids, weaves or unidirectional fibers, embedded in a polymer resin are commonly used for composite materials. Braids have demonstrated good crush resistance properties [43, 44]. Additionally, the intertwined fibers of a braid limits crack propagation, thus, offering good fatigue properties [7, 13]. Moreover, braided preforms can be produced to a near net shape of the final product, which is more difficult to realize with laminated processes. Laminated processes consist of creating a composite structure by stacking plies, where each ply is composed of fibers embedded in a polymer resin [45]. Traditionally manufactured for climbing ropes and fishing lines, braids are now found in structural composite parts used in the transportation industries and the medical sector [15]. Examples of these elements are aircraft fuselage frames, beams, marine propellers, skin structures and orthopedic and hip prosthesis [5-7, 46, 47].

Braids are formed by intertwining yarns. A yarn is a bundle of fibers, which represents a strand within the braid. In a typical braiding machine, each yarn spool is mounted on a spool tensioner, which keeps the yarn under tension throughout the braiding process. The spool tensioners are each attached to an individual carrier. The carriers are moved around a bedplate by rotating horngears, which have slots housing the carriers. The carriers follow a fixed path, called track, which is grooved into the machine's bedplate. Each carrier is equipped with guiding foot that is inserted into the track, which forces the carrier to follow the given track. Intersecting tracks force the carriers' path to cross, thus creating the braid. Figure 4.1a) present a top view of a maypole braiding machine bedplate. The braider is composed of 12 horngears. Ten spool tensioners are shown. Note that there are also 11 carriers shown, which are not coupled to a spool tensioner. Figure 4.1b) presents a close-up view of two adjacent horngears, where a track intersection can be visualized.

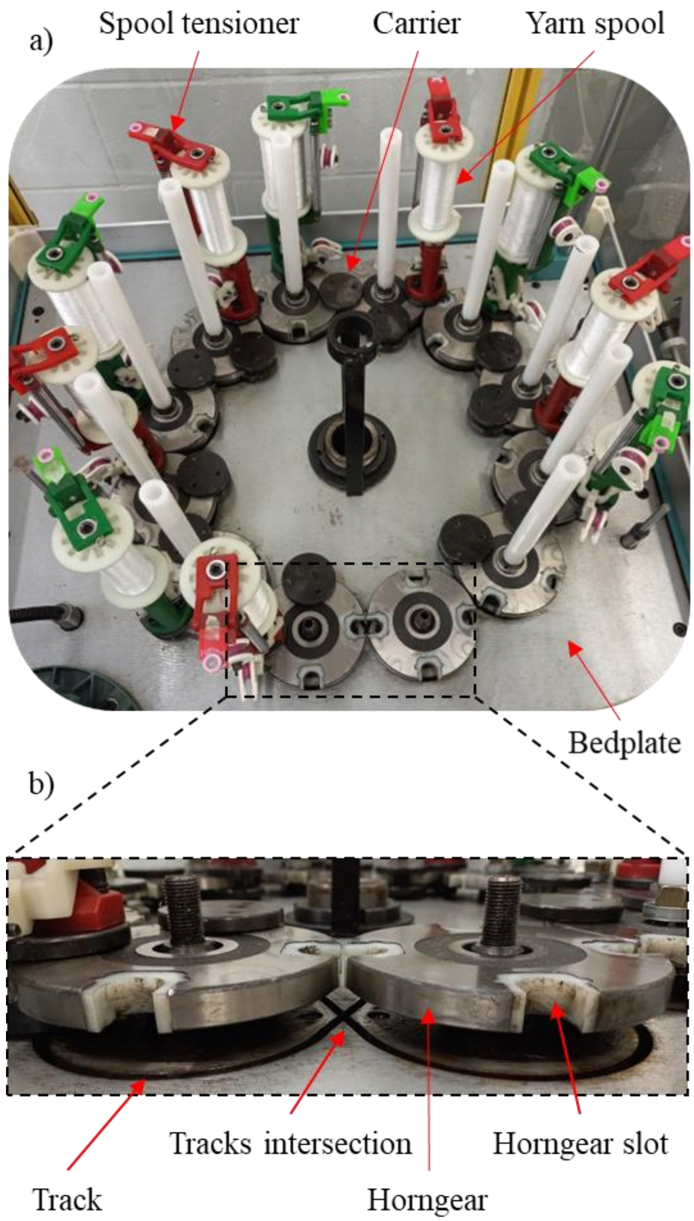

Figure 4.1 : a) Top view of a maypole braiding machine bedplate b) Close-up view of two adjacent honrgears and a track intersection.

The track and horngears arrangement is referred to as the bedplate's configuration. The carriers' placement with respect to the bedplate's configuration is referred to as the carrier arrangement. The bedplate's configuration and the carrier arrangement have a direct impact on the braid's architecture and the topology of its yarns. In addition, the mechanical properties of a braided product are linked to its architecture [9]. However, in the literature, there are very few design guidelines for bedplate's configuration and carrier arrangement of braiding machines, specifically for creating complex braids [6, 21]. Complex braids are generally designed for a specific application. Nonetheless, the quality of the design is highly dependent on the skills and the expertise of the designer. Tada et al. [21] have proposed bedplate's configurations for manufacturing square, rectangular and L-shaped braids. However, the methodology used to determine the carrier arrangement was not discussed.

The carrier arrangement is a key aspect to consider when designing a braid. The carriers must be placed in a specific manner to avoid collision during the braiding process. Collisions occurs when two carriers find themselves simultaneously at a track intersection. Figure 4.2 and Figure 4.3 illustrate the importance of the carrier arrangement. Two horngears, with four slots each, are placed according to an eight-shaped track. Horngears rotate in opposite directions. The green and orange circles represent a carrier. Figure 4.2 illustrates a collision caused by a wrong carrier arrangement. Figure 4.2a) shows the initial position of the carriers. Figure 4.2b) presents the intermediate position while Figure 4.2c) illustrates the collision at the track intersection. On the other hand, Figure 4.3 presents a collision-free carrier arrangement. Figure 4.3a) and Figure 4.3b) present the initial and intermediate positions of the carriers, while Figure 4.3c) presents a collision-free transfer of carriers between horngears.

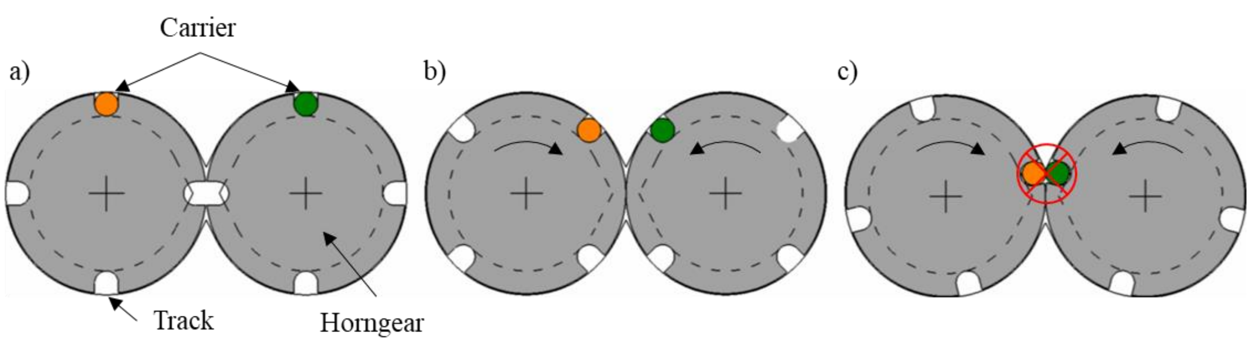

Figure 4.2 : Carrier arrangement causing a collision a) Initial position b) Intermediate position c) Carrier collision.

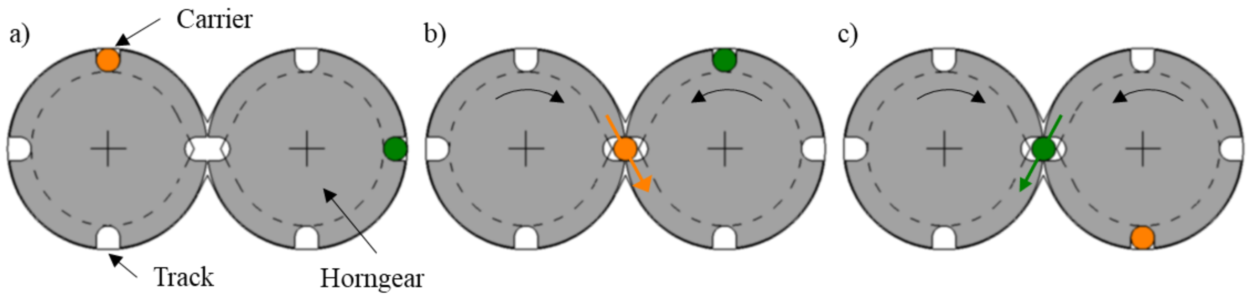

Figure 4.3 : Collision-free carrier arrangement a) Initial position b) Intermediate position c) Collision-free transfer.

Finding the proper carrier arrangement becomes more complex when increasing the scale of the braiding machine. Nonetheless, the theoretical background regarding the carrier arrangement is underdeveloped. Engineers rely mostly on expertise and on trial and error to properly place the carriers in order to avoid any collision during the braiding process [22, 23]. This method can be costly and highly inefficient in terms of time and resources.

A limited number of studies have tackled the carrier arrangement and collision issues. Yu et al. [6] proposed a method that can verify whether carriers will collide based on the number of horngear's slots in order to find a collision-free carrier arrangement. They focused on complex braided preforms obtained by splicing traditional flat braid machines tracks. This means that the bedplate's configuration is composed of flat braid tracks connected to each other to form a complex shape, such as a T, U, H, or a cross shape. Chengjie et al. [23] developed a mathematical model for the carrier arrangement of square rotary braiding machines. These types of machines are used to fabricate multi-layer braids, where layers are interlocked with each other's. Chengjie et al. [23] focused on complex braids having a symmetrical cross-section, such as rectangular or a C-shaped braid. Tubular or square shaped braids were not considered in the model. Kyosev [22] modeled the key braiding machine parts, which are the horngears, the carriers, and the tracks. He also modeled their interactions, which allowed him to simulate the braiding process, and thus, simulate the carriers' motion. Consequently, collisions can be detected through simulation before the actual trials. A collision is detected when the distance between carriers is too small. However, this method can be computationally intensive for large scale braiding machines where the distance between a vast number of carriers has to be verified.

Determining a collision-free carrier arrangement remains a complicated task. Although different methods have been developed to validate the carrier arrangement in the pre-production stage, most of them are either complicated, computationally intensive or are specific to a single type of braiding machine or bedplate's configuration. No method that can easily be implemented and versatile enough to be used for any type of braiding machines has yet been developed.

Collision detection is not limited to the field of braiding. This concept is shared by different fields of application, such as autonomous vehicles, robotics, communication networks and transportation networks. Graph theory, which is a branch of mathematics that studies the relation between objects within a network [48], has been utilized to detect and manage collisions within these networks. For example, graph theory has been used in transportation networks for traffic management and route planning [49, 50]. It has also been used for obstacle avoidance and path planning of autonomous mobile robots [51], as well as preventing identification collisions when using multi-reader radio frequency identification systems [52]. However, it has yet to be applied for detecting collisions in braiding machines.

The aim of this study is to develop a graph theory-based algorithm to detect collisions, which can be used for any kind of braiding machine and bedplate's configuration.

4.2 Graph definition

A graph $\boldsymbol{G}$ is defined by set of vertices $\boldsymbol{V}$ and set of edges $\boldsymbol{E}$, such as $\boldsymbol{G} = (\boldsymbol{V}, \boldsymbol{E})$. Each edge of the graph connects a pair of vertices [53]. A graph can be directed or undirected. In a directed graph, an orientation is assigned to each edge. The orientation is generally depicted by an arrow on the edge. For example, in a road network represented by a graph, the orientation of the edge could represent the flow of traffic on a one-way street. Moreover, in a braiding machine bedplate's configuration represented by a graph, the orientation of the edge could represent the direction in which the carrier moves along a track. On the other hand, in an undirected graph, edges have no orientation. For example, an undirected edge could represent a two-way street in the graph of a road network. Figure 4.4 presents two different graphs. Figure 4.4a) presents an undirected graph while Figure 4.4b) presents a directed graph.

Graphs can be weighted or un-weighted. In a weighted graph, a real number is associated to each edge. For example, in a road network, the weight of the edge could represent the distance between its two connected vertices, the time required to travel the edge or the displacement cost from one vertex to the other. On the other hand, in the unweighted graph, edges do not have an associated real number. Figure 4.4a) illustrates a weighted graph while Figure 4.4b) presents an unweighted graph.

Faces within a graph are defined as closed regions delineated by a set of vertices and edges. For example, the graph of Figure 4.4a) has two faces. Each face is identified by a circled number.

A cycle is defined as a path where the first vertex is the same as the last vertex. Additionally, the first vertex is the only one that is repeated. For example, the graph of Figure 4.4b) has two cycles. Since the graph is directed, the cycles have a direction: clockwise or counterclockwise. The graph in Figure 4.4b) has one clockwise cycle, which is depicted in orange, and one counterclockwise cycle, which is depicted in green.

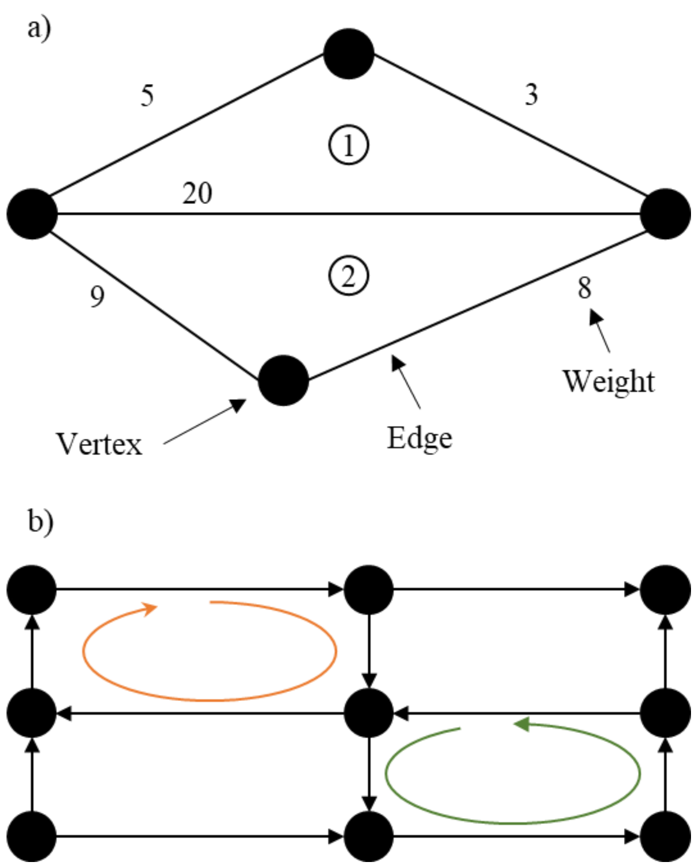

Figure 4.4 : Undirected weighted graph. Faces of the graph are identified by circled number b) Directed unweighted graph. A clockwise cycle is illustrated in orange. A counterclockwise cycle is illustrated in green.

4.3 Graph modeling of braiding machines bedplate configuration

In the graph of a braiding machine bedplate's configuration, horngears are represented by a face, while edges represent sections of the track that carriers can move along. Additionally, vertices represent horngears' slots.

In a traditional braiding machine, each horngear rotates in the opposite direction of its neighbors. The horngear rotational direction imposes the direction of the carriers' displacement, which cannot be modified during the braiding process. Therefore, during the braiding process, carriers can only move in a unilateral direction along the track. Consequently, the graph must be directed to represent the direction of the carriers' displacement.

The graph of the bedplate's configuration can be created according to the following steps:

1. Rotate the horngears until they are positioned for a carrier transfer. Slots of adjacent horngears should be positioned near the tack intersection, as shown in Figure 4.5.
2. Attribute vertices to the horngears slots. Slots near an intersection share a common vertex. A shared vertex indicates a track intersection.
3. Connect each vertex to the vertex representing its adjacent slot within the same horngear. Doing so, faces are created, each representing a horngear.
4. Attribute, for each face, the direction of the edges, according to the horngear rotational direction. If the horngear rotates in a clockwise direction, the cycle within the face will be clockwise. On the other hand, if the horngear rotates in a counterclockwise direction, the cycle within the face will be counterclockwise.
5. Attribute a weight for each edge if the graph must be weighted.
6. Determine the different tracks.
7. Allocate a number to each vertex.

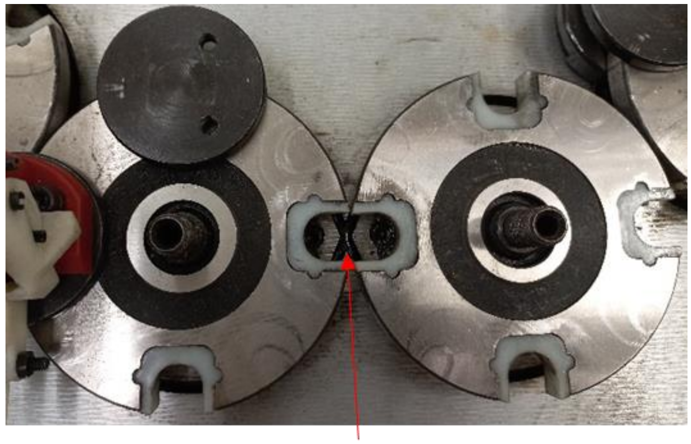

Figure 4.5 : Horngears positioned for a carrier transfer.

For example, let's take a maypole braiding machine composed of 12 identical horngears with 4 slots each, similar to Figure 4.1a). The horngears are placed in a circle. Step 1 is shown in Figure 4.6a). Each horngear is placed for a carrier transfer. Slots from adjacent horngears are near the track intersection. The track intersection is located between adjacent horngears, as shown in Figure 4.5. Step 2 is shown in Figure 4.6b). Each slot is represented by a vertex. The slots near a track intersection are represented by a common vertex. This common vertex indicates the track intersection, i.e., the carrier transfer point between horngears. Step 3 is presented in Figure 4.6c). Vertices from a same horngear are connected by edges. The vertices are connected according to the slot pattern of the horngear. This means that a given vertex is linked to the vertex representing its adjacent slot within the horngear. Step 4 is presented in Figure 4.6d). The rotational direction of each horngear is specified by an arrow. Therefore, the direction of each edge can be determined. The horngears are mechanically linked, by a gear system, to the same motor. Consequently, every horngear has the same tangential velocity. Therefore, the graph is unweighted. Step 6 is shown in Figure 4.6e), which illustrates the two tracks on the bedplate. Traveling along the black track, carriers move counterclockwise around the bedplate, while traveling along the magenta track, the carriers move clockwise around the bedplate. The last step is shown in Figure 4.6f), where each vertex is numbered.

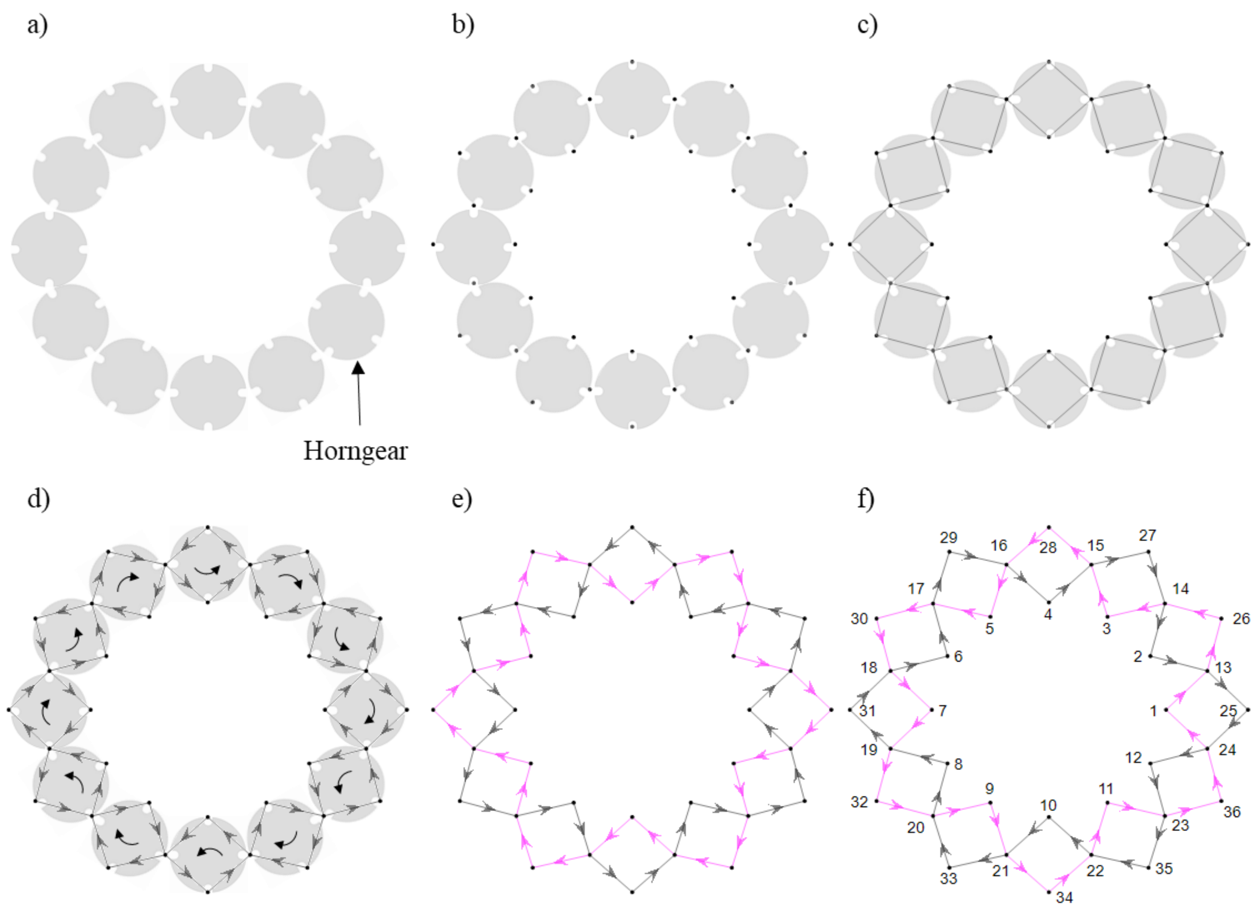

Figure 4.6 : Steps for creating the graph of a bedplate's configuration a) Step 1 b) Step 2 c) Step 3 d) Step 4 e) Step 6 f) Step 7.

4.4 Collision detection algorithm

The carrier's path can be defined by a series of vertices, where each vertex is adjacent to the next and edges between vertices have the same direction. Vertices belonging to the path denote different positions of the carrier at a given time of its displacement. One vertex can belong to more than one path, meaning that multiple paths can share the same vertex. However, if two carriers find themselves simultaneously on the same vertex, a collision occurs since both carriers will be at the same place at a given time, as depicted in Figure 4.2c).

Algorithm 4.1 detects carrier collisions. The inputs of Algorithm 4.1 are the bedplate's configuration graph, the number of carriers and the path of each carrier. It returns an error message if a collision between carriers is detected.

The path of a carrier is determined according to the track it is moving along. The first vertex of the path represents its starting position on the bedplate. For example, let's take a maypole braiding machine composed of 12 horngears, which its bedplate's configuration graph is illustrated in Figure 4.6f). Figure 4.7 presents the starting position of one carrier. The carrier is placed on vertex number 34 and is depicted by a magenta circle. The carrier is placed on the magenta track. Thus, it moves counterclockwise around the bedplate. According to the magenta track, the path of the carrier is described by Equation (4.1), which is the path taken by the carrier to travel around the bedplate until it comes back to its initial position.

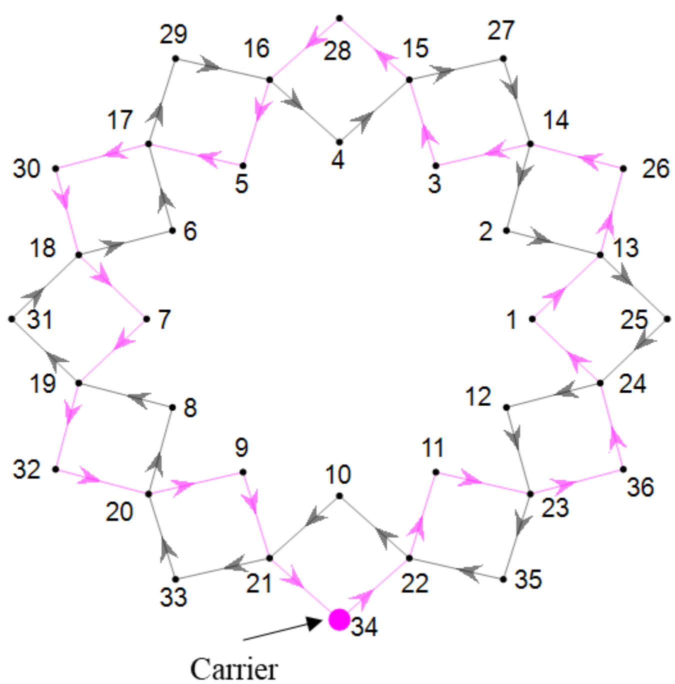

Figure 4.7 : Graph of a maypole braiding machine bedplate's configuration where the starting position of one carrier is shown. The carrier is placed on the magenta track. Therefore, the carrier moves counterclockwise around the bedplate. The carrier is depicted by a large magenta circle.

$$P = \{34\ 22\ 11\ 23\ 36\ 24\ 1\ 13\ 26\ 14\ 3\ 15\ 28\ 16\ 5\ 17\ 30\ 18\ 7\ 19\ 32\ 20\ 9\ 21\ 34\} \qquad (4.1)$$

Collision detection is performed by analyzing each displacement step (DS) of the carriers' path. The path of a carrier is specified by a series of vertices. A displacement step is defined as the movement from one vertex to the next, with respect to the path. Therefore, a displacement step represents the carrier movement between two adjacent vertices. In the path from Equation (4.1), the first displacement step represents the movement from vertex number 34 to vertex number 22. Thus, at the end of the first displacement step, the carrier is now on vertex number 22. The second displacement step represents the movement from vertex number 22 to vertex number 11. Therefore, at the end of the second displacement step, the carrier is now on vertex number 11.

For a given displacement step, the occupied vertices are determined. An occupied vertex is a vertex on which a carrier is positioned. Afterward, the number of occupied vertices is compared to the number of unique occupied vertices. If both numbers are different, this indicates that at least two carriers are positioned on the same vertex simultaneously. Therefore, a collision is detected since at least two carriers are at the same place at a given time. This analysis is made for every displacement step of the carriers' path.

In Algorithm 4.1, lines 1 to 5 identify all occupied vertices for a given displacement step (DS), which are stored in the variable named *OccupiedVertices*. The collision detection is undertaken at line 6, where *OccupiedVertices* is checked for repeated values, i.e., repeated vertices.

Algorithm 4.1 : *Collision detection for braiding machines*

Inputs : Unweighted and directed Graph G defined by vertices (V) and edges (E), such as $G \coloneqq (V, E)$
$k \leftarrow$ number of carriers
Carriers' path $P \coloneqq \{P_1, \dots, P_k\}$ where elements of $P_i \in V$ for $i \in [k] \coloneqq \{1, \dots, k\}$

1: **for** $j \leftarrow 1$ **to** number of elements in P_i for $i \in [k]$ **do** ▷ j represents the DS number
2: OccupiedVertices $\leftarrow \{\}$
3: **for** $i \in [k]$ **do** ▷ i represents the path number
4: *OccupiedVertices* $\leftarrow$ *OccupiedVertices* $\cup P_{i,j}$
5: **end for**
6: **if** Length(OccupiedVertex) $\neq$ Length(Unique(OccupiedVertex)) ▷ Verify repeated vertices at each DS
7: **error** Collision detected
8: **end if**
9: **end for**

To demonstrate the algorithm, two case studies are carried out. The first one is conducted on a maypole braiding machine, which produces tubular braids. The second one is conducted on a braiding machine designed for producing T-shaped braids. The bedplate's configuration of such machines is more complex than the one of a maypole braiding machine. Therefore, the first case study is a simple case, which helps understand how Algorithm 4.1 works. The second case study is a complex one. It represents the range of complex cases and demonstrates the capabilities of Algorithm 4.1 to detect collisions.

4.5 Case Study #1: collision detection on a maypole braiding machine

The purpose of this case study is to demonstrate the working principle of Algorithm 4.1. It will automatically validate or invalidate a carrier arrangement, which is usually done by manual trial and error by the machine operator. Twelve carriers are considered for the fabrication of a 12 yarns tubular braid using a maypole braiding machine. Similar to the example from Figure 4.6, the braiding machine is composed of 12 horngears having four slots each. Figure 4.8a) presents an overlap of the machine bedplate's configuration and its graph. The rotational direction of each horngear is indicated by an arrow.

Algorithm 4.1 is used to validate the carrier arrangement. A collision-free process will confirm that the carrier arrangement is correct. Otherwise, it needs to be modified.

Figure 4.8b) presents the carrier arrangement of 12 carriers. Carriers are portrayed by colored circles. Six carriers are placed on the clockwise track, depicted in black circles, and six carriers are placed on the contour clockwise track, depicted in magenta circles. In the case of Figure 4.8b), a collision is detected at the first displacement step on vertex number 14. At the first displacement step, the carrier from vertex number 27 and the carrier from vertex number 26 will find themselves simultaneously on vertex number 14, resulting in a collision. Therefore, the carriers are wrongfully placed. The carrier arrangement must be modified and verified once again until no collisions are detected.

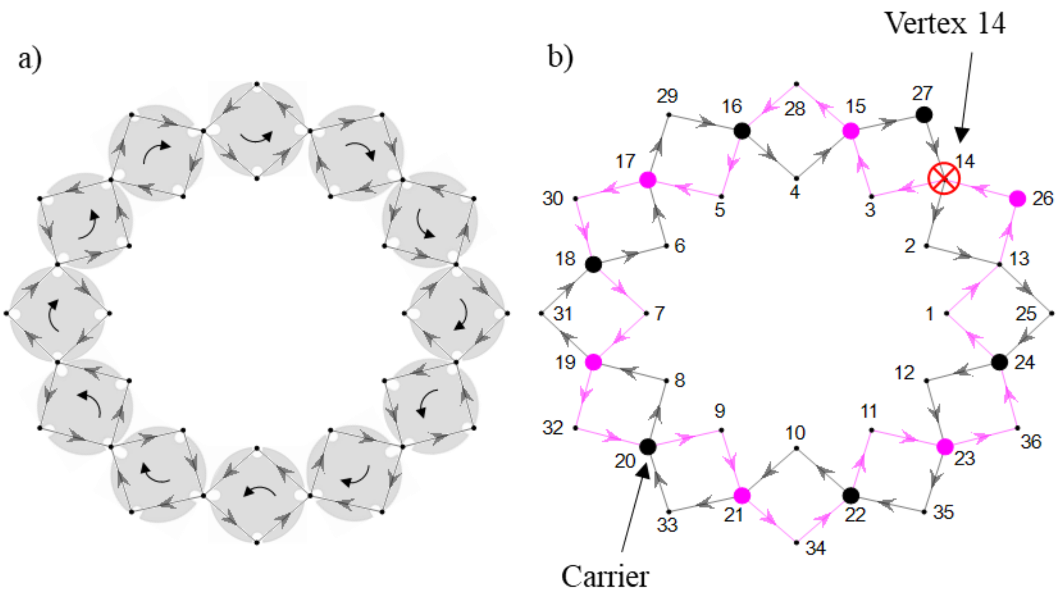

Figure 4.8 : a) Overlap of a 12 horngears maypole braiding machine's bedplate and its graph. The rotational direction of each horngear is indicated by an arrow. b) Carrier arrangement of 12 carriers. Carriers are represented by colored circles. The magenta carriers move along the magenta track, while the black carriers move along the black track. A collision will occur on vertex number 14 at the first displacement step.

Based on the carrier arrangement, the algorithm offers a simple method for detecting collisions, which does not require numerical modeling and simulation of the braiding process. Consequently, this method can be easily implemented.

4.6 Case Study #2: collision detection on a T-shaped braiding machine

The purpose of this case study is to demonstrate the versatility of Algorithm 4.1 as well as its ability to detect collisions. To do so, Algorithm 4.1 is used to automatically validate or reject the carrier arrangement of 24 carriers for the fabrication of a T-shaped braid [6]. The bedplate's configuration of a T-shape braider is more complex than a maypole braiding machine. The horngears are not identical: some have a larger diameter with a higher number of slots. In addition, the number of tracks is higher, which increases the likelihood of a collision. As a comparison, a maypole braiding machine has 2 distinct tracks, while the T-shape braider has four tracks.

The braiding machine is composed of 13 horngears arranged according to a T-shape, as shown in Figure 4.9a), which presents an overlap of the bedplate's configuration and its graph. Out of the 13 horngears, seven horngears have four slots, while six horngears have five slots. Since faces of the graph represent horngears and vertices represent the horngears' slots, faces representing horngears with five slots are composed of five vertices, while faces representing horngears with four slots are composed of four vertices. The shared vertex between faces represents the intersection of the tracks, i.e., the carrier transfer point between two adjacent horngears.

Horngears rotate in the opposite direction of their neighbors. The rotational direction of each horngear is indicated by an arrow on Figure 4.9a). This rotational direction, which dictates the direction of the carrier displacement, is fixed throughout the braiding process. Therefore, the graph is directed. Moreover, being mechanically linked to a single motor, each horngear has the same tangential velocity. The arc length between adjacent slots, measured on the horngear circumference, is identical for every horngear on the bedplate. This explains why horngears with a larger number of slots have a larger diameter. Therefore, the graph is unweighted.

The T-shaped braid is produced by splicing two flat braids perpendicular to each other. Yarns of both braids are intertwined to form a joint, hence creating the T-shaped braid. Thus, as shown in Figure 4.9a), the bedplate's configuration can be divided into two main branches: the horizontal branch and the vertical branch. A branch is defined as a set of adjacent horngears forming a straight line. Each branch produces a flat braid. The branches' intersection, where both flat braids are bonded, is also depicted in Figure 4.9a). Due to the bedplate's configuration, carriers are not transferred between branches during the braiding process. For example, a carrier moving along the vertical branch will stay on the vertical branch throughout the manufacturing process without ever being transferred to the horizontal branch.

Figure 4.9b) illustrates the four main tracks on the bedplate. Since each branch produces a flat braid, each branch is composed of two tracks. The magenta and black tracks form the horizontal branch. Carriers on the magenta track move from right to left, while carriers on the black track move from left to right. The orange and green tracks form the vertical branch. Carriers on the orange track move from bottom to top, while carriers on the green track move from top to bottom.

At the end of each branch, the carrier is forced to complete a full rotation around the horngear, which allows it to change tracks and move back up the branch. For example, at the end of the magenta track, the carrier cannot move further left into the branch. It is forced to move back toward the right direction. Therefore, the carrier is transferred from the magenta track to the black track until it cannot move further right into the branch. At this point, the carrier is transferred onto the magenta track. This cycle is repeated throughout the braiding process.

Collisions may occur within a branch where both tracks of the same branch intersect. Additionally, collisions may occur at the branches' intersections where tracks of different branches meet. Detecting collisions is more complicated since there are two types of collisions: within a branch or between branches. In the literature, both types of collisions are tackled as two separate problems [6, 23]. Each problem having its own mathematical model, which is specific to the bedplate's configuration. Algorithm 4.1 proposes a method that tackles both problems at once, regardless of the bedplate's configuration. In this case study, Algorithm 4.1 is used to validate the carrier arrangement of 24 carriers. A collision-free process will confirm that the carrier arrangement is correct. Otherwise, it needs to be modified.

Figure 4.10a) presents the carrier arrangement of 24 carriers. Carriers are portrayed by colored circles. There are 14 carriers placed on the horizontal branch, while 10 carriers are placed on the vertical branch. According to Algorithm 4.1, a collision will take place on vertex number 16 at the seventh displacement step. Figure 4.10b) to Figure 4.10f) depict the first five displacement steps. Figure 4.11 depicts the sixth displacement step, which represents the last displacement step before the collision on vertex number 16. As shown in Figure 4.11, carriers on vertex numbers 15 and 20 will collide at displacement step number seven. Therefore, the carriers are incorrectly placed in Figure 4.10a). The carrier arrangement must be modified to ensure a collision-free process.

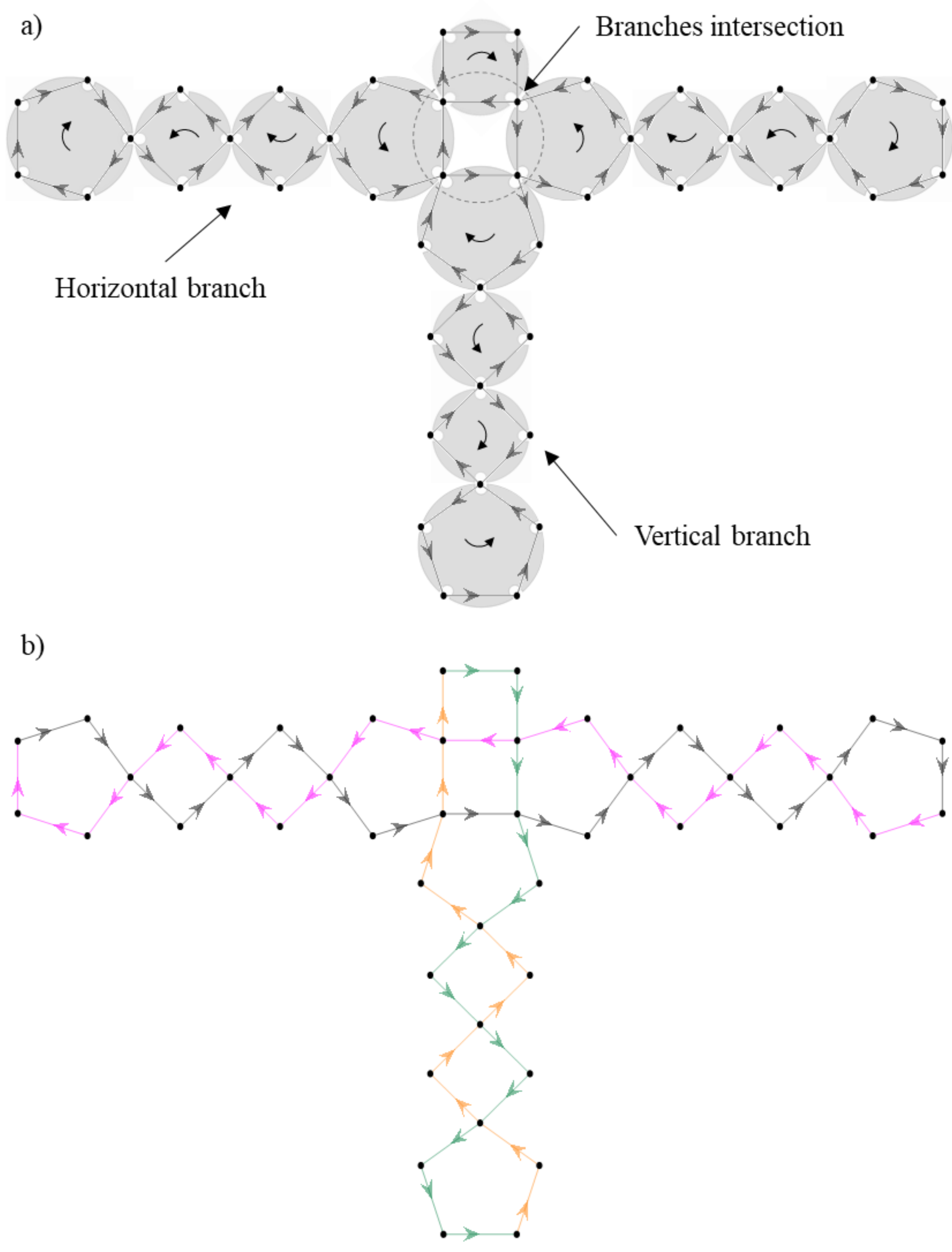

Figure 4.9 : a) Overlap of a 13 horngears T-shaped braiding machine bedplate's configuration and its graph. Out of the 13 horngears, seven have four slots and six have five slots. The rotational direction of each horngear is indicated by an arrow. b) Graph of a 13 horngears T-shaped braiding machine's bedplate. In black: the horizontal left to right track. In magenta:

horizontal right to left track. In green: the vertical top to bottom track. In orange: the vertical bottom to top track.

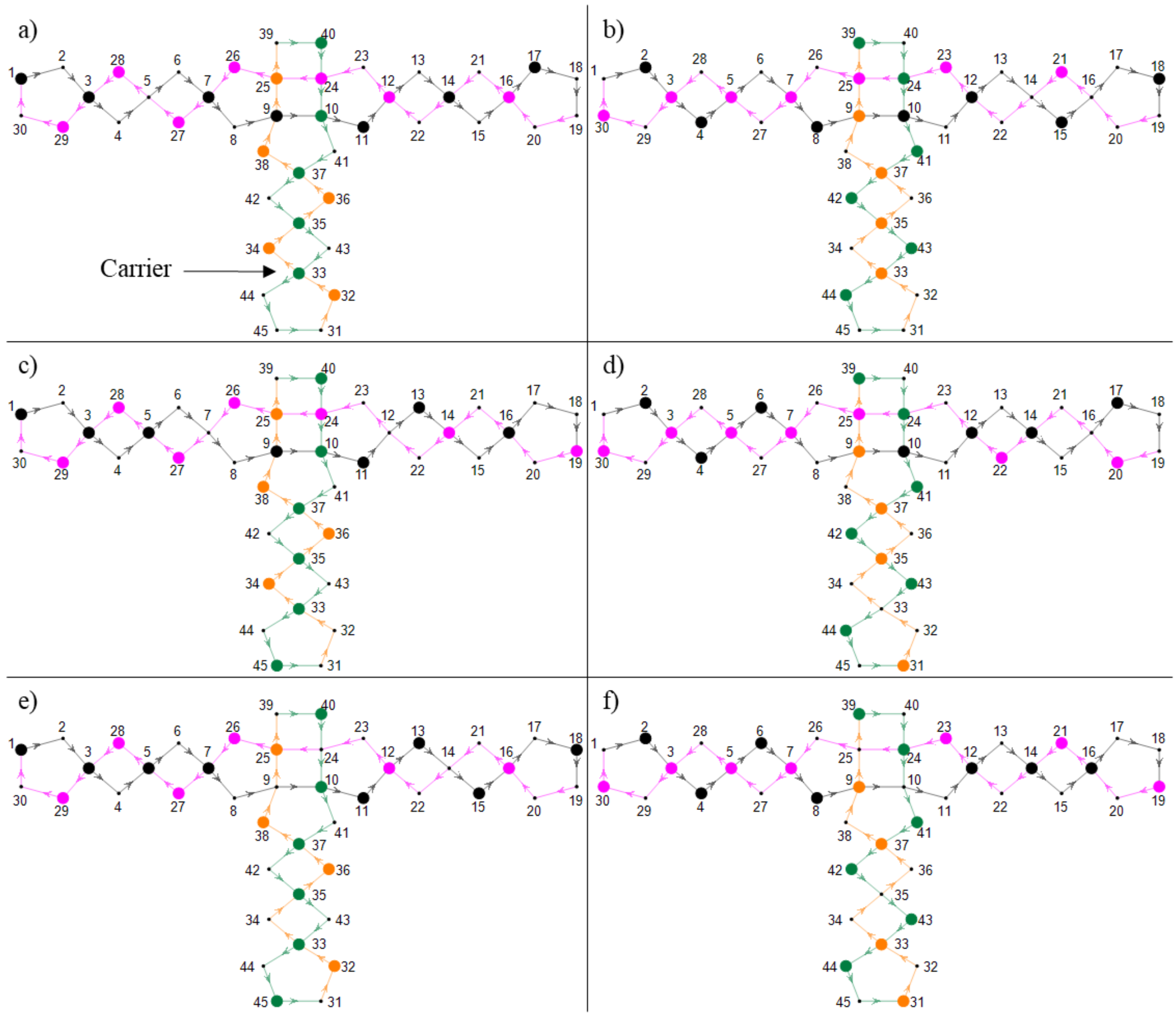

Figure 4.10 : First five displacement steps of the carrier's path. a) Carrier arrangement of 24 carriers. Carriers are represented by colored circles. Carriers move along their respective colored track. b) Displacement step 1 c) Displacement step 2 d) Displacement step 3 e) Displacement step 4 f) Displacement step 5.

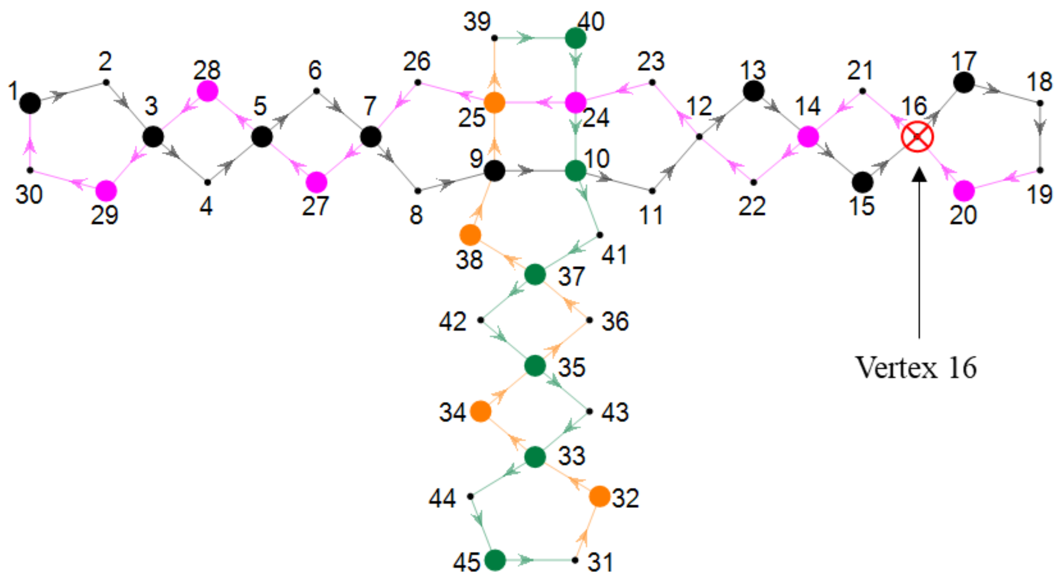

Figure 4.11 : Displacement step 6 of the carriers' path from carrier arrangement of Figure 5.10a). Displacement step 6 represents the last collision-free displacement step. At displacement step 7, two carriers collide on vertex number 16.

As shown in this case study, the developed algorithm offers a unique method that can be applied on any type of bedplate's configuration, which includes horngears with different diameters and different number of slots. In addition, the algorithm can take into consideration both types of collision: within branches and between branches.

4.7 Conclusion

We developed an algorithm that detects collisions between carriers based on the carrier arrangement using graph theory. To do so, the machine bedplate is represented by a graph, which is fed as input to the algorithm along with the number of carriers and the path of each carrier. To detect a collision, the algorithm checks for shared vertices between paths at each displacement step. Therefore, no carrier arrangement or machine bedplate's configuration could cause computational issues. Moreover, the algorithm can be used for any type of bedplate's configuration, which makes it a very useful tool for designing bedplates. Additionally, it can rapidly validate or reject the carrier arrangement before real life implementation. Two case studies were carried out to demonstrate the algorithm. The first one was conducted on a maypole braiding machine, while the second one was conducted on a T-shaped braider.

In order to be implemented, the algorithm does not require a specialized software, which can be expensive to acquire and long to master. Therefore, the algorithm can be implemented quickly and at a low-cost. Additionally, advance knowledge in mathematics or finite element analysis is not needed to implement and use the algorithm, which makes it accessible to all. Therefore, it eliminates the need for a highly qualified and experienced worker to ensure a collision-free process. Furthermore, the developed method is not computationally expensive. Using a standard desktop computer with an i9-9900K central processing unit (CPU) and 32 GB of random access memory (RAM), the algorithm took less than 15 milliseconds to run for each case study, which is much faster than a human decision-making process. Therefore, it allows the worker more time to focus on different tasks. Additionally, a method that automatically detects collisions reduces the risk of human mistakes, which can cost a lot of money in broken components and render the braiding machine inoperable.

In future work, multiple iterations will be done automatically to find every collision-free carrier arrangement for a given bedplate's configuration. Coupled with a finite element simulation of the braiding process, every possible braid patterns could be numerically determined and classified.

4.8 Declaration of Conflicting Interests

The Authors declare that there is no conflict of interest.

4.9 Funding

The authors disclosed receipt of the following financial support for the research, authorship, and/or publication of this article: This work was supported by the Natural Sciences and Engineering Research Council of Canada [NSERC, RDCPJ 543847-19]; and PRIMA Quebec [R18-13-003]; FilSpec Inc; Pultrusion Techniques; and Bauer Hockey ltd.

CHAPITRE 5 ARTICLE 2: 3D PRINTING PROCESS FOR TEXTILE COMPOSITES

P.Assi[1,2], S. Achiche[2], L. Laberge Lebel[1]

[1]Advanced Composites and Fibers Structures Laboratory (ACFSlab), High Performance Polymer and Composite Systems (CREPEC), Polytechnique Montreal, 2500 ch. Polytechnique, Montreal, Qc, Canada, H3T 1J4

[2] Laboratoire de Conception de Systèmes Intelligents et Mécatroniques(CoSIM), Polytechnique Montreal, 2500 ch. Polytechnique, Montreal, Qc, Canada, H3T 1J4

Publié dans *CIRP Journal of Manufacturing Science and Technology* – 11 février 2021

Abstract

The geometry of a braid influences its mechanical properties directly. On the other hand, the path of the carriers dictates the geometry of the braid. In traditional braiding machines, the carriers move along a fixed path, via horngears, which cannot be changed during the braiding process. This limitation does not allow braiding with variable geometry parameters along its axis, such as variable thickness and variable cross-sections. This paper presents a braiding machine design allowing a completely independent carrier movement. This process is analogous to 3D printing where layer-by-layer deposition produces a final part. In our case, controlling the position of each intertwining yarn will create a 3D braid. Each carrier can move without affecting the position of its neighbors allowing an easier and total control on the position and morphology of each intertwining yarn. A novel horngear design is proposed. The horngears are independently driven. They occupy the bedplate area in a hexagonal compact arrangement. The carrier path can be divided into multiple pre-defined unitary displacements. Driven by the horngears, the carrier follows these successive unitary displacements. A prototype of the braiding machine has been developed and tested with three independent carriers. As a first step, a flat braid with three yarns is produced. In the second step, a braid with a variable cross section is produced: a flat braid turning into yarn twisting. This proof of concept opens-up the possibility of 3D-printing textile composites with tailorable mechanical properties.

5.1 Introduction

The use of composite materials continues to increase in various industries, such as the aerospace, the automotive and the sports industry. Over the past 20 years, the mass percentage of aircraft attributed to composite materials has increased from 15 to 53% [1]. This increase is attributed to the excellent stiffness-to-weight and strength-to-weight ratios of composite materials. Composites commonly consist of a textile fabric impregnated in a polymer resin [3]. The textile fabric may vary from weaves, braids and unidirectional fibers. Braids are traditionally used to produce shoelaces, fishing lines and climbing ropes. It also made its way in structural composites for marine propellers, aircraft fuselage frame, and engine [5-7]. They offer good fatigue resistance since the intertwined fibers damps crack propagation [7, 13]. They have also shown good crush resistance properties[43, 44]. The mechanical properties and the shape of a braid are directly related to its architecture [9].

The braiding process consists of intertwining at least three parallel yarn in order to create a continuous structure [4]. Figure 5.1a) presents an isometric view of a typical braiding machine. Yarns are winded onto a spool. Each spool is mounted on a spool tensioner, which applies tension to the yarns during the braiding process. Every spool tensioner is bolted on a carrier, which moves along a pre-defined path, called “track”, grooved into the bedplate. Moving along the track, the path of the carriers intersect each other, causing the yarns to intertwine, hence creating the braid. A yarn is defined as a strand of the braid, which consists of a bundle of fibers.

Figure 5.1b) presents a top view of the bedplate. Half of the horngears are illustrated in order to visualize the track underneath them. Horngears are discs with a number of evenly spaced notches around its circumference. These notches house the carriers during their movement. Horngears are placed on the bedplate according to the track, as shown in Figure 5.1b). Each horngear rotates in the opposite side of its neighbours. When two notches of adjacent horngears are face to face, the carrier is transferred from one horngear to the other. Figure 5.1c) demonstrates the carrier transfer. The guiding foot is the carrier’s part that slide in the grooved track. Figure 5.1c) i) presents the initial position of the guiding foot and the horngears. Figure 5.1c) ii) presents the intermediate position. At this point, the track is forcing the guiding foot to transfer itself from one horngear to another. In Figure 5.1c) iii), the guiding foot has completed its transfer and is being moved around the track by a new horngear. A single horngear can hold more than one carrier but only one carrier at the time can be transferred between two adjacent horngears. A pull up mechanism is placed on top of the bedplate, as shown in Figure 5.1a), in order to pull the yarns and the braided product away from the bedplate.

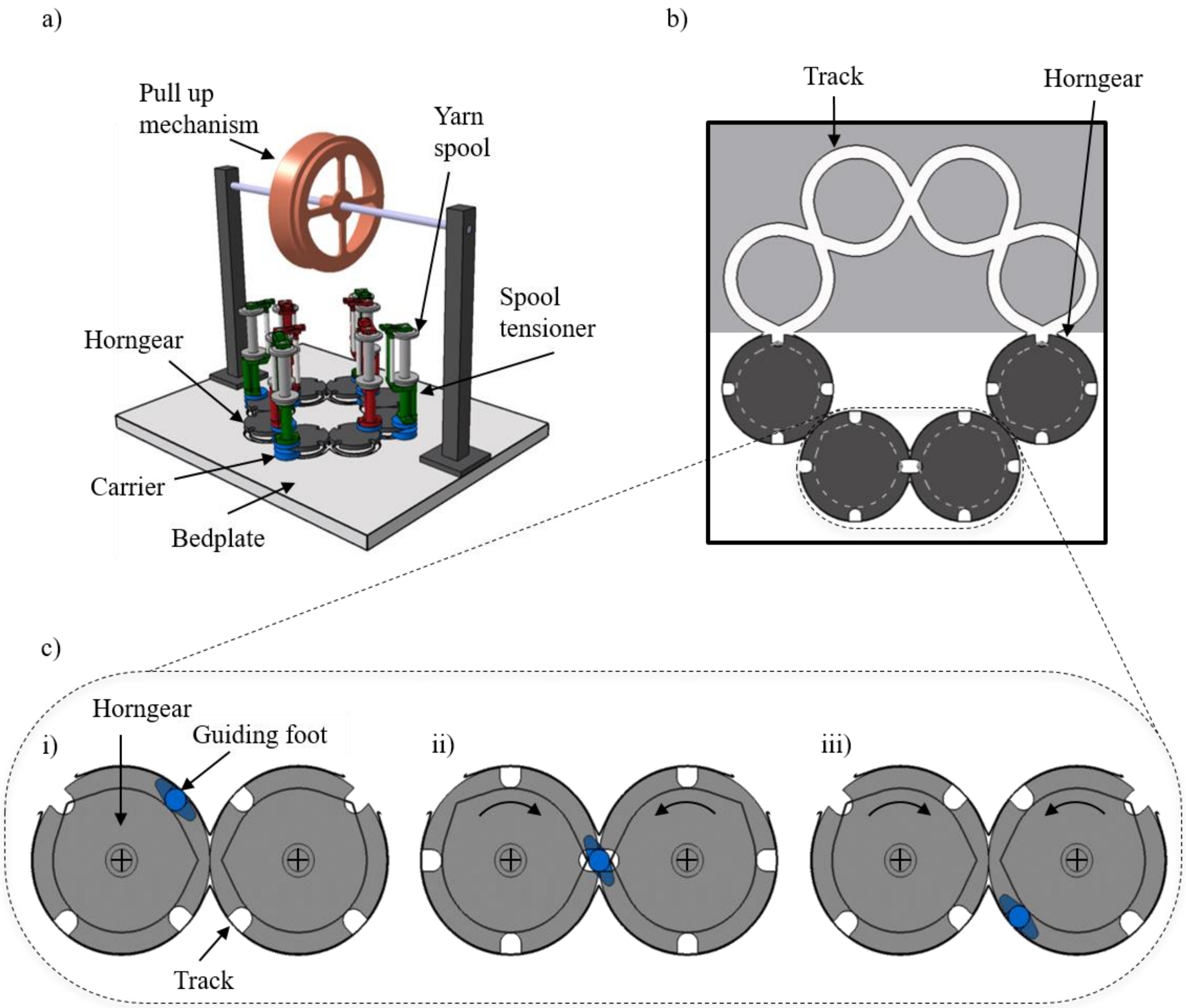

Figure 5.1 : a) Isometric view of a maypole-braiding machine and its main components. b) Top view of the bedplate. Half of the horngears are illustrated in order to visualize the track underneath them. c) Carrier transfer between two horngears i) Initial position ii) intermediate position final position.

The machine architecture presented in Figure 5.1 is commonly used to produce two dimensional (2D) braid. 2D braids are a single layer of intertwined fibers. Tridimensional (3D) braids can also be manufactured. The difference between a 2D and a 3D braid resides in the yarns' crossing topology [4, 7]. A 3D braid is a multilayered textile, where yarns of the braid connect every layer to each other. Therefore, 3D braids have yarns in the thickness's direction of the textile product, while 2D braids do not. Tridimensional (3D) braid is less prone to delamination than a two dimensional (2D) braid, while a 2D braid has better mechanical properties in the braid axis compared to a 3D braid [5, 15].

Several machine architectures were created to manufacture 3D braids. Bock *et. al.* presented a switch mechanism, which is placed between horngears along the track, to modify the carrier path [26]. This system is similar to a railway switch. It has two sets of tracks. The first one is an X-shaped track that allows the carrier to be transferred between horngears, as shown in Figure 5.1c) ii). The second set consists of two circular arcs, which create a discontinuity in the track between the two horngears. Therefore, the carrier cannot be transferred. It rotates around its initial horngear. The selected set of track depends on the switch mechanism status (open or closed).

Unlike the traditional horngear system, the carrier trajectory can be modified during the process. However, the machine needs to come to a complete stop in order to modify the switch status. According to the author understanding, a 3D braiding machine has been developed by Laourine [27] and Schneider [16, 29] using the technology presented in [26]. Each horngear is equipped with a brake and clutch mechanism allowing it to rotate or to come to a complete stop independently of its neighbours. Every switch status is controlled separately by a pneumatic actuator. However, this braiding process is stepwise. During one-step, the switch status can be changed or the horngears can rotate 90 degrees. Carriers can only be transferred from a horngear to another one at the time. In addition, the switch cannot change its status while having a carrier on top of it and neither while the horngears are turning.

Mungalov and Bogdanovich [35] designed a new transfer mechanism; also known as the "rotary gripping fork", allowing to interchange two carriers, simultaneously, between two adjacent horngears. The gripping forks are also placed along the track between each horngear. Each fork is independently driven and can either rotate 180 degrees or stay still. Two carriers can be placed on each side of the fork while being housed by two different horngears. Rotating the fork by 180 degrees interchanges the position of the carriers. Thus, two carriers are transferred simultaneously from one horngear to another and the path of the carrier can be flexible. When the fork stands still, the carriers are not transferred: they rotate around the horngear housing them. Allowing a carrier to be placed on top of the transfer mechanism, while switching its status, enables to have a larger number of spool tensioners on the bedplate. Nevertheless, the machine needs to come to a complete stop in order to activate the fork rotation.

The speed and the path taking by the carriers dictate the architecture of a braid. With the traditional horngear system, the path followed by the carrier is fixed by the track and cannot be altered. The track limits the braided product to a fixed overall shape and architecture. In order to cope with the increasing forms and mechanical properties requirements, such for an intake manifold or turbine blades, a new braiding technology, allowing a complete control over the position and the carriers' path, is needed. This will enable the fabrication of complex preforms with a continuous variable cross-section.

So far, braiding machines with a variable carrier path have a stepwise process. The machine must come to a complete stop when the carriers' path is altered. Additionally, each development still uses horngears that can house more than one carrier. When a horngear rotates, every carrier's position located on it is altered. Hence, the displacement of the carrier cannot be totally controlled individually and independently. Another limitation of the technologies listed above is that some kind of switching device must be used in conjunction with the horngears. This adds up a layer of complexity in the machine architecture and control that limits the capability of braiding truly evolving fibrous structures.

The main goal of this study is to develop a braiding machine architecture allowing an independent carrier movement. To do so, we propose a new design of horngears and remove any switching devices in order to lower the control complexity of the machine. Each carrier can move separately, without affecting the positions of its neighbors. Yarns can also be added or removed from the braid without any human intervention slowing down the process. This paper presents the design of the novel braiding machine architecture as well as two braids produced by a prototype: a flat braid and braid with a variable cross-section (flat braid turning into yarn twisting turning back into a flat braid). The machine function is also validated by producing braids with various pitches.

5.2 Proposed machine architecture

5.2.1 Design methodology

The concept presented in this study was developed using a standard sequential design process [54]. The specific design requirements were detailed and different solutions were laid out by brainstorming within our research group, which is composed of 12 specialists in braiding, mechanical design and engineering design. The design evaluation followed a simplified version of the Multi-criteria Mechatronic Profile (MMP). The MMP has been validated through several complex designs from robotic systems, biomedical prosthesis to autonomous unmanned aerial vehicles (UAVs) [55-57]. The simplified MMP was used to compare the design proposed in this work to the existing benchmark and will be briefly introduced further in the paper.

The developed solutions, for this paper, at the preliminary stages of design can be classified into two main categories: an active carrier and a passive carrier. An active carrier is equipped with its own drivetrain and can move in an autonomous manner while a passive carrier moves through a fixed tooling and cannot move in an autonomous manner. Since the operating time of an active carrier depends on battery life, we decided to go forward with a passive carrier solution. The selected concept was developed and validated through prototyping. Although there may be other more optimal solutions allowing an independent carrier movement, we present in this paper a unique viable and feasible concept, which has been validated by a functional prototype.

5.2.2 Horngear and carrier design

Figure 5.2 shows a horngear with nine equidistant notches. *R* is the nominal radius of the horngear. The large dashed circle is the horngear nominal circumference. The dimension *b* is the horngear notches spacing. This is the straight-line length between two adjacent notches center, taken at the end of the nominal radius. The notches, represented by the small dashed circle, have a diameter *D.* The notch diameter is tangent to the horngear nominal circumference. Figure 5.2b) illustrates a hexagonal compact arrangement of three horngears. The horngears are in close contact. The dimension *x* is the free length between a horngear nominal circumference and the contact point between two adjacent horngears. Figure 5.2c) illustrates a typical chain made by three cylindrical shafts tied together with two links. This chain replaces the traditional carrier. The length of each link is *b,* that is, matching the horngear notches spacing. The diameter of each cylindrical shaft (*D)* must be large enough to prevent mechanical blockage. An approximate design rule is that *D* must be close to *b*, while letting the horngear teeth extend to the horngear nominal circumference, as shown in Figure 5.2a).

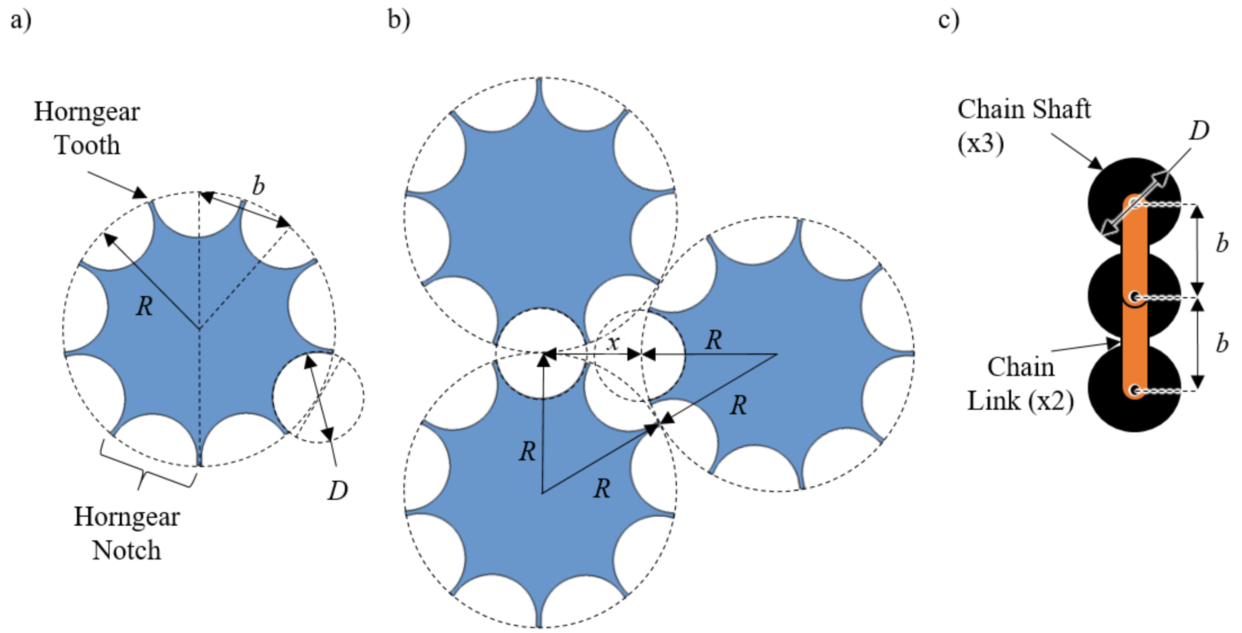

Figure 5.2 : a) Horngear with 9 equidistant notches. The large dashed circle represents the nominal circumference of the horngear. R is the nominal radius of the horngear. b is the straight-line length between two notch centers. The small dashed circle is the notch circumference of diameter D. b) A hexagonal compact arrangement of three horngears where x is the free length between a horngear nominal circumference and the contact point between two adjacent horngears. c) Representation of a chain with three shafts and two links.

Every horngear on the bedplate has the same dimension. By the Pythagoras' theorem, the dimension x is calculated according to,

$$x = (\sqrt{3} - 1)R \qquad (5.1)$$

The right-angle triangle is illustrated on Figure 5.2b). It has a hypotenuse of 2R. The two legs of the right-angle triangle measure R and (x + R). The dimension *b* is calculated according to,

$$b = 2\mathrm{R}\sin\left(\frac{\pi}{\mathrm{N}}\right) \tag{5.2}$$

Where *N* is the number of notches in the horngear.

The number of notches must be selected according to the following guidelines:

- In order to prevent the carrier chain from buckling and also prevent mechanical blockage when transitioning from a horngear to another,

$$b < \mathrm{x} \tag{5.3}$$

- To facilitate the engagement of the carrier chain in the adjacent horngear, which is responsible for steering, *b* must be close to *x*.

By replacing the Equations (5.1) and (5.2) in Equation (5.3), the number of notches in the horngear can be expressed by,

$$N > \frac{\pi}{\sin^{-1}\left(\frac{\sqrt{3}-1}{2}\right)} \tag{5.4}$$

Therefore, the number of notches N is obtained by rounding up the right-hand side of Equation (5.4). The ideal number of notches is 9.

5.2.3 Carrier movement

Figure 5.3 illustrates the displacement of a carrier in a hexagonal compact horngear arrangement. Four horngears (HG) are shown as well as one carrier. The carrier consists of three cylindrical shafts connected by two links, which form a chain. By attaching a spool tensioner on top of the carrier, the yarn spool can be moved around the bedplate. In order to simplify the illustration and to focus on the carrier movement, the spool tensioner and the yarn spool are not shown in Figure 5.3. The assembly of the carrier, spool tensioner and yarn spool can be seen in Figure 5.4.

Each HG is independently driven by an electric actuator. The yellow HG are rotating clockwise (CW), the purple HG are rotating counterclockwise (CCW) and the white HG are standing still. In order to move the carrier around the bedplate, three adjacent horngears, in contact with the carrier, need to rotate simultaneously. For example, to proceed from position in Figure 5.3b) to the position in Figure 5.3c) iii, HG #1 needs to rotate CW while HG #3 and #2 need to rotate CCW. Figure 5.3c) i and Figure 5.3c) ii present the intermediate positions of the carrier and HG in order to pass from Figure 5.3b) to Figure 5.3c) iii. Before rotating the three HG adjacent to the carrier, by a 60 degrees turn, the carrier needs to be oriented in the proper direction. In order to do so, the HG housing the first cylindrical link of the chain is responsible to steer the carrier. In Figure 5.3a), HG #3 holds this responsibility. By rotation 10 degrees CW, HG #3 orients the carrier horizontally, as shown in Figure 5.3b). Following the 60 degrees turn from HG #1, #3 and #4, the front chain's link ends up in a notch of a new HG. In this case: HG #2, as shown in Figure 5.3c) iii. To complete the cycle of displacement, the HG connected to the rear chain's link rotates by an addition 10 degrees, as shown in Figure 5.3d). This last step straightens the carrier. In addition, one of two HG, #2 or #4, can steer the carrier for its next movement. From the position shown in Figure 5.3d), the carrier can either go up-right, down-right, up-left or down-left.

The displacement cycle can be divided into three sequential steps:

1. A 10-degree rotation of the HG responsible to steer the carrier in a particular direction, as shown in Figure 5.3b).
2. A 60-degree rotation of the three adjacent HG allowing to move the carrier, as shown in Figure 5.3c) i to Figure 5.3c) iii.
3. A 10-degree rotation of the HG responsible for straightening the carrier, as shown in Figure 5.3d).

Therefore, the HG are performing two roles: (1) steering the carrier, and (2) moving the carrier. This dual role is a key feature of this design. No other mechanism, such as a switch, a guiding foot, or a transfer mechanical system is required to steer and move the carriers on the bedplate. Instead, the carrier moves around the bedplate by successively operating sets of three HG in a predetermine manner. There are six pre-defined unitary displacements, along which the carrier can move. The carrier's path can be composed by multiple subsequent unitary displacements. In addition, a grooved track is no longer required.

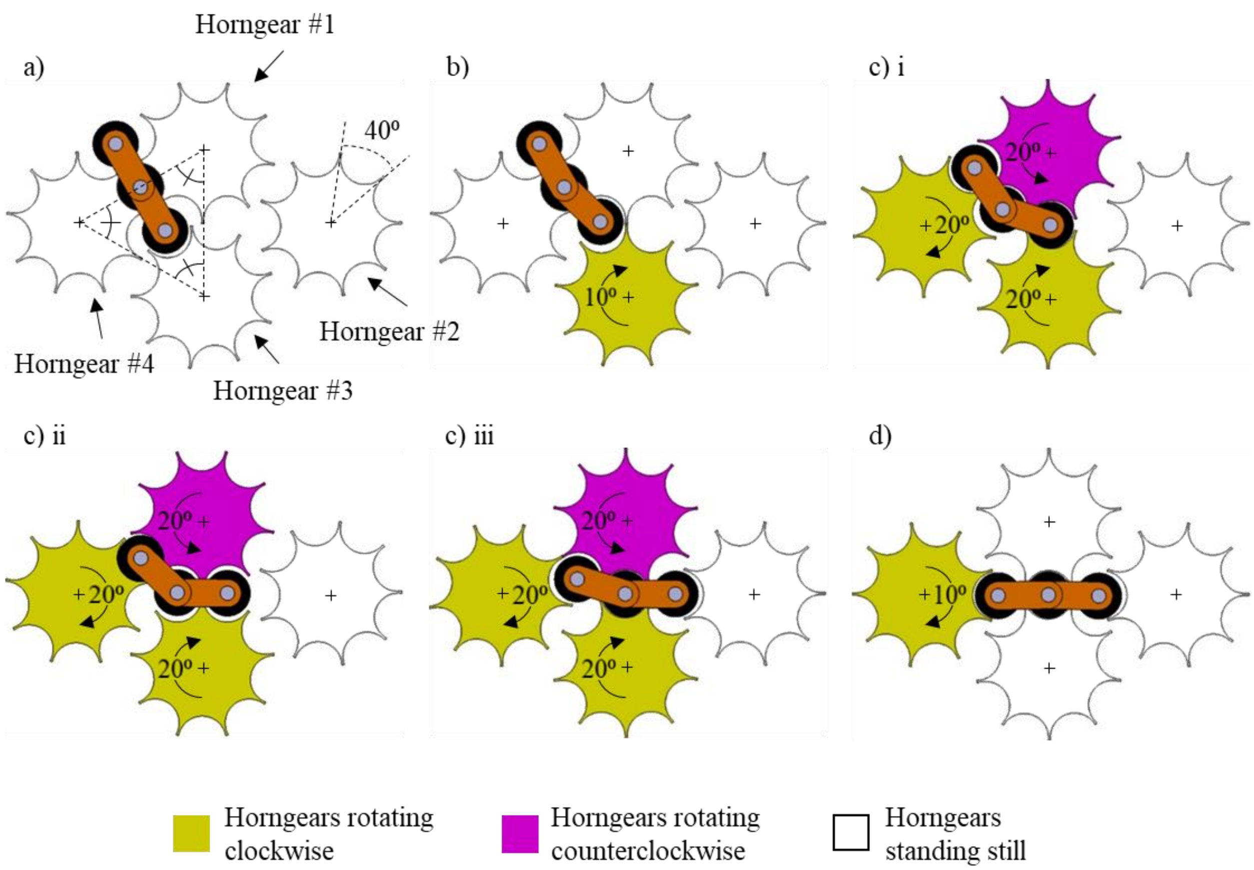

Figure 5.3 : Displacement cycle. The yellow HG are rotating (CW), the purple HG are rotating counterclockwise (CCW) and the white HG are standing still. a) Initial position of the HG and the carrier as well as an equilateral triangle formed by the center of three adjacent HG. b) HG #3 rotates CW by 10 degrees to steer the carrier horizontally. c)i to c)iii HG 4 and #3 rotate CW while HG #2 rotate CCW, by 60 degrees, in order to move the carrier. d) HG #2 rotates CW to straighten the carrier.

Since each HG has nine equidistant notches around its circumference, a notch is enclosed within a 40-degree angle, as shown on HG #2 from Figure 5.3a). A 40-degree rotation will turn the HG one notch further while a 20-degree rotation will turn the HG half a notch further. In each figure from Figure 5.3c) i to Figure 5.3c) iii a 20-degree rotation is depicted. A 40-degree rotation occurs from the position shown in Figure 5.3b) to the position shown in Figure 5.3c) ii as well as from the position shown in Figure 5.3c) i to the position shown in Figure 5.3c) iii. To move from position shown in Figure 5.3b) to position shown in Figure 5.3c) iii, the horngears rotate one and a half notches further, i.e. 60-degree.

In the hexagonal compact HG arrangement presented in Figure 5.3, a set of three adjacent HG forms an equilateral triangle with the center of each HG as vertices. In Figure 5.3a), an equilateral triangle formed by the center of HG #1, #3 and #4, is illustrated by dashed lines. The notch of HG #3 must be centered with respect to the angle formed by the edges of the triangle in order to prevent mechanical blockage when receiving the front chain's link. Therefore, to pass from position shown in Figure 5.3a) to position shown in Figure 5.3b), a 10-degree rotation is required.

5.3 Experimental results and discussion

As a proof of concept, the first prototype of the machine is presented in Figure 5.4. Eighteen identical horngears are machined by laser cutting. Each horngear has a radius of 33.25 mm and has nine notches. The diameter of each notch is 21.93 mm. They are positioned in a hexagonal compact arrangement. Each horngear is independently driven by a servo actuator (AX-12A, Dynamixel). This actuator is selected for its high torque and relatively compact frame. All the actuators are controlled by a microcontroller (ArbotiX-M Robocontroller, Dynamixel). The main components are also shown on Figure 5.4, such as the yarn spools, the bedplate, the spool tensioners, the carriers, the horngears and the pull up mechanism. The prototype can accommodate three carriers at the time. Therefore, braids with three yarns were produced.

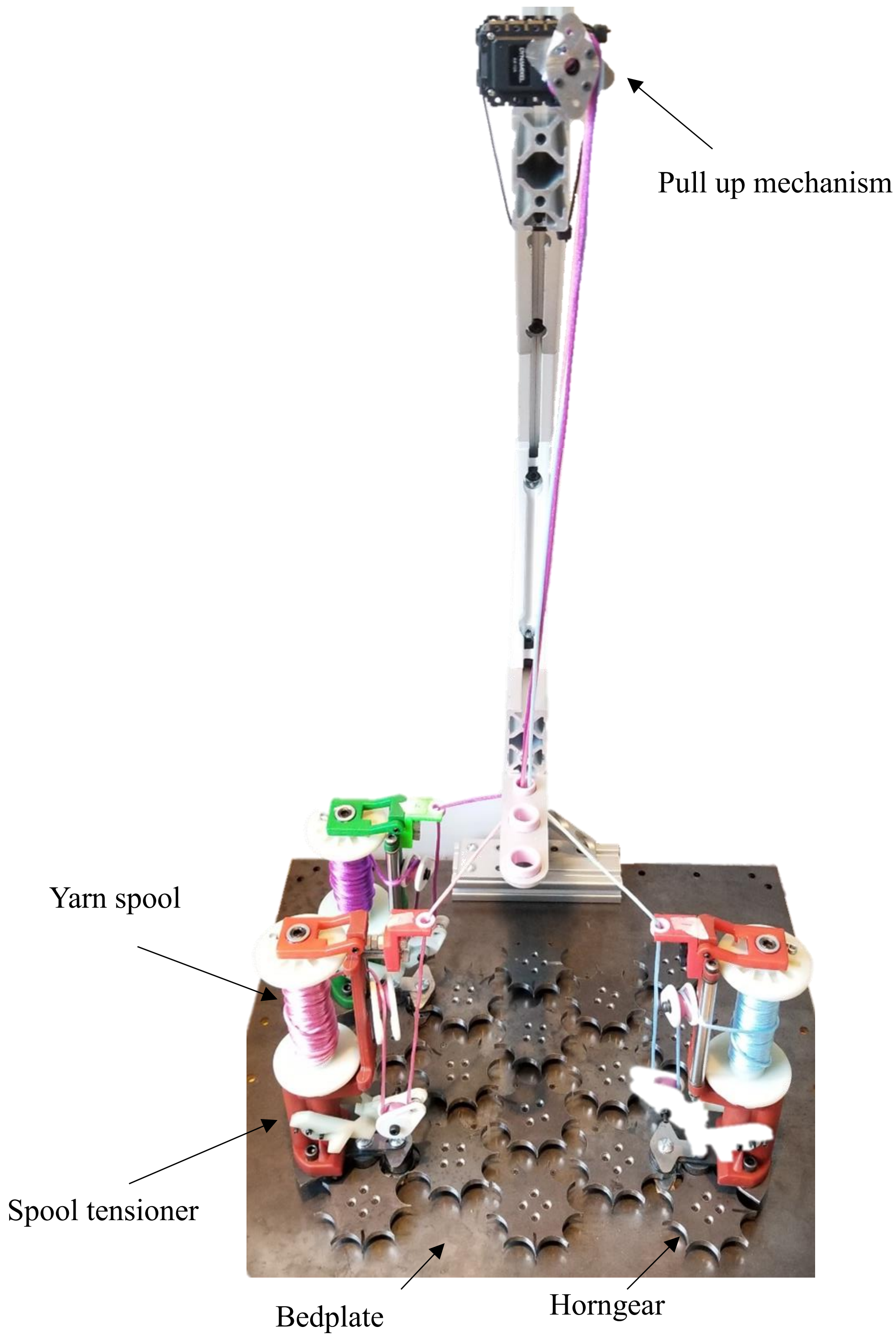

Figure 5.4 : A prototype of the proposed machine design and its main components.

5.3.1 Three yarns flat braid

To fabricate a flat braid composed of three yarns, three spool tensioners, taken from a maypole-braiding machine (KBL24-1-110, Xuzhou Henghui Braiding Machine Company Ltd), were used. Each of them was bolted to a separate carrier. The initial position of the carriers is shown in Figure 5.4. The carriers were moved around the bedplate one after the other, i.e., one at a time. This simplifies collision management and programming.

The braid pitch is defined as the longitudinal distance of the repeated section of the braid. Figure 5.5 shows a pitch length where all yarns form two crossovers with each other until they return to their circumferential initial position. The carriers were moved around the bedplate using carrier displacement cycles similar to the one shown at Figure 5.3. Each individual carrier movement is defined as a step. Each step has its own departure and arrival point on the bedplate. A total of 12 steps, i.e. four steps per carrier, were programmed to create one braid pitch shown in Figure 5.5. After these 12 steps, the carriers' position was identical to their initial position. In addition, at every four steps, the puller, i.e. pull up mechanism, was activated for a specified pulled distance. As a result, to fabricate one pitch, 12 steps, as well as three pulls were required. The sequence is defined as the set of steps and pulls needed to produce one pitch. The braiding sequence description is available in the Annex A.

Once the overall carriers' trajectory is divided into steps, each step is subdivided in multiple subsequent unitary displacements and fed as input to a *Matlab* script. The script outputs a text file containing the movement of every actuator for each unitary displacement. This text file is then read by the controller that moves the motors accordingly.

Figure 5.5 presents a standard flat braid fabricated with the proposed design and prototype. The braid portrayed in Figure 5.5 has a pitch length of 27.7 mm ± 0.7 mm. It was measured using *ImageJ* on calibrated images.

Figure 5.5 : Three yarns flat braid.

5.3.2 Variable cross-section braid

In order to demonstrate the versatility of the proposed machine architecture, we choose to fabricate a braid with a variable cross-section. Figure 5.6 shows a braid with two cross-section changes. First, a flat braid is converted into a filament winding. The filament winding is composed of two yarns twisting around each other and a third one wrapping around them with at a different pace. The second cross-section change consists of the filament winding tuning back into a flat braid. To fabricate the braid shown in Figure 5.6, the carriers' paths were altered automatically during the braiding process. The flat braid sections were manufactured using the same sequence as the braid from Figure 5.5. The filament winding section was fabricated using a different sequence, which is available in the Annex A. Both cross section changes correspond to a change in the carriers' paths.

Figure 5.6 : Variable cross-section braid.

5.3.3 Characterization of the prototype

In traditional braiding machines, the braid pitch (P) can be expressed has a function of the take up speed (V) and the rotation speed of the carriers (ω), as,

$$P = \frac{V}{\omega} \quad (5.5)$$

In order to characterize the relationship between the take up speed of the prototype and the pitch length of the braid, five different three yarns flat braids were fabricated. Table 5.1 groups the parameters and measurements for each test condition. As previously defined in section 4.3.1, a sequence is the set of steps and pulls needed to produce one pitch. Therefore, the sequence duration is the required time to fabricate one pitch. The sequence duration was measured using a chronometer. The pulled distance is the overall braid length pulled by the pull up mechanism during a sequence. Since the pull up mechanism is activated 3 times during the sequence, the effective take up speed is the total pulled distance during a sequence divided by its duration. Furthermore, the effective rotation speed is the speed at which the carriers complete the sequence and return to their starting position on the bedplate. Therefore, the effective rotation speed is computed as the inverse of the sequence duration. Finally, the computed pitch is the pitch calculated according to Equation (5.5) and the measured pitch is the pitch's length measured on the braid. In Table 5.1, each row represents a different test condition. For each test condition, only the pulled distance was varied to change the braid pitch. Since the horngears' rotation speed and the pull up mechanism speed were constant, the increase in pulling distance was generated by a longer pull up mechanism activation time. This explains the increase in the sequence duration for a longer braid pitch.

Table 5.1 shows that the computed pitch is close to the pitch measured on each sample. The average of the five absolute errors is 0.9°. For each condition, the absolute error between the measured and computed pitch is slightly higher than the standard deviation on the measured pitches. This error is explained by delays in the execution of the sequence by the controller and imprecision on the sequence duration measurement. Both issues will be resolved in an improved prototype. Nevertheless, results from Table 5.1 demonstrate the proper functioning of this braiding machine architecture since the relationship between the machine's parameters (P,V,ω) is similar to that of traditional machines, which is dictated by Equation (5.5).

Table 5.1 : Parameters of each sample in order to determine the relationship between the take up speed and the pitch length of the braid.

Sequence duration (s)	**Pulled distance (mm)**	**Effective take up speed (mm/s)**	**Effective rotation speed (s^{-1})**	**Computed Pitch (mm)**	**Measured Pitch (mm)**	**Absolute Error on Pitches (mm)**
109.3 ± 0.3	26.14	0.23	0.0091	26.13	27.7 ± 0.8	1.6
109.6 ± 0.6	32.67	0.29	0.0090	32.67	35.5 ± 0.7	2.8
111.5 ± 0.3	39.21	0.35	0.0090	39.21	37.4 ± 2.2	-1.8
114.7 ± 1.2	45.74	0.40	0.0087	45.74	47.9 ± 1.7	2.2
115.4 ± 0.4	52.27	0.45	0.0087	52.28	52.0 ± 1.3	-0.3

5.3.4 Comparison with existing designs

Among the few design evaluation technics available for complex systems, the Multi-Criteria Profile for Mechatronic System (MMP), developed by Mohebbi *et. al.* [56, 57], proposes a methodology to compare designs quantitatively. The MMP uses five criteria to evaluate and compare designs: the machine intelligence, the system reliability, the design complexity, the design flexibility and the cost. Due to the available information on the existing machines and considering that our design is in the prototyping phase, we limited the evaluation, and therefore the comparison, to the complexity of the machine. Based on the MMP, the following elements of the machine complexity are assessed: number of components, architecture complexity and control complexity.

We've compared the new developed design to a traditional braiding machine (see Figure 1), the braiding machine developed by Laourine [27] and Schneider [16, 29], referred here as the "railway switch" braiding machine, and the concept developed by Mungalov and Bogdanovich [35], referred here as the "rotary fork" braiding machine. Our proposed design is referred here as the "3D textile printing" machine.

5.3.4.1 Main components

The MMP evaluates and compares the total number of components for each design, such as the number of actuators, sensors and drivers. In this study, we decided to assess the number of different types of components, since the number of components depends on the machine size and the type of braid manufactured. Additionally, there is no common rule within each machine on how the number of components scales with it size. Therefore, unless the designs are compared to a fixed machine size, comparing the total number of components doesn't fairly evaluate the designs' complexity for benchmarking purposes.

Table 5.2 enumerates the different types of components for each design. Components are primary parts or assemblies of a design. For example, an electric motor assembly includes its driver, gearbox and encoder. The railway switch braider has the highest number of different components, followed by the rotary fork braider, with 9 and 7 respectively. The 3D textile printing braider has the lowest number of different components, which is 5. Since it doesn't have a carrier guiding track, it has one less type of component than the traditional braider.

Table 5.2 : Main types of components for the traditional braiding machine, the railway switch braiding machine, the rotary braiding machine, and the 3D textile printing braiding machine.

	Traditional (see Figure 5.1)	**Railway switch [13-15]**	**Rotary fork [16]**	**3D textile printing [This work]**
	- HG - Electric motor for the HG - Carriers - Control system - Pull up mechanism - Carrier guiding track	- HG - Electric motors for the HG - Carriers - Control system - Pull up mechanism - Clutch system for the HG - Brake system for the HG - Railway switch - Pneumatic actuators for the railway switch	- HG - Electric motors for the HG - Carriers - Control system - Pull up mechanism - Rotary fork - Pneumatic actuators for the rotary fork	- HG - Electric motors for the HG - Carriers - Control system - Pull up mechanism
Total	**6**	**9**	**7**	**5**

5.3.4.2 Architecture complexity

As defined by the MMP, the degree of architecture complexity of a design is determined by the number of interconnections. These connections relate the interdependency, from a functionality point of view, between components. Figure 5.7 presents the interconnections for the traditional, railway switch, rotary fork, and 3D textile printing braiding machine. The interconnection count for each machine is shown by numbers close to the interconnection arrows. It is important to note that the goal is to reduce machine complexity for the same task to be achieved by the design.

The railway switch diagram of Figure 5.7 is explained in detail since it is the most complex. The same reasoning can be applied for the other designs. The control system manages the railway switch actuators, the horngears motors, the pull up mechanism, the clutch as well as the brake system, which explains interconnection (IC) #9, #13, #1, #2 and #3 respectively. Since the horngears rotate via a clutch and a brake system, an IC exists between these components. The brakes allow to slow down and stop the horngears from rotating (IC #7) while the clutch system delivers power from the motor to the horngear (IC #6 and #4). The same reasoning is applied for the IC #10 and #8: railway switches are activated by the railway switch actuators and the carriers are moved around the bedplate via horngears. In addition, the railway switches and the horngears cannot be activated simultaneously, which clarifies IC #12. Moreover, a railway switch cannot change its status while having a carrier on top of it, which justify IC #11. Finally, the clutch and the brake systems are interdependent (IC #5) since they work together to stop and activated the horngears.

The 3D textile printing braiding machine has the simplest architecture followed by the traditional braiding machine, with a degree of architecture complexity of 4 and 5 respectively. These scores would classify them as roughly equivalent. Considering that the 3D textile printing braiding machine is not equipped with a carrier guiding track, it has one less IC than the traditional braider. With a degree of architecture complexity of 13, the railway switch braiding machine has the most complex architecture followed by the rotary fork braiding machine, which has a degree of architecture complexity of 8.

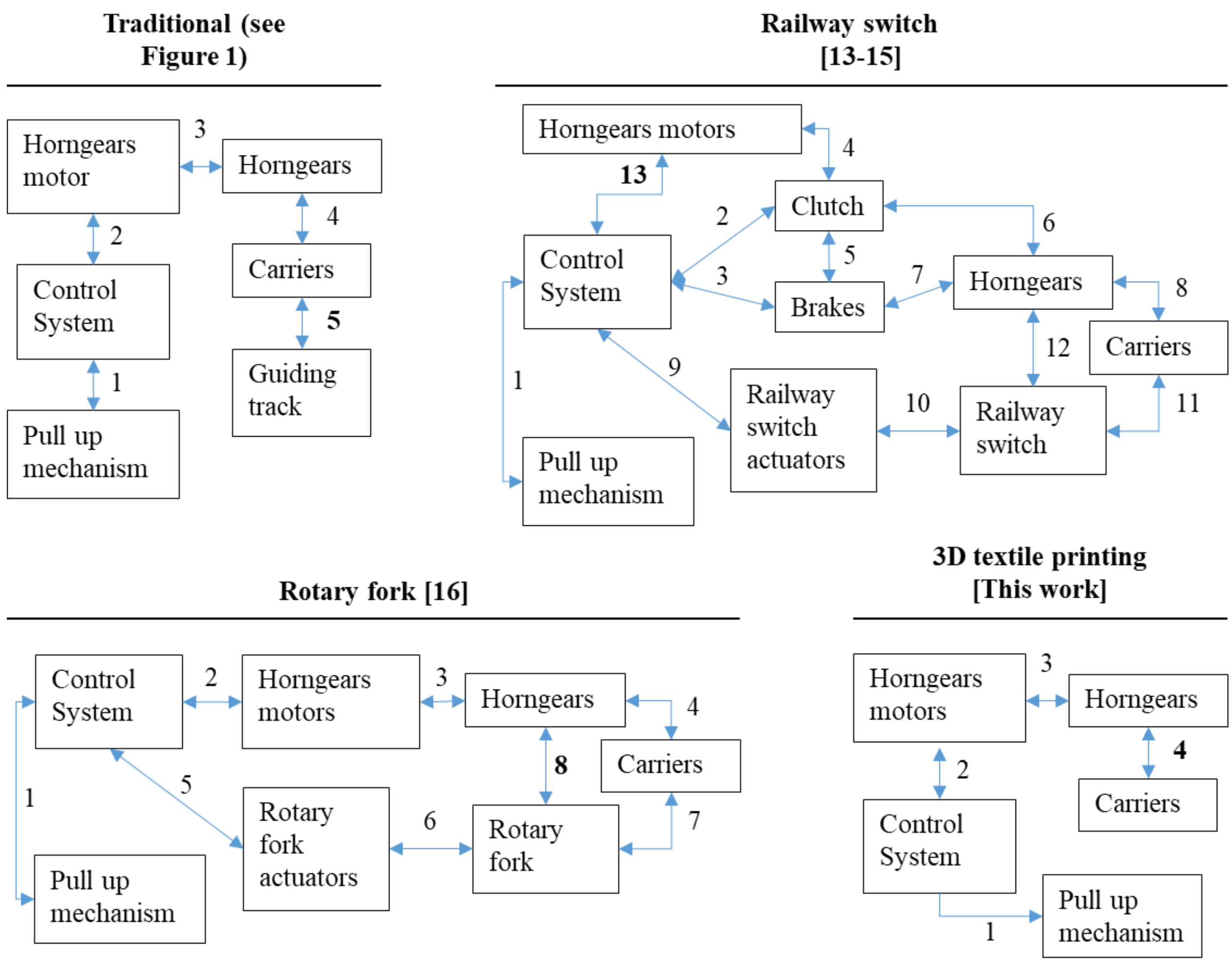

Figure 5.7 : Interconnections diagram for the traditional braiding machine, the railway switch braiding machine, the rotary braiding machine, and the 3D textile printing braiding machine. The interconnection count for each machine type is shown by numbers close to the interconnection arrows.

5.3.4.3 Control complexity

Furthermore, the control complexity is evaluated by the number of closed loop in the control system. Here, we concentrate on the control system required to move one carrier. In both the railway switch and the rotary fork braiding machines, the number of closed loop is 5. One for each four switching devices located around the horngear and one for the horngear itself. The number of closed loop for the 3D textile printing braiding machine is 4, since four horngears are required to move one carrier. Finally, the number of closed loop is 1 for the traditional braiding machine.

Indeed, there is only one motor enabling the horngears' rotation: horngears are connected to the motor through multiple gears.

Table 5.3 summarizes the number of main components, architecture complexity and control complexity for each concept. Overall, traditional braiding machines remain the simplest concept. However, these machines don't allow modifications in the carrier path. The 3D textile printing design presented in this paper has an overall score higher than the traditional braiding machines. However, it has the lowest score in every category compared to other designs allowing a variable carrier path. Therefore, our new design is less complex than existing designs.

Table 5.3 : Summary of the number of different types of components, degree of architecture complexity and degree of control complexity for the traditional, railway switch, rotary fork and 3D textile printing braiding machine.

	Traditional (see Figure 5.1)	**Railway switch [13-15]**	**Rotary fork [16]**	**3D textile printing [this work]**
Number of components types	6	9	7	5
Degree of architecture complexity	5	13	8	4
Degree of control complexity	1	5	5	4
Total	12	27	20	13

5.4 Conclusion

This paper proposes a novel braiding machine architecture. A new horngear design is presented as well as a new carrier design. Carries are moved and steered around the bedplate by the horngears. The machine architecture is exempt from any kind of track or switching devices. As a proof of concept, a prototype is assembled. Two braids are fabricated: a flat braid with three yarns and a braid with a variable cross section.

In addition, the design matches traditional prediction regarding the pitch and the take up speed. The proposed braiding machine design allows an independent carrier movement. Carriers are able to move simultaneously around the bedplate, without affecting the position of its neighbors. This allows a variable carriers' path during the braiding process. It also allows independent carrier moving speed. These enable the production of variable braiding pattern and variable cross section braids having fluctuating mechanical properties along its axis. Filament winding, 2D and 3D braids as well as a combination of all three can be produced with the novel braiding machine architecture. Furthermore, the independent carrier movement allows adding and removing carriers automatically during the braiding process. Hence, yarns can be added and removed automatically from the braid during its fabrication. Therefore, we consider that this braiding machine can 3D print textile structures. It allows control on the number, position and shape of yarn crossovers, layer-by-layer, along the braid longitudinal axis.

The control of the machine is simplified be removing all kinds of switches or mechanical transfer. On a larger scale, controlling simultaneously multiple electric motors could become a challenge. If the actuators where to come out of sync, horngears could work against each other and/or create a mechanical jam. In order to overcome this possible limitation, controlling in torque, instead of angular positions, two out of three horngears during the second step of the carrier displacement cycle can be an option to consider. The position controlled horngear could set the speed and the angular displacement while being assisted by the two others to move the load. The torque controlled horngears could provide a constant or a variable workforce during the displacement with respect to the position controlled horngear, thus, providing a master/slave control method rather than controlling each actuator independently. Moreover, by increasing the number of carriers, the size of the bedplate can rapidly increase. Theoretically, a minimum of four horngears per carrier is required to enable the carriers' movement while avoiding collisions.

Furthermore, the inertia of the carriers and the horngears was not comprehensively studied for this proof of concept. In future work, a thorough study on the inertial forces will be carried out in order to determine the torque needed to accelerate and decelerate the carriers at normal operating speed. Based on existing designs, stopping and starting the horngears repetitively should not invalidate the design presented in this paper. However, inertia forces must be taken into consideration, especially when sizing the actuators. Additionally, in future work, a bigger machine will be assembled allowing 48 carriers on its bedplate and a control algorithm will be further developed in order to validate and address these limitations.

5.5 Acknowledgment

The authors would like to acknowledge the financial support from the Natural Sciences and Engineering Research Council (NSERC, RDCPJ 543847-19) of Canada, PRIMA Quebec (R18-13-003) and FilSpec Inc, Pultrusion Techniques, and Bauer Hockey ltd.

CHAPITRE 6 ARTICLE 3: APPLICATION OF GRAPH THEORY FOR PREVENTING CARRIERS' COLLISIONS IN VARIABLE PATH BRAIDING MACHINES

P.Assi[1,2], S. Achiche[2], L. Laberge Lebel[1]

[1]Advanced Composites and Fibers Structures Laboratory (ACFSlab), High Performance Polymer and Composite Systems (CREPEC), Polytechnique Montreal, 2500 ch. Polytechnique, Montreal, Qc, Canada, H3T 1J4

[2] Laboratoire de Conception de Systèmes Intelligents et Mécatroniques(CoSIM), Polytechnique Montreal, 2500 ch. Polytechnique, Montreal, Qc, Canada, H3T 1J4

Publié dans *The International Journal of Advanced Manufacturing Technology* – 21 avril 2023

Abstract

Braided preforms are now used for structural composite parts. They have made their way into the aeronautic and the automotive sectors. With the development of variable carriers' paths braiding machines, the braid geometry can now be tailored to specific needs and be fabricated to a near net shape of the final product. However, the carrier's path variability brings complexity to the manufacturing process: carriers can collide with each other while braiding the desired structure. Manual trial and error is still needed to program a collision-free braiding process, which is time and resource consuming. We proposed a method, based on graph theory, to automatically prevent collisions during the braiding process. This method can be applied onto variable carriers' paths braiding machines. To do so, the bedplate of the braiding machine is modeled as a graph. Faces represent horngears and edges represent carriers' path. Vertices can represent one of the following three: a horngear's slot, a track intersection, or possible stationary carrier's position. A collision is prevented by delaying the displacement of one or more carriers. A prevention algorithm is presented, which prescribe a delay to each carrier in order to achieve a collision-free process. To demonstrate the algorithm, a case study is carried out on a 3D textile printing braiding machine. The algorithm offers an automatic and efficient method to prevent collisions in variable carriers' paths braiding machines.

6.1 Introduction

Composite materials offer excellent mechanical properties for a fraction of the usual weight. They play an important role in reducing the weight of vehicles, such as cars and aircraft, to increase their energy efficiency and reduce their greenhouse gas emission. In the past twenty years, the use of composite materials has widely increased to combat global warming. As an example, the mass percentage of composite material of aircraft has climbed from 15% to 53% [1], resulting in lighter vehicles.

A composite material is a combination of different components, which forms a heterogeneous material [3]. However, fibers impregnated in a polymer resin are commonly used for composite materials. Continuous fiber yarns can be arranged in many forms, such as weaves, unidirectional fibers, and braids. Braids offer many benefits including good fatigue and crush resistance properties [7, 13, 43, 44]. More importantly, braiding enables the fabrication of near net shape preforms. This means that the preforms are produced very close to the final shape of the product, which reduces the number of manufacturing steps as well as raw material waste [58]. Braids can be found in structural composite parts, such as beams, fuselage frames and marine propellers. They are also used in the medical field for hip and orthopedic prosthesis [5-7, 15, 46, 47].

Braids are fabricated by interlacing yarns. To do so, yarn bobbins are mounted on carriers, which are moved around a bedplate following different paths, called tracks. The tracks are machined into the braider's bedplate. As the tracks cross each other, the yarns intertwine and create the braid. The carriers are moved along the tracks by horngears. Figure 6.1 presents a top view of a maypole braiding machine bedplate, which is used to fabricate tubular braids. The braider's bedplate in Figure 6.1 is composed of eight horngears. However, only six horngears are shown to visualize the track as well as a track intersection.

As mentioned, horngears enable the carriers' displacement. They are equipped with slots, which can house a carrier, as shown in Figure 6.2. When rotating, the horngears move the carriers. To move around the bedplate, carriers must be transferred from horngear to horngear. The transfer is carried out at the track intersection by means of the carrier's guiding foot. Each carrier is fitted with a guiding foot, which is placed in the track. Therefore, the carrier is forced to follow the track. Additionally, in a traditional braiding machine, each adjacent horngear rotates in the opposite direction. Figure 6.2 illustrates a carrier transfer between two horngears. Both horngears have four slots. They rotate in opposite direction, as indicated by the arrows. The carrier is depicted in orange. The carrier's guiding foot is also shown. Figure 6.2a) presents the initial position of the carrier. As the horngears rotate, the carrier is moved according to the track. Once the carrier reaches the track intersection, as shown in Figure 6.2b), it is forced to transfer to the adjacent horngear due to the shape of the guiding foot. Figure 6.2c) presents the final position once the carrier transfer is completed. The carrier is now being displaced by a new horngear.

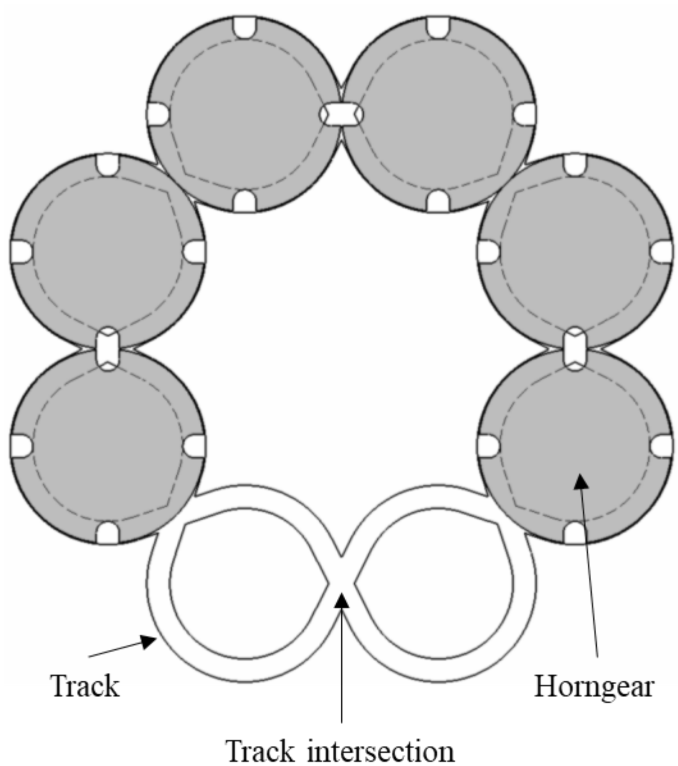

Figure 6.1: Top view of a maypole braiding machine bedplate composed of 8 horngears. Only six horngears are shown to visualize a track intersection

In traditional braiding machines, the path taken by a carrier is fixed and cannot be modified during the braiding process. This is a major drawback since traditional braiding machines are unable to produce different cross-section braids, i.e., different braid architectures. They are limited to a single cross-section braid. The braid architecture dictates its mechanical properties [9]. Therefore, the achievable mechanical properties are limited to a single architecture. Once the tracks are machined into the bedplate, the braid's cross section is fixed. In order to modify it, the bedplate needs to be redesigned with a new set of tracks. Thus, for each braid's cross-section, a specific set of tracks is required. Changing the bedplate is time consuming, which can cause a lot of unwanted production downtime whenever multiple changes are needed. Additionally, designing the correct bedplate is a complicated task, which requires high expertise as well as multiple trials and errors [21, 59]. The tracks must be designed in the approved manner and the horngears must be accurately sized and placed to achieve the desired cross-section.

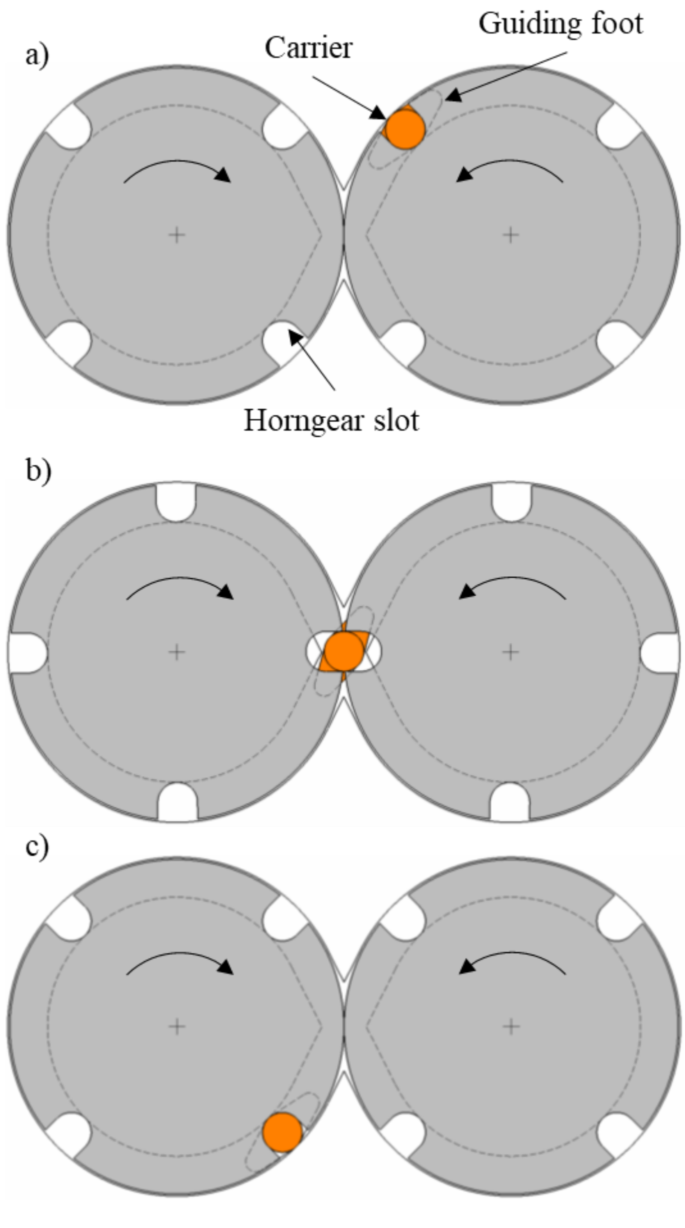

Figure 6.2 : Carrier transfer between horngears. The arrows indicate the direction of rotation of the horngears a) Initial position b) Carrier transfer at a track intersection c) Final position : carrier transfer is completed

Different braiding machines have been developed to enable variable carriers' paths, hence avoiding the hassle of modifying the bedplate for each different cross-section braid. This allows the production of braids with flexible geometry parameters along its axis, i.e., variable braid thickness and variable cross sections. Laourine [27] and Schneider [16, 29] developed a braiding machine that uses a switch mechanism placed between each horngear. Depending on the switch status, the carriers can either be transferred, or not, from one horngear to another. Mungalov *et al.* [35] proposed a system that allowed the transfer of two carriers simultaneously between adjacent horngears. The system, placed between each horngear, is referred as the "rotary fork." Carriers can only be transferred to another horngear by activating the fork. Assi *et al.* [60] recently introduced a braiding machine, called the 3D textile printing braiding machine, where carriers are moved around the bedplate by individually driven horngears, without the use of a transfer mechanism. The three above-mentioned machine architectures are presented and discussed in more details in [60].

Programing variable carriers' paths braiding machines is challenging to accomplish due to their architecture complexity. Carriers must move without colliding with transfer mechanisms, horngears or between themselves. It requires highly skilled and experienced engineers to program such machines. Nevertheless, engineers heavily depend on trial and error, which is time and resource consuming, since no other method is available according to the literature surveyed. A small number of studies have presented methods to detect carriers' collisions in variable carriers' paths braiding machines by simulating the braiding process [22, 30]. However, whenever a collision is detected, engineers must manually reprogram the machine in order to have a collision free process. The studies aforementioned do not propose a method to prevent collisions in variable carriers' paths braiding machines. Additionally, the flexibility of the carrier displacement has yet been exploited to prevent collisions, which could extend the variety of braided geometries and reduce the pre-production process time.

Detecting and preventing collisions between objects is not limited to the world of braiding. It's a concept common to many different sectors, such as the telecommunication and transportation sectors. Several proposed methods to solve collision problems are based on graph theory since it studies the relationship between different objects within a network. It also provides a visual representation, which can help better understand complex networks. For example, it has been used for planning collision-free train routes within a train station [61]. It has been used to manage traffic within transportation networks, such as air transportation networks [49]. It has also been used for planning routes of autonomous robots, while taking into account obstacles and avoiding them [51]. Graph theory can also be used to design telecommunication network [62] and allocate physical cell ID in large wireless network [63]. Additionally, it has been used to properly assign frequencies to radio transmitters in order to prevent transmitter interference [64]. Graph theory has also been utilized to avoid interference in design changes of complex systems [65]. However, it has yet been applied for preventing collisions in variable carriers' paths braiding machines.

The aim of this study is to develop a graph theory-based algorithm to prevent collisions in variable carriers' paths braiding machines by exploiting the flexibility of the carriers' displacement. Graphs terminology and definitions are established in section 6.2, followed by the methodology and a case study in sections 6.3 and 6.4 respectively.

6.2 Graphs terminology and definitions

A graph G is characterized by a set of edges ***E*** and a set of vertices ***V***. Therefore, a graph can be defined as ***G***=(***V***,***E***), where each pair of vertices is connected by an edge. The disjoint paths problem is a fundamental problem in graph theory: for a given graph ***G*** and a set of ***k*** pairs of vertices (s_1,t_1), (s_2,t_2), …, (s_k,t_k) in ***G***, it studies the existence of ***k*** disjoint paths $P_1,P_2,\ldots,P_k$ connecting each pair of vertices, so that P_i links s_i to t_i, for $i \in [1,2,\ldots,k]$. However, the disjoint-path problem does not take into consideration the temporal dimension.

The concept of time-disjoint paths, also known as time-disjoint walks, has been introduced by Bayen et al. [66]. It allows paths to share multiple vertices, as long as no paths use the same vertex simultaneously. This can become handy for planning collision-free routes of autonomous vehicles, for example. A walk is defined as a path having a temporal dimension. Two vertex-disjoint walks are two paths that never share the same vertex simultaneously. However, a given vertex can be utilized by both walks at different times. Further information on graph theory can be found in[53].

6.3 Methodology

The proposed methodology is divided into two steps: modeling the braiding machine bedplate into a graph and developing a graph theory-based algorithm to prevent collisions in variable carriers' paths braiding machines.

6.3.1 Graph modeling of braiding machines bedplate

In a graph of a braiding machine bedplate, edges represent paths along which the carriers can move. Vertices can represent horngears' slots, a track intersection, or possible stationary carrier positions. Moreover, faces represent horngears.

The graphs of traditional braiding machines are directed, since the carriers are forced to move in a unilateral direction, which is imposed by the direction of rotation of the horngears. All the horngears are mechanically linked to the same actuator. Therefore, the direction of rotation of the horngears is set at the beginning of the braiding process and cannot be modified. On the other hand, in variable carrier's paths braiding machines, the direction of rotation of each horngear can be modified at any time, since each horngear is independently driven. Therefore, carriers can move back and forth along the same track. For that reason, the graphs of variable carrier's paths braiding machines are undirected.

For example, let's consider the bedplate of a 3D textile printing braiding machine [60] composed of 18 horngears as shown in Figure 6.3a). Figure 6.3a) presents an overlap of the machine's bedplate and its graph. Each horngear is represented by a face. The edges on the graph represent paths, between the horngears, which the carrier can take. The horngears are placed in a hexagonal compact arrangement. Therefore, each face has six edges.

In our example, each vertex shown in Figure 6.3a) represents an intersection between two or three possible paths. As mentioned in [60], this type of braiding machine architecture eliminates the need for a track. However, each time the carrier finds itself between three adjacent horngears, it can move in three different directions. As shown in Figure 6.3a), a carrier is depicted by a large purple circle. The carrier is placed between three adjacent horngears. The orange, green and blue arrows represent the three possible paths, which the carrier can take. Additionally, during the braiding process, a carrier may be stationary between two adjacent horngears, as shown in Figure 6.3b). To represent this position, a vertex is added at the center point of each edge of Figure 6.3a).

Figure 6.3b) shows the graph of the machine's bedplate with the added vertices, which represent positions between two adjacent horngears. Moreover, each horngear is identical and is set to turn at the same speed. Therefore, the graph is unweighted.

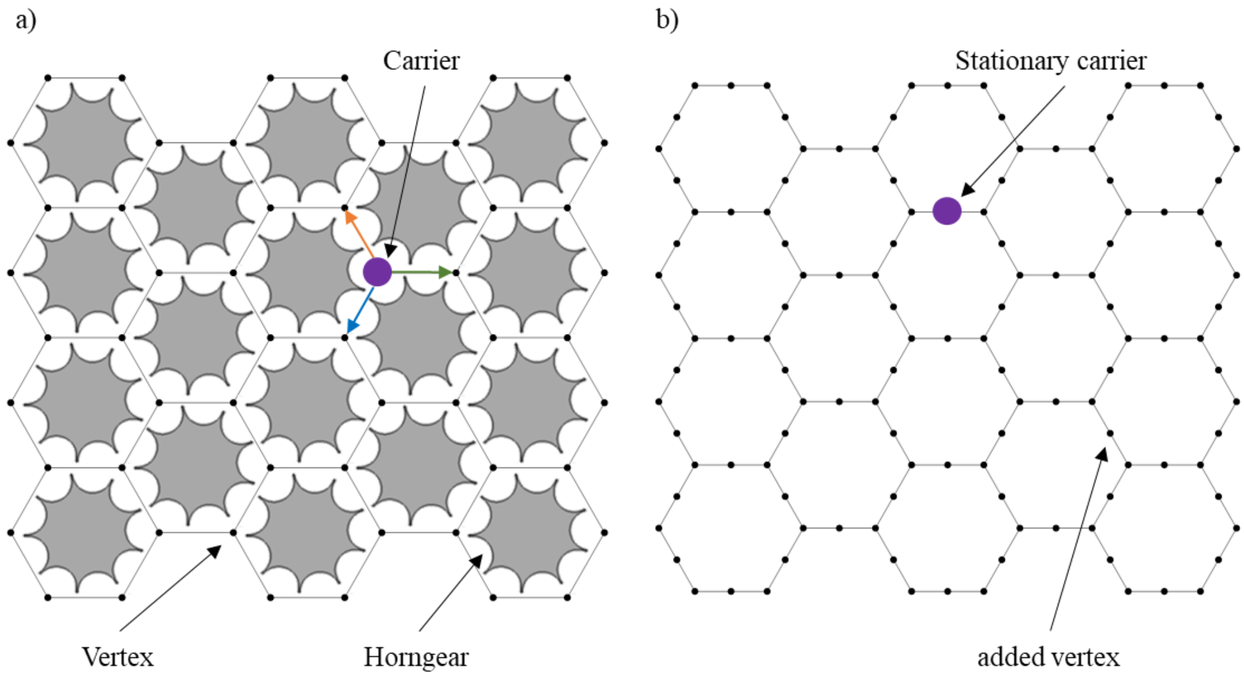

Figure 6.3 : a) Overlap of a 3D textile printing braiding machine bedplate and its graph. A carrier represented by a large purple circle is positioned between three adjacent horngears. The orange, green and blue arrows represent the three possible paths of the carrier. b) Graph of the machine's bedplate. Vertices added to the middle of each edge represent possible stationary carrier positions between two adjacent horngears

6.3.2 Collision prevention algorithm

The path of a carrier can be characterized by a sequence of vertices, where each vertex designates a position of the carrier at a given time. It could be assumed that vertex-disjoint carrier's paths will ensure a collision-free process, since no carriers will ever occupy the same vertex, i.e., the same position on the bedplate. However, in some cases, having vertex-disjoint paths will not ensure a collision-free carrier displacement.

For instance, let's consider two carriers moving in a 3D textile printing braiding machine. Figure 6.4 shows a collision between two carriers even if both carriers occupy different vertices. Each carrier is depicted by a small disk and a large circle. The small disk represents the center of the carrier, which occupies a vertex. The large circle represents the footprint of the carrier. In Figure

6.4, both large circles intersect each other, meaning that the carriers are in collision from being too close to one another. In this case, to prevent such collisions, carriers should have face-disjoint paths: horngears should only house one carrier at the time. Doing so will guarantee a collision-free displacement. Another way to prevent such collisions is to enlarge the size of the horngear. A larger horngear increases the number of carriers that it can house without them colliding from being too close to one another. However, increasing the horngear size also increases the braiding machine footprint. Therefore, due to space constraints, increasing the horngear size is not always a feasible solution.

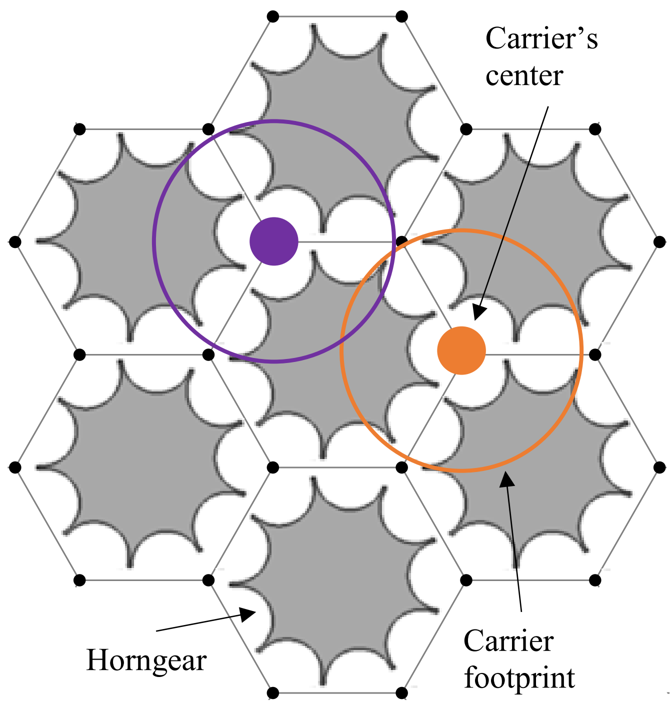

Figure 6.4 : Collision of two carriers sharing the same face, i.e., the same horngear, but different vertices. The small disk represents the center of the carrier while the large circle represents the footprint of the carrier

Depending on the braiding machine architecture, carriers should have either vertex-disjoint or face-disjoint path to ensure a collision-free process. Nonetheless, it is not always possible to have disjoint paths. For example, let's consider the displacement of two carriers, C1 and C2, in a 3D textile printing braiding machine. Their initial position is depicted on Figure 6.5a). C1 is illustrated by a large orange circle while C2 is illustrated by a large purple circle. Figure 6.5b) presents the final position of both carriers as well as the path taken by each one. The path taken by C1 is depicted in orange, while the path taken by C2 is depicted in purple. The shared faces between both paths are indicated by a red X mark within a circle.

In a 3D textile printing braiding machine, a carrier is moved around the bedplate by sets of two or three adjacent horngears, which are adjacent to the carrier [60]. Therefore, edges at the extremity of the bedplate, i.e., edges belonging to a single face, cannot be considered for the carrier's path. The carrier must remain between at least two horngears in order to be displaced. Therefore, there is no vertex-disjoint or face-disjoint paths allowing the displacement of C1 and C2 for the example in Figure 6.5. However, if the temporal dimension is taken into consideration, the paths shown in Figure 6.5b) become vertex-disjoint walks.

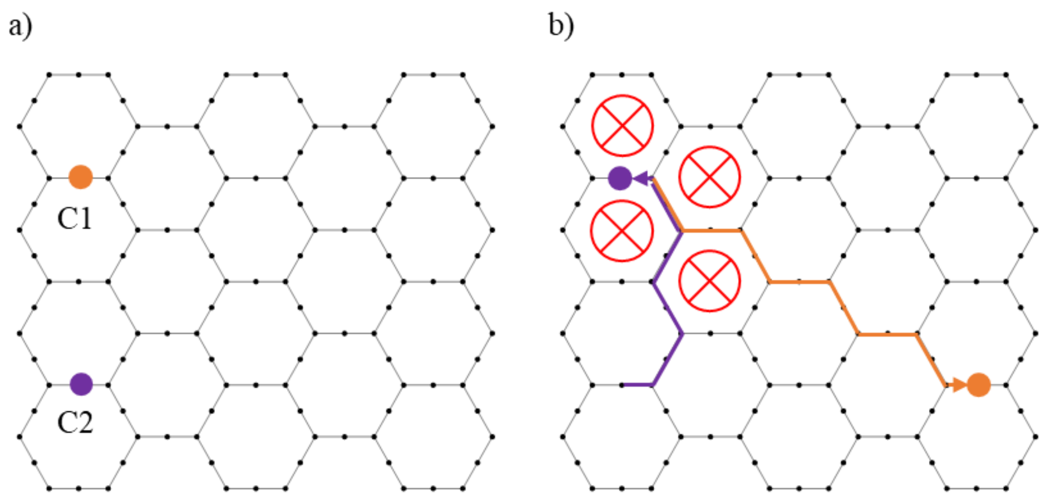

Figure 6.5 : Initial position of two carriers, C1 and C2, in a 3D textile printing braiding machine. Carriers are illustrated by large circle b) Final position of each carrier as well as their respective path. The path taken by C1 is illustrated in orange, while the path taken by C2 is illustrated in purple. Shared faces between both paths are indicated by a red X mark within a circle

We define two types of collision: a vertex collision and a face collision. The first one occurs when a vertex is simultaneously occupied by more than one carrier, i.e., carriers colliding from being at the same place at the same time. The second one occurs when multiple carriers simultaneously share the same face, i.e., carriers colliding from being too close to one another as shown in Figure 6.4.

In this paper, we present an algorithm that prevents collisions in variable carriers' paths braiding machines. Here, we focus on managing face collisions, i.e., solving the face-disjoint walks problem, since managing vertex collisions, i.e., solving the vertex-disjoint walks problem, has been done by Bayen *et al.* [66]. Similar to vertex-disjoint walks problem, the face-disjoint walks problem is solved based on the working principle of delays [66]. The main idea behind this principle is to postpone the departure of a carrier's displacement to prevent a collision.

Each carrier's walk has a starting point and an end point. The carrier walk is composed of a series of vertices. A displacement step (DS) is defined as the carrier's displacement from one vertex to next with respect to its walk. Additionally, the carriers' displacement is synchronized, meaning that each displacement step is synchronized. A delay refers to the number of displacement steps one carrier must wait before engaging its displacement. Therefore, a delay is not measured in time, but rather in displacement steps.

Algorithm 6.1 prevents face collisions in variable paths braiding machines. The main steps of the algorithm are described as follows:

1. Algorithm 6.1 takes as input the graph of the braiding machine bedplate, the number of carriers as well as the walk of each carrier. The walks are sorted into a list according to a user-define criteria, such as their length.
2. Each walk is checked for collisions with the walks listed before it. A collision occurs when two walks share the same face simultaneously.
3. When two walks collide, the vertices from each walk belonging to the shared face are determined and stored into a variable. This is done at line 7 and line 8 from Algorithm 6.1
4. Delays causing a collision between both walks are calculated at line 13 of Algorithm 6.1 and are stored into the variable *CollisionDelay*. These delays are calculated for every combination of vertices determined at step 3. Each time a delay is calculated, two vertices, one from each walk, are taken into consideration. The displacement steps (DS) used to calculate the delay are determined at line 11 and line 12.
5. Once every delay causing a collision is calculated, the delay value allowing a collision-free displacement is therefore determined according to line 20 of Algorithm 6.1. It determined as the smallest positive integer which does not belong to *CollisionDelay*.

At the end of each carrier's displacement, i.e., each carrier's walk, the delays are reset. Therefore, for each new set of walks, the delays are recalculated.

Algorithm 6.1 : *Face collision prevention in braiding machines*

Inputs : Unweighted and undirected Graph defined by vertices (V) and edges (E), such as $G \coloneqq (V, E)$
$k \leftarrow$ number of carriers
Carriers' walk $W \coloneqq \{W_1, \dots, W_k\}$ where elements of $W_i \in V$ for $i \in [k] \coloneqq \{1, \dots, k\}$

$Delay \leftarrow \{\}$
for $i \in [k]$ **do** ⊳ i represents the walk considered
  $CollisionDelay_i \leftarrow \{\}$
  for $j \in [i-1]$ ⊳ j represents a walk listed before W_i
    $CollisionDelay_{i,j} \leftarrow \{\}$
    for $w \in F_i \cap F_j$ **do** ⊳ w represents the number of shared faces
      $N_{j,w} \leftarrow W_j \in (F_i \cap F_j)$ ⊳ F_i and F_j represent the faces of W_i and W_j
      $N_{i,w} \leftarrow W_i \in (F_i \cap F_j)$ ⊳ Vertices of W_i belonging to the shared face
      for $l \leftarrow 1$ **to** *number of elements in* $N_{j,w}$ **do**
        for $m \leftarrow 1$ **to** *number of elements in* $N_{i,w}$ **do**
          $DS_j \leftarrow W_j \in (W_j \cap N_{j,w}[l])$ ⊳DS of W_j corresponding to the vertex $N_{j,w}[l]$
          $DS_i \leftarrow W_i \in (W_i \cap N_{i,w}[m])$
          $CollisionDelay \leftarrow Delay_j + DS_j - DS_i$
          $CollisionDelay_{i,j} \leftarrow CollisionDelay_{i,j} \cup CollisionDelay$
        end for
      end for
    end for
  $CollisionDelay_i \leftarrow CollisionDelay_i \cup CollisionDelay_{i,j}$
  end for
$Delay_i \leftarrow \min(\mathbb{Z}_{\geq 0} \setminus CollisionDelay_i)$
end for

6.4 Case study: Collision prevention on a variable path braiding machine

This case study aims to validate Algorithm 6.1 when braiding on variable paths braiding machine. A three yarns flat braid produced on a 3D textile printing braiding machine is used as an example for this case study. As mentioned in [60], the pitch of a three yarns flat braid can be achieved by 12 distinct carrier displacements, i.e., four displacements per carrier, where each carrier's displacement has its initial and final position on the bedplate. Here, we focused on three displacements, i.e., one displacement per carrier, since the collision prevention principle is similar for all 12 displacements.

Similar to Figure 6.3, the braiding machine bedplate is composed of eighteen horngears placed in a hexagonal compact arrangement. Since horngears are independently driven, delays can be assigned to the carriers to prevent collisions. The algorithm is used to prescribe delays to each carrier in order to avoid collisions. Note that when every delay is zero, carriers can start their displacement simultaneously without colliding with each other.

Figure 6.6a) presents the graph of the machine bedplate as well as the initial position of three carriers: C1, C2 and C3. Figure 6.6b) presents the final position of each carrier as well as their walk. As illustrates in Figure 6.6c), when each carrier moves simultaneously, C1 and C2 collide on the same face at their third displacement step. Therefore, the walk of C1, C2 and C3 are fed as input to Algorithm 6.1. As a result, to prevent the collision, the algorithm prescribes a delay of six displacement steps for C2. Figure 6.6d) illustrates the first six displacement steps of C1 and C3 while C2 is not moving. After six displacement steps, C2 starts to move, as shown in Figure 6.6e). Figure 6.6e) presents displacement steps 7 and 8. Figure 6.6f) illustrates displacement step 9 to the final position of each carrier. As shown in Figure 6.6d), e) and f), collisions can be avoided by applying delays prescribed by the algorithm without rerouting the carriers or changing the initial carrier arrangement.

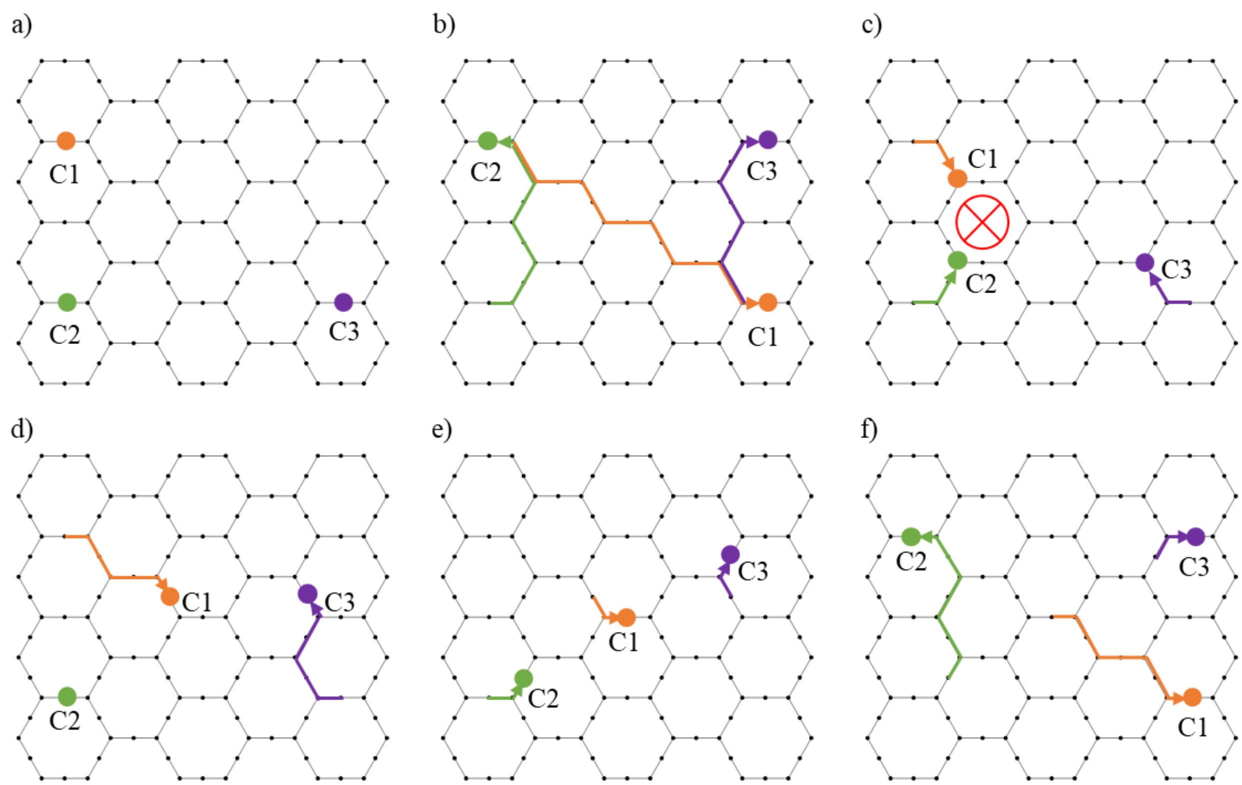

Figure 6.6 : a) Initial position of three carriers: C1, C2 and C3 b) Final position of each carrier and their respective walk c) Simultaneous displacement of carriers resulting in a collision d),e) and f) Implementation of the delay prescribed by the algorithm resulting in a collision free displacement d) Displacement steps 1 to 6 e) Displacement steps 7 and 8 f) Displacement step 9 to the final position

In previous work [60], carriers had to move around the bedplate one at the time in order to complete the carriers' displacement from Figure 6.6a) to Figure 6.6b). Doing so simplified collision management and programming, which had to be done manually. However, as shown in this case study, the proposed algorithm can automatically detect and manage collisions, which simplifies the programming of the machine. It also increases the braiding machine efficiency by enabling simultaneous carrier displacements.

6.5 Conclusion

Based on graph theory, we presented an algorithm that prevents collisions between carriers in variable carriers' paths braiding machines through the application of delays. The machine bedplate was represented by a graph. By applying delays to the carrier displacement, collisions can be prevented without changing the carrier arrangement or rerouting the carriers.

The algorithm takes as input the walk of each carrier. The walks are sorted into a list either randomly or according to a user-define criteria, such as their length. However, the order in which the walks are sorted has an impact on the braid manufacturing time i.e., the time it takes for each carrier to complete its displacements. Delays are prescribed sequentially according to the list's order. Hence, by changing the order of the list, the delay prescribed to each carrier will change. Therefore, the list's order could be optimized to reduce the total manufacturing time. In addition, the delays could easily increase and slow down the manufacturing process when fabricating a complex braided structure requiring multiple carriers and long displacements. To mitigate this issue, the carriers' displacement could be subdivided into shorter displacements around each crossing, therefore reducing the number of delays.

The algorithm offers an automated solution for preventing collisions. It took less than 40 milliseconds to run for the case study using a standard desktop computer equipped with 32 GB of random access memory (RAM) and an i9-9900K central processing unit (CPU). This is significantly faster than the time it would take for a human to make a similar decision by a manual trial an error method. Therefore, programming variable carriers' paths braiding machines can now be done more efficiently. With the right user interface, the algorithm can be eventually used by any machine operator. Consequently, highly skilled and experienced engineers are no longer required to guarantee a collision free braiding process. The algorithm becomes a very handy tool when it is time to fabricate a novel braid geometry for which the proper machine settings and carrier arrangement are unknown. From the 3D model of a braid, the positions of each yarn can be determined at any given point along the longitudinal braid axis. To fabricate the braid, the yarns' positions must be translated into carriers' positions on the bedplate and the carriers must move to those desired positions without colliding which each other. This is where the algorithm becomes useful: with the required carriers' positions, the algorithm ensures a collision free displacement. For the algorithm to function, each carrier must have a start and an end position, which are user-defined. As future work, we will automatically determine the carriers start and end position based on the desired braid geometry. Programing variable carriers' paths braiding machines could then be fully automated.

6.6 Funding Acknowledgements

This work was supported by The Natural Sciences and Engineering Research Council of Canada [NSERC, RDCPJ 543847-19]; PRIMA Quebec [R18-13-003]; FilSpec Inc; Pultrusion Techniques; and Bauer Hockey ltd.

CHAPITRE 7 DISCUSSION GÉNÉRALE

Bien que les métiers à tresser à trajectoires fixes existent depuis plusieurs années, déterminer et valider l'arrangement des chariots est encore une tâche compliquée qui nécessite l'expertise d'un personnel hautement spécialisé ainsi que plusieurs essais-erreur. La méthode présentée au chapitre 4 offre une solution simple, permettant de valider ou d'infirmer l'arrangement des chariots. Cette dernière peut être utilisée sur n'importe quel métier à tresser. Aucun logiciel spécialisé n'est requis pour implémenter cette méthode, ce qui permet de réduire les coûts et économiser du temps, car ces logiciels sont généralement coûteux et longs à maîtriser. Par ailleurs, des connaissances avancées en mathématique ainsi qu'en analyse d'éléments finis ne sont pas requises. Donc, la main-d'œuvre spécialisée n'est plus nécessaire pour assurer un procédé de fabrication sans collision. Cette dernière peut désormais se concentrer sur différentes tâches. De plus, une méthode automatique réduit le risque d'erreur qui peut être coûteux en termes de matériels endommagés ou rendre la machine inopérable.

À l'achat d'un métier à tresser traditionnel, les fabricants livrent la machine avec les chariots installés selon un arrangement prédéfini. Évidemment, cet arrangement ne crée aucune collision. Il permet de maximiser le nombre de chariots sur le plan de travail, donc, de maximiser le nombre de fils dans la tresse. Toutefois, cet arrangement permet la création d'un nombre très limité d'architectures de tresse. En changeant l'arrangement des chariots prédéfini par le fabricant, différentes architectures peuvent être fabriquées, telles que 1x1, 3x3, 2x2, 3x2, enroulement filamentaire, etc. Cependant, les différents arrangements possibles ne sont pas fournis par le fabricant. La méthode présentée au chapitre 4 permet de déterminer rapidement et de façon automatique tous les arrangements de chariots valides, ce qui permet de connaître et d'utiliser le plein potentiel du métier à tresser.

Au chapitre 5, une nouvelle technologie pour la fabrication de tresses 3D est présentée. Cette dernière permet de contrôler la position et l'orientation de chaque fils, ce qui permet la fabrication de pièces en composites tressés mieux adaptée aux requis de forme et offre une plus grande liberté de conception aux ingénieurs. La technologie n'utilise aucun mécanisme de transfert, ce qui simplifie l'architecture et le contrôle de la machine. Les pièces à géométrie complexe, telles que les cadres et les fourches de vélos, peuvent désormais être fabriquées en une seule étape de fabrication, et ce, de façon automatique. Ceci permet de maintenir la continuité des fibres, contrairement aux méthodes de fabrication traditionnelles, telles que le positionnement manuel de tissés plans (2D), offrant donc de meilleures propriétés mécaniques. Le retrait et l'ajout des chariots peuvent également se faire automatiquement sans arrêter le procédé de fabrication, ce qui améliore l'efficacité de ce dernier.

Les fibres de carbone sont souvent utilisées pour la fabrication des pièces en composites en raison de leur faible masse volumique et de leurs fortes propriétés mécaniques. Malheureusement, la production des fibres de carbone est extrêmement énergivore. La matière première utilisée pour créer les fibres de carbone, aussi nommée le précurseur, est le polymère polyacrylonitrile (PAN). Cette structure est principalement composée d'azote, de carbone et d'hydrogène. Tout d'abord, le précurseur est mis sous tension pour aligner les chaînes de polymère. Les chaînes étirées sont ensuite placées dans un four, pour plusieurs heures, à des températures variant entre 200ºC et 300ºC. Le PAN est par la suite carbonisé, ce qui consiste à chauffer les filaments du précurseur jusqu'à des températures variant entre 1000ºC et 2000ºC et ce, pour environ 40 minutes. Suite à la carbonisation, les filaments subissent une graphitisation pour augmenter leur module d'élasticité : chauffage entre 2000ºC et 3000ºC. Non seulement le processus complet requiert un apport en énergie énorme, mais il produit aussi des gaz tels que du méthane, du dioxyde de carbone et de l'hydrogène. Par ailleurs, les méthodes de fabrication traditionnelles des matériaux composites ont un impact très négatif sur l'environnement, car elles produisent énormément de rebuts difficilement recyclables. La technologie présentée au chapitre 5 présente une solution permettant de minimiser, voire d'éliminer, toute forme de rebut lors de la fabrication des pièces. Par le positionnement de chaque fil, la solution proposée permet la création de pièces optimisées tout en étant fabriquées aux dimensions finales. Cela permet d'abaisser la quantité de matériel requis et de réduire la quantité de matériel gaspillé. Conséquemment, la quantité de matière nécessaire à la fabrication de pièces en composites est réduite, ce qui entraîne une réduction de la consommation énergétique liée à cette fabrication.

Lors des essais de caractérisation du prototype, présenté au chapitre 5, les chariots ont été déplacés de façon séquentielle. En d'autres mots, un chariot à la fois était en mouvement pendant que les autres étaient stationnaires. Cela a permis de faciliter la programmation manuelle des déplacements. Cela a également permis d'éviter plus facilement des collisions entre les chariots. Malgré le mouvement séquentiel des chariots, les relations fondamentales entre les paramètres de la tresse et les paramètres du prototype ont été respectées, démontrant une bonne fonctionnalité du concept. Toutefois, l'efficacité du procédé était grandement affectée. Par l'automatisation de la programmation et de la gestion des collisions, les résultats présentés au chapitre 6 ont rendu possible le déplacement simultané des chariots, améliorant ainsi l'efficacité du procédé. De plus, la programmation automatique élimine les erreurs humaines pouvant être coûteuses en matériel et en temps.

En couplant les résultats présentés au chapitre 6 avec la technologie présentée au chapitre 5, les ingénieurs peuvent désormais se concentrer davantage sur la conception des nouvelles géométries tressées sans se soucier de l'arrangement des chariots ni de la programmation du métier à tresser, car cette dernière peut maintenant se faire automatiquement tout en évitant les collisions entre les chariots. Les travaux du chapitre 6 serviront de jalon pour la programmation automatique des métiers à tresser à trajectoires variables. Il est important de mentionner que la programmation complexe et manuelle de telles machines limite leur utilisation et leur commercialisation. Grâce à la solution simple et efficace détaillée au chapitre 6, les propriétés mécaniques des composites tressés 3D pourront être exploitées davantage.

CHAPITRE 8 CONCLUSION ET RECOMMANDATIONS

L'objectif principal du projet de recherche était de développer un procédé de fabrication pour les tresses 3D permettant de positionner en tout temps et de façon indépendante les chariots supportant les bobines de fil. Cet objectif a été atteint en accomplissant trois sous-objectifs.

Le premier sous objectif était de développer un algorithme pour la détection de collisions entre les chariots pouvant être implémenté indépendamment du type de métier à tresser. Cet objectif a été atteint. Il est présenté au chapitre 4. Pour ce faire, le plan de travail est représenté par un graphe constitué de faces, de nœuds et d'arêtes. Les roues à encoches sont représentées par les faces et les encoches des roues sont représentées par les nœuds. Les nœuds représentent également l'intersection de deux trajectoires. Les arêtes représentent les trajectoires que les chariots peuvent emprunter. L'algorithme prend en entrée la trajectoire de chaque chariot ainsi que le graphe du plan de travail. À partir de ces informations, l'algorithme valide ou réfute l'arrangement des chariots. Une collision se produit lorsque deux chariots se trouvent au même endroit simultanément. Sur le graphe, cela implique que deux chariots se trouvent simultanément sur le même nœud. L'algorithme vérifie donc que chaque nœud est uniquement occupé par un chariot en tout temps. Dans le cas contraire, cela indique une collision. Cette méthode a été implémentée sur deux différents métiers à tresser : un métier traditionnel ainsi qu'un métier à tresser pour des tresses en forme de « T ». Ce dernier est plus complexe que les métiers à tresser traditionnels, car il est composé de plusieurs trajectoires ainsi que différentes géométries de roue à encoches. Il représente l'éventail des cas complexes et démontre les capacités et la polyvalence de l'algorithme.

Le second sous objectif était de concevoir et de fabriquer un métier à tresser permettant un déplacement indépendant des chariots. Cet objectif a été atteint. Il est présenté au chapitre 5. Un nouveau chariot a été conçu. Ce dernier est composé d'une chaîne de trois maillons. Il se déplace sur un plan de travail composé de roues à encoches. Ces dernières sont positionnées selon un arrangement hexagonal compact. Les lignes directrices de conception concernant le dimensionnement des roues à encoches sont également présentées au chapitre 5. Le déplacement du chariot s'effectue par l'entremise des roues à encoches. Le système est similaire à celui d'un système chaîne-pignon. Le cycle du déplacement du chariot est divisé en 3 étapes. La première consiste à orienter le chariot. Cette étape est effectuée par la rotation d'une roue à encoches qui oriente le premier maillon de la chaîne. La deuxième étape concerne le déplacement du chariot.

Pour se faire, les trois roues adjacentes au chariot tournent simultanément. Finalement, la dernière étape du cycle correspond au redressement de la chaîne. Cette étape est effectuée par la rotation d'une roue à encoches. En répétant les étapes du cycle de déplacement, le chariot peut être déplacé sur le plan de travail. Un prototype a été fabriqué pour valider le concept. À partir de ce prototype, deux tresses ont été fabriquées. La première est une tresse standard à trois fils. La deuxième est une tresse comprenant deux changements de section transversale. Cette dernière débute par une tresse standard à trois fils. Elle se transforme par la suite en un enroulement filamentaire de 3 fils, où deux fils s'enroulent ensemble et le troisième enroule les deux premiers à un pas différent. Filament, l'enroulement filamentaire se transforme en tresse standard à 3 fils. Ces changements de section ont été effectués de façon automatique, sans arrêter le procédé de fabrication. Il est donc possible de contrôler la position de chaque chariot.

Le troisième sous objectif était de développer un algorithme de contrôle permettant d'éviter les collisions dans les métiers à tresser à trajectoires variables en exploitant la flexibilité du déplacement des chariots. Cet objectif a été atteint. Il est présenté au chapitre 6. De façon similaire au chapitre 4, l'algorithme présenté au chapitre 6 se base également sur la théorie des graphes. Pour ce faire, le plan de travail est également représenté par un graphe. Les roues à encoches sont représentées par les faces du graphe, tandis que les arêtes représentent les trajectoires que les chariots peuvent emprunter. Contrairement au chapitre 4, les nœuds ne représentent pas les encoches des roues, mais bien l'intersection des trajectoires ou des positions stationnaires entre deux roues adjacentes. L'algorithme présenté au chapitre 6 prend en entrée le graphe du plan de travail ainsi que la trajectoire de chaque chariot. Dans les cas d'éventuelles collisions, l'algorithme prescrit un délai à chaque chariot. Ces délais retardent le déplacement des chariots permettant ainsi d'éviter une collision. Une étude de cas a été effectuée sur le prototype présenté au chapitre 5, où une collision a été évitée en retardant le déplacement d'un chariot. Cela a permis un déplacement simultané des chariots.

8.1 Limitations

8.1.1 Plan vertical

Les tresses fabriquées à l'aide du prototype ont été réalisées sur un plan de travail horizontal (parallèle au sol). Cependant, sur un plan vertical (perpendiculaire au sol), le concept du chariot, tel que présenté au chapitre 5, n'est pas fiable. En effet, sous l'effet de la gravité, le chariot risque de rester coincé entre les roues. La Figure 8.1 présente un chariot sur un plan vertical bloqué entre les roues. Le chariot se déplace vers la gauche et seulement les deux premiers maillons constituant la chaîne du chariot sont présentés.

Figure 8.1 : Blocage mécanique du chariot sur un plan vertical

La gravité entraîne les maillons du chariot vers le bas. Le premier maillon (celui de gauche à la Figure 8.1) vient donc se heurter contre la dent d'une roue, plutôt que de s'enligner dans l'encoche de la roue, créant ainsi un blocage mécanique. Afin de pallier cette limitation et de rendre possible le tressage sur un plan vertical, des modifications doivent être apportées au chariot. Entre autres, un mécanisme permettant de maintenir un alignement rectiligne entre chaque maillon du chariot sous l'effet de la gravité, tel qu'un système de ressort, pour assurer l'alignement entre le premier maillon du chariot et l'encoche des roues.

8.1.2 Fils axiaux et vitesse du procédé

Dans les métiers à tresser traditionnels, les roues à encoches sont actionnées par un moteur commun et un système d'engrenage. Le système d'engrenage permet la création d'un trou de passage au centre de chaque roue à encoches. Des fils axiaux peuvent donc être facilement intégrés à la tresse.

Les bobines des fils axiaux sont stationnaires et positionnées en dessous du plan de travail. Les fils passent par le trou de passage au centre des roues à encoches avant de s'intégrer à la tresse.

Dans le concept présenté au chapitre 5, chaque roue à encoches est directement actionnée par un moteur électrique. Elles sont fixées sur l'arbre du moteur. Il est donc impossible de créer un trou de passage au centre de chaque roue à encoches pour accommoder des fils axiaux. Un actionnement indirect pourrait pallier cette limitation. Cela permettrait de décaler l'arbre du moteur du centre de la roue à encoches afin d'accommoder des fils axiaux.

De plus, avec un actionnement direct des roues à encoches, la grosseur des actuateurs est limitée. Les moteurs doivent être placés l'un à côté de l'autre selon un arrangement hexagonal compact, similaire aux roues à encoches. Pour ce faire, la circonférence des moteurs doit être plus petite ou égale à celle des roues, sans quoi, les moteurs devront partager un espace commun, ce qui est physiquement impossible (interférence physique entre les moteurs). L'actionnement indirect permettra d'éliminer cette contrainte d'espace et d'augmenter la vitesse de déplacement des chariots en utilisant des actionneurs plus puissants et plus volumineux.

8.2 Recommandations futures

Pour obtenir une géométrie bien précise, dès lors, des propriétés mécaniques spécifiques, il faut être en mesure de relier la trajectoire des chariots à la géométrie de la tresse générée (cinématique directe) et vice versa (cinématique inverse). Les méthodes pour relier la trajectoire à la géométrie sont connues. Cependant, il n'existe aucune méthode reliant la géométrie du textile aux trajectoires des chariots. La capacité à déduire l'entrelacement des fils, or la trajectoire des chariots, à partir d'une tresse ou d'un modèle de tresse donné est réservée aux experts. Par expérience et par observation, ils sont les seuls à pouvoir déterminer le trajet des chariots et la technique utilisée pour produire la tresse. Il serait intéressant d'élaborer une méthode pour résoudre la cinématique inverse.

L'analyse des sections transversales de la tresse pourrait être une piste de solution. En attribuant à chaque fil une couleur et en effectuant une analyse d'image sur plusieurs coupes transversales selon l'axe longitudinal de la tresse, la position de chaque fil pourrait être déterminée de coupe en coupe. En enregistrant la position de chaque fil, la trajectoire de ces derniers pourra être déterminée. Pour créer la tresse à l'aide du métier à tresser, les chariots devront reproduire les trajectoires des fils sur le plan de travail.

RÉFÉRENCES

[1] R. Slayton and G. Spinardi, "Radical innovation in scaling up: Boeing’s Dreamliner and the challenge of socio-technical transitions," *Technovation,* vol. 47, pp. 47-58, 2016.

[2] V. Giurgiutiu, *Structural Health Monitoring of Aerospace Composites*: Elsevier, 2016.

[3] P. K. Mallick, *Fiber-reinforced composites: materials, manufacturing, and design*: CRC press, 2007.

[4] Y. Kyosev, *Advances in braiding technology: Specialized techniques and applications*: Woodhead Publishing, 2016.

[5] Z. Wang, G. Zhang, Y. Zhu, L. Zhang, X. Shi, and W. Wang, "Theoretical analysis of braiding strand trajectories and simulation of three-dimensional parametric geometrical models for multilayer interlock three-dimensional tubular braided preforms," *Textile Research Journal,* 2019.

[6] Q. Yu, Z. Sun, Y. Qiu, S. Zhou, Y. Chen, J. Wu*, et al.*, "Study on the braiding of preform with special-shaped sections based on the two-dimensional braiding process," *Textile Research Journal,* vol. 89, pp. 172-181, 2017.

[7] F. K. Ko, C. M. Pastore, and A. A. Head, *Atkins & Pearce handbook of industrial braiding*: Atkins & Pearce, 1990.

[8] L. Pei, Z. Xiao, L. Geng, J. Wu, F. Zhang, and Y. Sun, "Surface parameters measurement for braided composite preform based on gray projection," *Journal of Engineered Fibers Fabrics,* vol. 14, 2019.

[9] Z. ming Huang. (2000, The mechanical properties of composites reinforced with woven and braided fabrics. *Composites science and Technology 60(4),* 479-498.

[10] D. Boris, L. Xavier, and S. Damien, "The tensile behaviour of biaxial and triaxial braided fabrics," *Journal of Industrial Textiles,* vol. 47, pp. 2184-2204, 2018.

[11] P. Potluri, A. Manan, M. Francke, and R. Day, "Flexural and torsional behaviour of biaxial and triaxial braided composite structures," *Composite Structures,* vol. 75, pp. 377-386, 2006.

[12] W. Hao, Z. Huang, L. Zhang, G. Zhao, and Y. Luo, "Study on the torsion behavior of 3-D braided composite shafts," *Composite Structures,* vol. 229, p. 111384, 2019.

[13] P. Potluri, A. Rawal, M. Rivaldi, and I. Porat, "Geometrical modelling and control of a triaxial braiding machine for producing 3D preforms," *Composites Part A: Applied Science Manufacturing,* vol. 34, pp. 481-492, 2003.

[14] M. Saiman, M. S. Wahab, and M. U. Wahit, "The effect of fabric weave on the tensile strength of woven kenaf reinforced unsaturated polyester composite," in *Proceedings of the International Colloquium in Textile Engineering, Fashion, Apparel and Design 2014 (ICTEFAD 2014)*, 2014, pp. 25-29.

[15] K. Bilisik, "Three-dimensional braiding for composites: a review," *Textile Research Journal,* vol. 83, pp. 1414-1436, 2013.

[16] A. Pickett, M. Schneider, B. Wulfhorst, and Langer, "Design and Manufacture of 3D-Braided Textiles As a Reinforcement for Composites," *Materials for Transportation Technology*, vol. 1, pp. 169-175, 2000.

[17] X. Sun, "Micro-geometry of 3-D braided tubular preform," *Journal of composite materials,* vol. 38, pp. 791-798, 2004.

[18] D. Brunnschweiler, "Braids and braiding," *Journal of the Textile Institute Proceedings,* vol. 44, pp. P666-P686, 1953.

[19] Y. Kyosev, *Braiding technology for textiles: Principles, design and processes*: Elsevier, 2014.

[20] L. Laberge-Lebel, "Manufacturing of braided thermoplastic composites with commingled fibers," Concordia University, 2005.

[21] M. Tada, T. Uozumi, A. Nakai, and H. Hamada, "Structure and machine braiding procedure of coupled square braids with various cross sections," *Composites Part A: Applied Science Manufacturing,* vol. 32, pp. 1485-1489, 2001.

[22] Y. Kyosev, "Machine configurator for braided composite profiles with arbitrary cross section," in *16th European conference on composite materials ECCM*, 2014.

[23] D. Chengjie, M. Zhuo, Z. Yujing, and S. Yize, "Modeling and analysis of the carrier arrangement in square rotary braiding," *Textile Research Journal,* vol. 89, pp. 4208-4219, 2019.

[24] H. Reichel, "MACHINE FOR BRAIDING KNOTLESS NETTING," Germany Patent US3894470, 1975.

[25] H. Berger, "Apparatus for Braiding Knotless Netting," Germany Patent US3866512, 1975.

[26] K. Bock, H. Cranz, and G. Flohr, "PROCESS AND MACHINE FOR PRODUCTION OF BRAIDED PACKING," US4096781, 1975.

[27] E. Laourine, M. Schneider, and B. Wulfhorst, "Production and analysis of 3D braided textile preforms for composites," presented at the Texcomp, 2000.

[28] A. Pickett, M. Schneider, B. Wulfhorst, and P. J. M. f. T. T. Langer, "Design and Manufacture of 3D-Braided Textiles As a Reinforcement for Composites," vol. 1, pp. 169-175, 2000.

[29] M. Schneider, A. Pickett, and B. Wulfhorst, "A new rotary braiding machine and CAE procedures to produce efficient 3D-braided textiles for composites," in *International Sampe Symposium and Exhibition,* 2000, pp. 266-276.

[30] Y. Kyosev, "Numerical modelling of 3D braiding machine with variable paths of the carriers," *Applied Composite Materials,* vol. 25, pp. 773-783, 2018.

[31] Y. Kyosev, M. Hübner, and C. Cherif, "Virtual development and numerical simulation of 3D braids for composites," in *texcomp13*, 2018.

[32] C. Du, Z. Meng, Y. Sun, and J. Yu, "Optimal design of the horn gear for rotary three-dimensional braiding machine," *The Journal of The Textile Institute,* pp. 1-7, 2020.

[33] A. Bogdanovich and D. Mungalov, "A Novel 3-D Braiding Technology, Complex Shape Preforms and Composites," in *ASME 2002 International Mechanical Engineering Congress and Exposition*, 2002, pp. 31-35.

[34] A. Bogdanovich and D. Mungalov, "A Novel 3-D Braiding Technology, Complex Shape Preforms and Composites," in *ASME International Mechanical Engineering Congress and Exposition*, 2002, pp. 31-35.

[35] D. Mungalov and A. Bogdanovich, "AUTOMATED 3-D BRAIDING MACHINE AND METHOD," US Patent US 6,439,096, 2002.

[36] D. Mungalov and A. Bogdanovich, "Connecting design and manufacture of complex shape 3-D braided preforms," presented at the 49th International SAMPE Symposium and Exhibition: Materials and Processing Technology, 2004.

[37] A. Mungalov, "Complex shape 3-D braided composite-preforms: Structural shapes for marine and aerospace," vol. 40, pp. 7-21, 2004.

[38] P. Gleßner and Y. Kyosev, "Pattern design with the variation braider VF of company Herzog GmbH," in *Narrow and smart textiles*, ed: Springer, 2018, pp. 149-158.

[39] F. Schreiber, F. Ko, H. Yang, E. Amalric, and T. Gries, "Novel three-dimensional braiding approach and its products," in *17th International Conference on Composite Materials, Edinburgh, UK*, 2009.

[40] G. Guyader, A. Gabor, and P. Hamelin, "Analysis of 2D and 3D circular braiding processes: Modeling the interaction between the process parameters and the pre-form architecture," *Mechanism Machine Theory,* vol. 69, pp. 90-104, 2013.

[41] T. D. Kostar and T.-W. Chou, "A methodology for Cartesian braiding of three-dimensional shapes and special structures," *Journal of materials science,* vol. 37, pp. 2811-2824, 2002.

[42] K. Bilisik, "Cartesian 3D braiding," in *Advances in braiding technology*, ed: Elsevier, 2016, pp. 107-145.

[43] M. Okano, A. Nakai, and H. Hamada, "Axial crushing performance of braided composite tubes," *International Journal of Crashworthiness,* vol. 10, pp. 287-294, 2005.

[44] H. Hamada, "Can braided composites be used for crushing elements in cars," presented at the ICCM, 1997.

[45] B. Harris, *Fatigue in composites: science and technology of the fatigue response of fibre-reinforced plastics*: Woodhead Publishing, 2003.

[46] J. de Oliveira Simões and A. T. Marques, "Determination of stiffness properties of braided composites for the design of a hip prosthesis," *Composites Part A: Applied Science Manufacturing,* vol. 32, pp. 655-662, 2001.

[47] H. Mehboob and S.-H. Chang, "Application of composites to orthopedic prostheses for effective bone healing: A review," *Composite Structures,* vol. 118, pp. 328-341, 2014.

[48] G. Agnarsson and R. Greenlaw, *Graph theory: Modeling, applications, and algorithms*: Prentice-Hall, Inc., 2006.

[49] A. H. Farrahi, A. T. Goldberg, L. Bagasol, and J. Jung, "Applying graph theory to problems in air traffic management," in *17th AIAA Aviation Technology, Integration, and Operations Conference*, 2017, p. 3775.

[50] R. Likaj, A. Shala, M. Mehmetaj, P. Hyseni, and X. Bajrami, "Application of graph theory to find optimal paths for the transportation problem," *IFAC Proceedings Volumes,* vol. 46, pp. 235-240, 2013.

[51] G. Farid, S. Cocuzza, T. Younas, A. A. Razzaqi, W. A. Wattoo, F. Cannella, *et al.*, "Modified A-Star (A*) Approach to Plan the Motion of a Quadrotor UAV in Three-Dimensional Obstacle-Cluttered Environment," *Applied Sciences,* vol. 12, p. 5791, 2022.

[52] Z. Ding, J. Li, M. Yang, Z. Yan, B. Li, and W. Chen, "A Multi-channel Anti-collision Algorithm in Multi-reader RFID Networks," in *International Conference on Smart Grid and Internet of Things*, 2020, pp. 220-238.

[53] J. A. Bondy and U. S. R. Murty, *Graph theory with applications* vol. 290: Macmillan London, 1976.

[54] K. T. Ulrich, S. D. Eppinger, and M. C. Yang, *Product Design and Development. 7th ed.*: McGraw-Hill Education, 2020.

[55] M. Ramananarivo, M. Raison, O. Barron, and S. Achiche, "Biofidelic design of the forearm of a myoelectric prosthesis with maximum functional volume," in *DS 87-1 Proceedings of the 21st International Conference on Engineering Design (ICED 17) Vol 1: Resource Sensitive Design, Design Research Applications and Case Studies, Vancouver, Canada, 21-25.08. 2017*, 2017, pp. 479-488.

[56] A. Mohebbi, S. Achiche, and L. Baron, "Mechatronic multicriteria profile (MMP) for conceptual design of a robotic visual servoing system," in *Engineering Systems Design and Analysis*, 2014, p. V003T15A015.

[57] A. Mohebbi, S. Achiche, and L. Baron, "Multi-criteria fuzzy decision support for conceptual evaluation in design of mechatronic systems: a quadrotor design case study," *Research in Engineering Design,* vol. 29, pp. 329-349, 2018.

[58] D. Marini, D. Cunningham, and J. R. Corney, "Near net shape manufacturing of metal: a review of approaches and their evolutions," *Proceedings of the institution of mechanical engineers, Part B: journal of engineering manufacture,* vol. 232, pp. 650-669, 2018.

[59] Q. Yu, Z. Sun, Y. Qiu, S. Zhou, Y. Chen, J. Wu, *et al.*, "Study on the braiding of preform with special-shaped sections based on the two-dimensional braiding process," *Textile Research Journal,* vol. 89, pp. 172-181, 2019.

[60] P. Assi, S. Achiche, and L. L. Lebel, "3D printing process for textile composites," *CIRP Journal of Manufacturing Science Technology,* vol. 32, pp. 507-516, 2021.

[61] D. Wang, X. Chen, and H. Huang, "A graph theory-based approach to route location in railway interlocking," *Computers Industrial Engineering,* vol. 66, pp. 791-799, 2013.

[62] M. Hayashi and T. Abe, "Evaluating reliability of telecommunications networks using traffic path information," *IEEE Transactions on reliability,* vol. 57, pp. 283-294, 2008.

[63] L. M. Abdullah, M. D. Baba, S. G. A. Ali, A. O. Lim, and Y. Tan, "New graph colouring algorithm for resource allocation in large-scale wireless networks," in *2014 IEEE 5th Control and System Graduate Research Colloquium*, 2014, pp. 233-238.

[64] J. L. Gross, J. Yellen, and M. Anderson, *Graph theory and its applications*: Chapman and Hall/CRC, 2018.

[65] U. Chouinard, S. Achiche, and L. Baron, "Integrating negative dependencies assessment during mechatronics conceptual design using fuzzy logic and quantitative graph theory," *Mechatronics,* vol. 59, pp. 140-153, 2019.

[66] A. Bayen, J. Goodman, and E. Vinitsky, "On the Approximability of Time Disjoint Walks," *Journal of Combinatorial Optimization,* pp. 1-22, 2020.

ANNEXE A SUPPLEMENTARY MATERIAL OF CHAPTER 5

Title: 3D printing process for textile composites

Authors: P.Assi[1,2], S. Achiche[2], L. Laberge Lebel[1*]

Author affiliation:

[1]: Advanced Composites and Fibers Structures Laboratory (ACFSlab), High Performance Polymer and Composite Systems (CREPEC), Polytechnique Montreal, 2500 ch Polytechnique, Montreal, Qc, Canada, H3T 1J4

[2]: Laboratoire de Conception de Systèmes Intelligents et Mécatroniques(CoSIM), Polytechnique Montreal, 2500 ch Polytechnique, Montreal, Qc, Canada, H3T 1J4

Figure A8.2 illustrates the sequence required to produce one pitch for a three yarns flat braid. Horngears are represented by hexagons. Each carrier is portrayed by three in line circles. For every step, the carriers are positioned at their departure point and the arrow connected to the carrier marks their arrival point on the bedplate. Every four steps, the pull up mechanism is activated for a specified pulled distance. To fabricate one pitch, a set of 12 steps and three pulls are required.

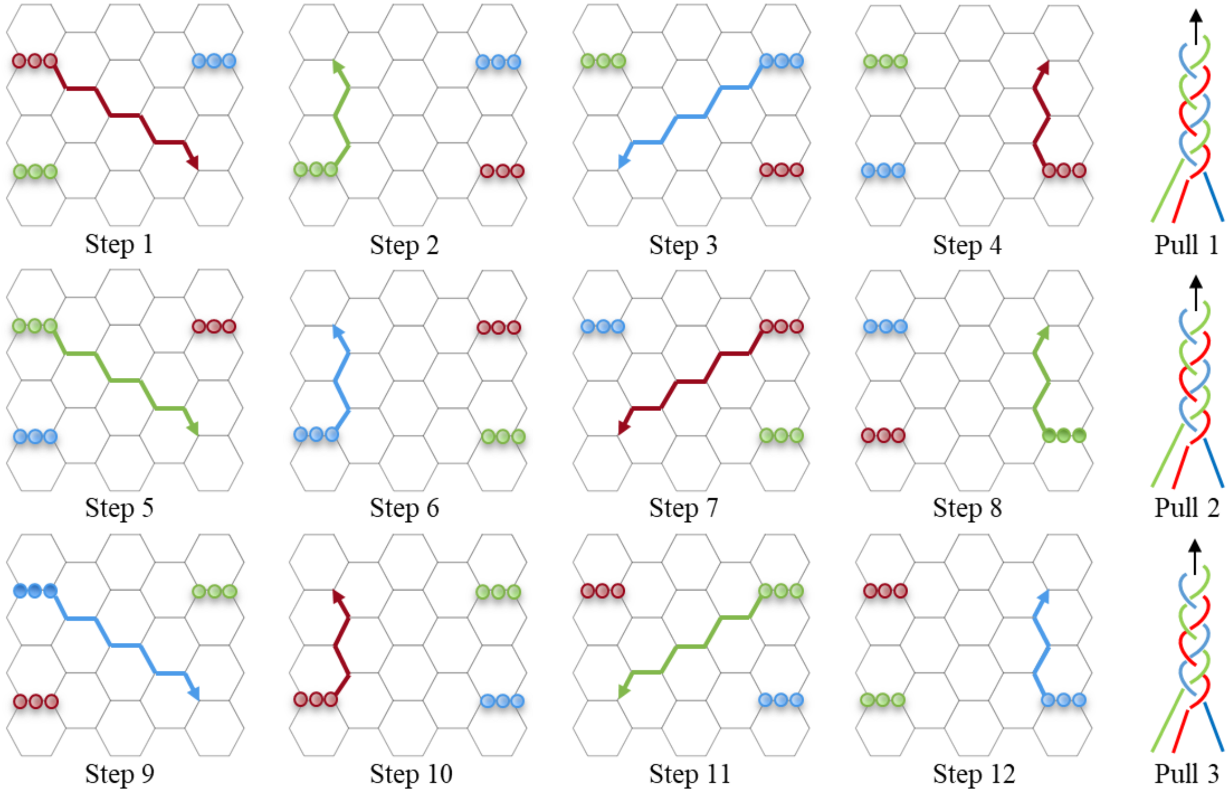

Figure A8.2 : The sequence required to produce one pitch for a three yarns flat braid.

Figure A8.3 illustrates the sequence required to produce one pitch for a filament winding. Similarly to Figure A8.2, horngears are represented by hexagons, carrier are portrayed by three in line circles and for every step, the carriers are positioned at their departure point and the arrow connected to the carrier marks their arrival point on the bedplate. Additionally, steps are combined when carriers move simultaneously, as shown in Figure A8.3b). Figure A8.3a) presents the transitional steps from a flat braid sequence to a filament winding sequence. For the filament winding sequence, one carrier, depicted in blue, was set aside. Only two carriers were used to produce the filament winding from Figure 5.6. The third yarn was wrapped around the two others automatically due to strain in the yarns. Figure A8.3b) presents the sequence to fabricate one pitch of filament winding and Figure A8.3c) presents the transitional steps from a filament winding sequence to a flat braid sequence.

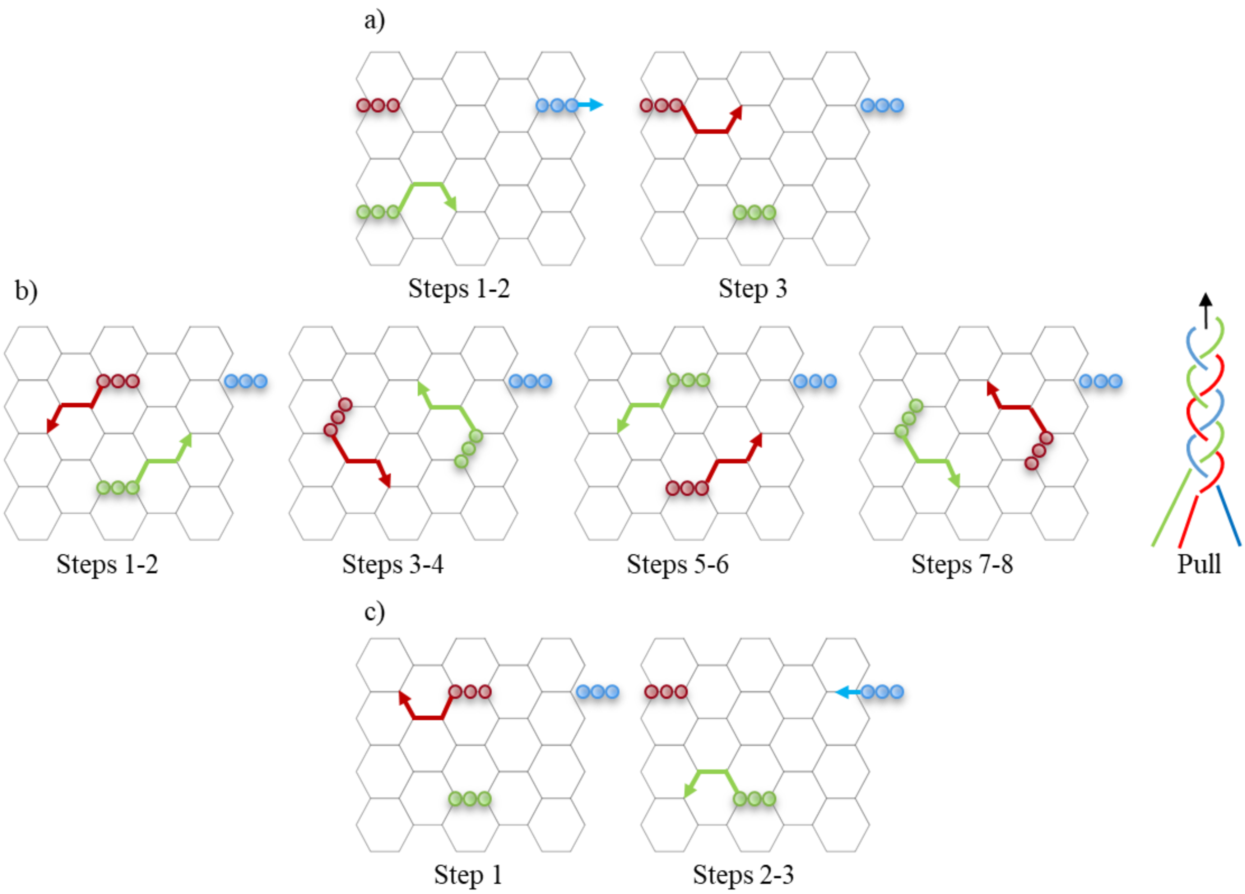

Figure A8.3 : The sequence to produce one pitch of filament winding a) transition steps from a flat braid to filament windings b) sequence to produce one pitch of filament winding c) transition steps from a filament windings to a flat braid.